University of Montana

# ScholarWorks at University of Montana

Graduate Student Theses, Dissertations, & Professional Papers

Graduate School

2006

# Spatial variability of soil hydrophobicity after wildfire

Anna Chapman Birkas
*The University of Montana*

Follow this and additional works at: https://scholarworks.umt.edu/etd

# Let us know how access to this document benefits you.

# THE SPATIAL VARIABILITY OF SOIL HYDROPHOBICITY AFTER WILDFIRE

By

Anna Chapman Birkás

B.S. Humboldt State University, 2002

presented in partial fulfillment
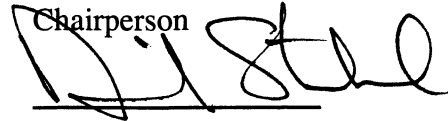
for the degree of

Master of Science

The University of Montana

May 2006

Approved by:

_____

Chairperson

_____

Dean Graduate School

6 - 1 - 06

Date

UMI Number: EP35263

# UMI®

Dissertation Publishing

UMI EP35263

# ProQuest®

Birkás, Anna C. M.S. May 2006                                                Forestry

The Spatial Variability of Soil Hydrophobicity after Wildfire

Director: Scott W Woods  ✎

   Increased levels of erosion and runoff after wildfire are often attributed to soil hydrophobicity. The potential of runoff and erosion caused by water repellent soil depends on its spatial contiguity and strength. Lack of information on the spatial characteristics of soil hydrophobicity limits efforts to manage for erosion and runoff after wildfire. We studied the spatial characteristics of soil hydrophobicity on two medium to high severity fires in the Colorado and Montana in 2002 and 2003. We also looked at the effects of soil moisture, soil texture, microtopography, and ash depth on spatial characteristics and strength of soil hydrophobicity. The Critical Surface Tension test was used to assess the presence and degree of soil hydrophobicity. Tests were applied in the field every 1m in $225^2$m grids and every 0.25m in $1m^2$ grids. Sampling interval and grid size was based on a pilot study in which soil hydrophobicity was tested in 20m transects every 0.5m and in 1m transects every 0.1m. Hydrophobicity tended to cover a greater area and be higher on medium severity plots, followed by high, low, and unburned plots. In most cases, soil hydrophobicity tended to be autocorrelated at a distance between 0.5 and 4 meters. Hydrophobicity was strongest at the surface and, in general, decreased with depth. Ash depth, soil texture, and microtopogrpahy were not correlated with soil hydrophobicity. Soil moisture appeared to be significantly correlated to soil hydrophobicity in some cases. Both burned and unburned plots contained 10-23 hydrophobic patches and the patches in burned plots were up to three times larger and closer together than in unburned plots. Plot M1 had 75% hydrophobic area, approximately twice as much as other burned plots, and was the only plot in which patches were laterally connected. This suggests that "Hortonian" overland flow generated by soil hydrophobicity may infiltrate near its point of origin unless a certain threshold of percent hydrophobic area is reached. The $1m^2$ plots were too small to capture the spatial characteristics of soil hydrophobicity. This may explain the variation in runoff measurements from small plots found by other researchers.

# TABLE OF CONTENTS

# TABLE OF FIGURES

# ACKNOWLEDGMENTS

# INTRODUCTION

Increased runoff and erosion from burned hillslopes is a common occurrence after wildfire (e.g. Helvey, 1980; Moody and Martin, 2001; Meyer and Wells, 1997; Meyer et al, 2001; DeBano, 2000; Johnsen et al., 2001), and can result in decreased soil productivity, risks to humans and their property due to increased flooding and debris flow, and adverse impacts to streams and wetlands. Millions of dollars are spent annually to decrease the impacts of wildfire on soil and water resources (Robichaud et. al., 2000). Understanding the factors contributing to increased runoff and erosion after wildfire is a critical part of effective post-fire management.

Fire-induced soil water repellency (hydrophobicity) is one of the key factors contributing to increased runoff and erosion after wildfires because it reduces infiltration and increases the potential for overland flow (DeBano, 1981; DeBano and Krammes, 1966;Hussain et al., 1969; Shakesby et. al., 2000; Letey, 2001). Soil water repellency is caused by naturally occurring hydrophobic compounds from the duff and leaf litter that are present in the soil prior to the fire (Letey, 2001; DeBano et al, 1970; DeBano, 1981; Savage, 1974; DeBano et al, 1976). During a fire these compounds vaporize, move down the soil temperature gradient, and condense on soil particles, forming a water-repellent layer (1981; DeBano et al.,1998; DeBano and Krammes, 1996; DeBano et al, 1976). Although many soils are naturally hydrophobic (DeBano, 1981; Doerr et al., 2000) fire generally increases the strength of the water repellency because it concentrates the hydrophobic compounds into a discrete layer near the soil surface (DeBano and Krammes, 1996; DeBano, 1981; Savage, 1994).

The strength of post-fire soil water repellency is determined by the fire severity, soil texture, antecedent soil-water content (DeBano et al., 1976; Robichaud and Hungerford, 2000; Wells et al, 1979; DeBano, 1998; Huffman et. Al., 2001), vegetation type (DeBano, 1981; Imeson et al., 1992; Doerr et al., 1998; Scott, 2000), soil moisture (Huffman et al., 2001; Robichaud and Hungerford, 2000), and time since burning (Huffman et al., 2005; DeBano, 2000). Soil water repellency generally increases up to a point with greater soil heating (Tiedeman et al., 1979; DeBano, 2000; DeBano et al, 1976). High fuel loads and dry soils increase the soil temperature during burning, resulting in higher severity fires and increased water repellency (Letey, 2001). Coarse grained soils tend to have greater water repellency than fine grained soils, possibly because they have a lower specific area and distillates more easily condense and fill pore spaces between them (Meeuwig,1971; DeBano 1981; DeByle, 1973). Vegetation type affects the degree of soil water repellency because plants contain different types and amounts of the resinous compounds that cause hydrophobicity (DeBano, 1981; Imeson et al., 1992; Doerr et al., 1998; Scott, 2000). The antecedent soil moisture has an indirect effect on soil water repellency because soil temperatures during a fire are generally not as high in wetter soils due to the heat capacity of water. If the soil is exposed to moisture after the fire it will eventually "wet-up", and become less hydrophobic. If the soil dries out again, however, soil hydrophobicity may return. The strength of fire induced soil hydrophobicity generally declines with time since burning, and usually returns to background levels within 1 to 2 years after the fire. However increased soil water repellency has been observed for up to 6 years after a fire (Dyrness, 1976)

Fire severity, soil texture (Gaston et al., 2001), soil moisture (Hawley et al., 1983; Ehrenfeld et al., 1997), and vegetation (Ehrenfeld et al., 1997) all tend to vary spatially. Since soil water repellency is a function of these factors, it is also likely to be spatially variable. Understanding the spatial characteristics of soil water repellency is important because of its potential effect on runoff and erosion. If soil water repellency is spatially continuous, then overland flow will be more effective in mobilizing and transporting soil particles. Conversely, if the water repellency is "patchy" then surface runoff from a water repellent patch of soil may infiltrate when it reaches a non-water repellent region, resulting in less continuous overland flow and reduced soil erosion (Shakesby et al., 2000).

Much of the existing information on the spatial characteristics of water repellency is based on inference from indirect observations. Several authors have noted a high degree of variability in soil water repellency between isolated point measurements (MacDonald and Huffman, 2004; Robichaud, 2000; Dekker, 2001). Runoff rates from $1 m^2$ plots on burned hillslopes in Portugal were more variable than those from adjacent $16 m^2$ plots (Shakesby et al., 2000). The authors attributed this to the fact that the small plots were able to fit on or between hydrophobic patches while the larger plots spanned them. These and other studies strongly suggest that water repellency after wildfire is spatially variable, but there is almost a complete lack of studies that have systematically measured the spatial characteristics of soil water repellency at scales relevant to hillslope runoff and erosion.

The current lack of information on the spatial variability of fire-induced soil water repellency in burned regions limits scientist's ability to predict fire effects on runoff and

erosion. Such data are needed so that models to predict post-fire hillslope scale erosion and runoff can be developed, so that prescribed burns can be applied in ways that limit erosion and runoff, and so that foresters can manage burned areas for decreased erosion and runoff. This study addresses some of these research needs by examining the spatial characteristics of soil hydrophobicity following two mid-elevation wildfires in Montana lodgepole pine (*Pinus contorta*) and Colorado ponderosa (*Pinus ponderosa*) and Douglas-fir (*Pseudotsuga menziesii*) ecosystems. The study objectives were to determine: 1) to what extent is soil water repellency spatially variable; and 2) to what extent is the spatial variability of soil water repellency dependent on site factors such as soil moisture, ash depth, and soil texture.

# STUDY SITES

Fieldwork was conducted in areas burned during the 2001 Moose Fire in northern Montana and the 2002 Hayman Fire in central Colorado (Figure 1). The Moose Fire was selected because it was the largest mixed severity fire in Montana in 2001, the year preceding the beginning of the study. The Hayman Fire was selected because it was the largest mixed severity fire in the Rocky Mountain region in 2002, the year preceding the second year of data collection.



Figure 1. Location of the Moose and Hayman fires in Montana and Colorado.

## Moose Fire

The Moose Fire, located approximately 16 km north of Columbia Falls in northern Montana (Figure 2), was started on August 14th 2001 by a lightning strike (USDA, 2002). The fire was mostly contained by October 2nd 2001 having burned 28000 ha. Of this burned area, 14300 ha were in the Flathead National Forest, 10782 ha were in

Glacier National Park, 2742 ha were in Coal Creek State Forest, and 381 ha were on private land.

The area burned in the Moose fire ranges in elevation from 990 m to 2045 m. The dominant tree species prior to the fire were lodgepole pine (*Pinus contorta*), subalpine fir (*Abies lasiocarpa*), Englemann spruce (*Picea engelmannii*), ponderosa pine (*Pinus ponderosa*), whitebark pine (*Pinus albicaulis*), western larch (*Larix occidentalis*), and Douglas fir (*Pseudotsuga menziesii*) (USDA 2002). Understory species included beargrass (*Xerophyllum tenax*) and huckleberry (various *Vaccinium* species). Annual precipitation increases with elevation in the burned area, ranging from 71 cm to 157 cm per year (USDA, 2001 and 2003). At higher elevations approximately 60% of the precipitation falls as snow. The area is underlain by Precambian meta-sedimentary argillites, siltites, quartzites and limestones, with glacial till, glacial outwash, and glacial lacustrine deposits in the valley bottoms (USDA 2001; soil survey, 1999). Soils in the area have a volcanic ash influence surface layer, a silt loam texture, and contain 5 to 15% coarse fragments (USDA 2001 and 2003; Soil survey, 1999).

## Moose Fire Site Locations



1. Control — Transects 1,2,3. - Grid MC
2. Control — Transects 4,5,6.
3. Low Severity — Transects 1,2,3.
4. Low Severity — Transects 4,5,6.
5. Medium severity — Transects 1,2,3. - Grid M1, M2.
6. Medium Severity — Transects 4,5,6.
7. High severity — Tansects 1,2,3.
8. High Severity — Transects 4,5,6. - Grid M3.

Site Locations
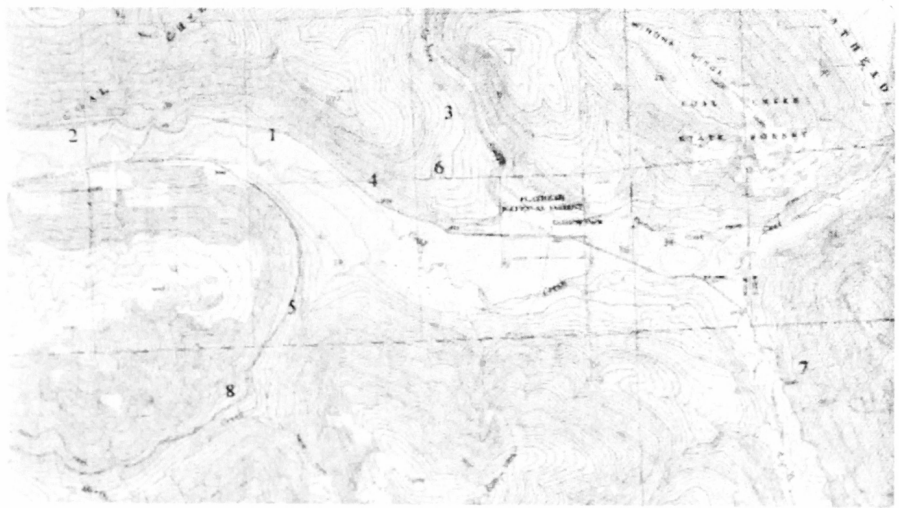


Figure 2. Location of the Moose Fire in Northern Montana, and location of field sites within the fire perimeter.

**Hayman Fire**

The Hayman Fire (Figure 3), located 48 km southwest of Denver, Colorado, started under severe to extreme drought conditions on June 8$^{th}$ , 2002 (USDA, 2002; Robichaud et al. 2003). The fire was mostly contained by early July, having burned 55200 ha. Approximately 72% of the fire was on national forest land, with the remainder mostly on private land. The Hayman Fire exhibited a mixed fire regime with 32% burned at high severity, 20% at moderate severity, 31% at low severity, and 17% unburned (USDA, 2002; Robichaud et al. 2003). The burned area ranges in elevation from 1981 m to 2743 m. Prior to the fire the dominant tree species were ponderosa pine on south and west facing slopes, and Douglas-fir on north facing slopes, with small amounts of blue spruce and aspen . Soils in the area are formed mostly from the underlying granite of the Pike Peak batholith and are within the Sphinx, Sphinx/rock outcrop, and Legault soil series (Robichaud et al. 2003).

Hayman Fire Site Locations

1. Medium severity        - Grid H1
2. Low medium severity  - Grid H2
3. High medium severity - Grid H3
4. Control                    - Grid HC

Denver

Hayman Fire

Colorado Springs
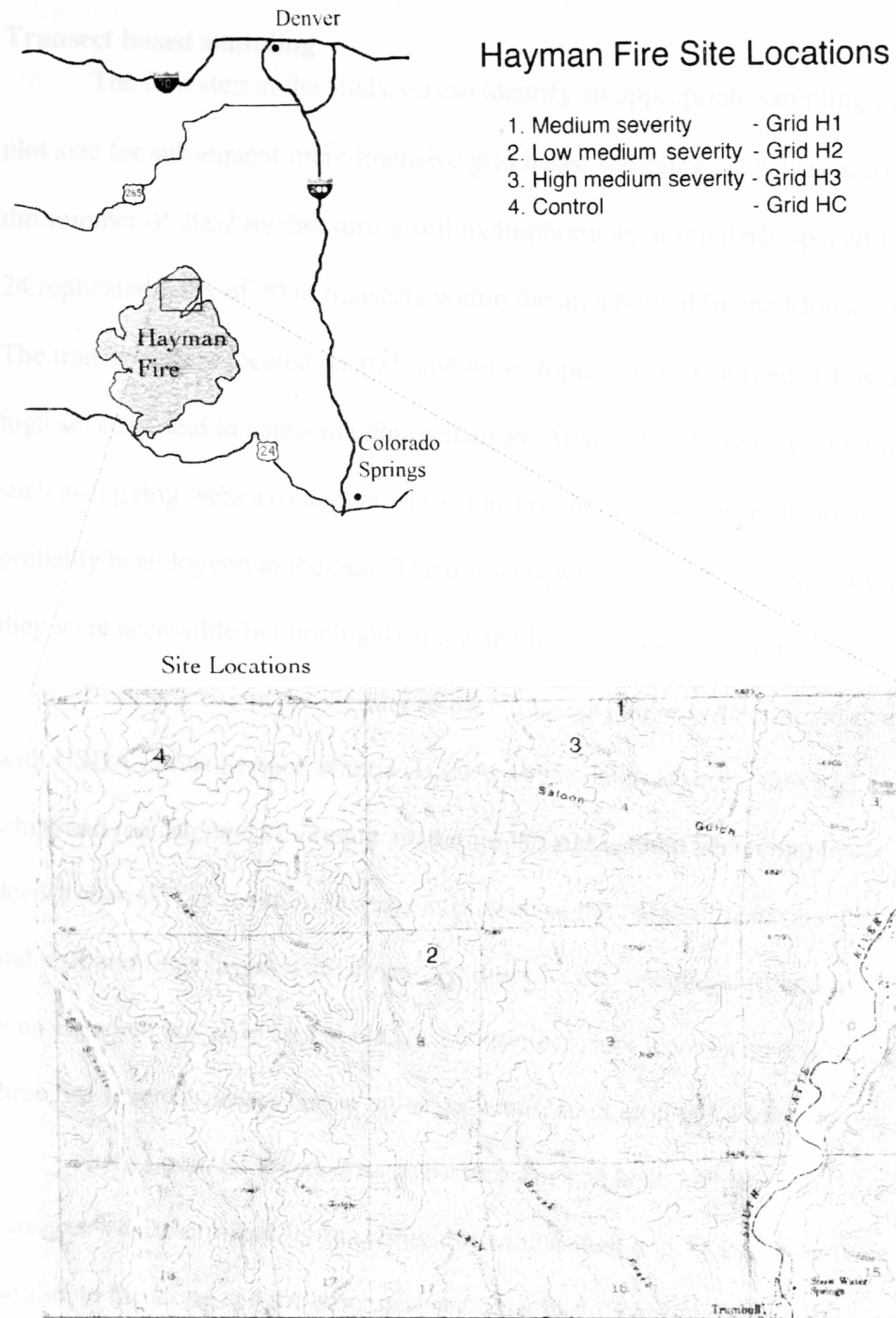
Site Locations

Figure 3. Location of the Hayman Fire in southwestern Colorado, and of the field site locations within the fire perimeter.

# METHODS

## Transect based sampling

The first step in the study was to identify an appropriate sampling interval and plot size for subsequent more intensive grid based sampling. This was accomplished in the summer of 2002 by measuring soil hydrophobicity at regularly spaced intervals along 24 replicated pairs of 20 m transects within the area burned by the Moose Fire (Figure 4). The transects were located on 10% and 40% slopes, in areas burned at low, moderate and high severity, and in adjacent unburned areas. Areas with obvious recent human impacts such as logging were avoided, however most of the transects were in areas that had probably been logged in the past. The transects were within 20 to 500 m of a road so that they were accessible but not highly impacted by road associated activities.

Burn severity in the vicinity of each transect pair was determined in accordance with USDA Forest Service criteria (USDA, 1995). High severity sites had either black or white and red ash, and all organic matter on the surface had been completely burned or deeply charred. On medium severity sites most of the organic matter had been consumed and duff and litter layers were absent. At low severity sites the duff and litter layers had been scorched but were largely intact. Six transect pairs were located within each of the three fire severity classes and in unburned areas, for a total of 24 transect pairs.

Once a general location for a transect pair had been identified the center of the transects was determined by randomly throwing a steel peg. One transect was aligned parallel to the slope and the other perpendicular to it. Hydrophobicity was measured every 0.5 m along each 20 m transect, and also at 0.1 m intervals along a randomly selected 1 m section within each transect (Figure 4).

The soil water repellency at each location was measured using the Critical Surface

Tension (CST) test (Letey, 1969). Fifteen ethyl alcohol solutions with molarities ranging

from zero (de-ionized water) to 5.6 M ethyl alcohol were used for the tests. Five drops of

each solution, starting with the lowest molarity, were dropped onto bare mineral soil after

the ash and duff layer had been scraped away. Soils at each location were classified as

hydrophilic, or slightly, moderately, strongly or very strongly hydrophobic depending on

the surface tension of the highest molarity solution for which all drops infiltrated the soil

within 5 seconds (Table 1) (Watson and Letey, 1970). Surface tension values ranged

from 71.3 dynes cm$^{-1}$ for de-ionized water to 36.5 dynes cm$^{-1}$ for the 5.6 M solution, so

that lower surface tension values indicate higher hydrophobicity.
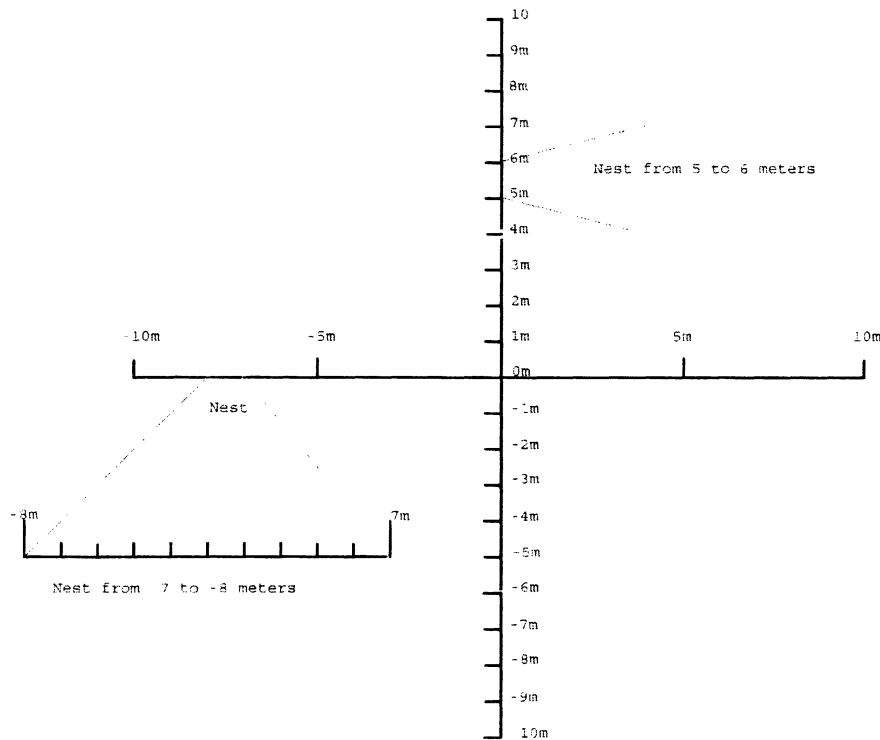


Figure 4. Sampling design for transect locations at the Moose Fire in 2002.

Soil volumetric water content in the 0 to 12 cm depth interval was measured at

each end of the transect and in the middle of the transect using a Hydrosense soil

moisture meter (Campbell Scientific Inc, Logan, Utah). Soil samples from the same three

locations and depth interval were analyzed for soil texture (Gee and Bauder, 1986).

Slope, aspect and air temperature at the time of sampling were also measured and

recorded.

Table 1. Classification of soil hydrophobicity based on surface tension of ethyl alcohol
solutions.

| Molarity of solution | Surface tension at $20^{\circ}C$ (dynes $cm^{-1}$) | Soil Hydrophobicity Class |
|---|---|---|
| 0 | 72.3 | Hydrophilic |
| 0.4, 0.8, 1.2, 1.6 | 50.1 – 65 | Slightly hydrophobic |
| 2, 2.4, 2.8 | 43.4 – 50.1 | Moderately hydrophobic |
| 3.2, 3.6, 4, 4.4 | 36.5 – 43.4 | Strongly hydrophobic |
| 4.8, 5.2, 5.6, 6 | < 36.5 | Very strongly hydrophobic |

**Data Analysis for transect based measurements**

The transect based soil hydrophobicity data were analyzed using the S-Plus

statistical analysis software (Insightful corporation, version 6.0, 1999-2005). Variograms

were created for each plot to determine at what distance soil hydrophobicity was

correlated. The minimum and maximum correlation distance was determined for the

entire data set. Directional variograms were created for the two directions of the

transects. The maximum separation distance for these variograms was eight. This is the

greatest distance at which points are tested to see if they are spatially related. This

distance was chosen because it is half the total distance available to measure, and beyond this point accuracy decreases due to having fewer pairs of points at these distances.

**Grid based sampling**

Spatially intensive grid based sampling was conducted on the Moose and Hayman fires in the summer of 2003. Hydrophobicity was measured within eight grids, four each on the Moose and Hayman fires. Three of the grids at each site were located in areas that had burned at medium to high severity to maximize the possibility of detecting hydrophobicity. The fourth grid was a control, and it was located in the closest comparable unburned area. Grid size and sampling intervals were based on the information obtained from the transect based sampling. Each grid was 15 m x 15 m and the hydrophobicity was measured at 1 m intervals using the CST test previously described. One 1 m x 1 m grid square was randomly selected within each grid and the hydrophobicity in this grid square was measured at 0.25 m intervals. Sampling at 1 m intervals in the 15 m x 15 m grid and at 0.25 m intervals within one 1 m x 1 m grid resulted in a total of 256 measurements per site. The variability of hydrophobicity with depth was measured at every fifth measurement location until the soil was no longer hydrophobic. If the surface of the mineral layer was not hydrophobic, depth measurements were not taken.

At each grid, the slope, aspect, air temperature, soil moisture, soil texture, microtopography, duff depth, and ash depth were measured at and recorded. Soil volumetric water content was measured using a Hydrosense soil moisture meter (Campbell Scientific Inc.). Soil moisture was measured at every point where

hydrophobicity was measured on the Moose Fire and at every fifth measurement location on the Hayman Fire. Volumetric water content was measured at fewer points at the Hayman Fire because of a shortage of spare parts and limited time. Ten soil samples were collected from each grid and analyzed for soil texture following the same methods used in transect-based sampling. Microtopography was assessed at every point where the soil hydrophobicity was measured. If at least three out of four sides of a site sloped either up or down then the site was classified as being either on a hump or a dip, respectively. Sites that were on neither a hump nor a dip were classified as flat. Duff thickness was recorded when present. If the duff appeared to have been redeposited from upslope then it was not included in the duff thickness estimate because it was assumed that it was not present during the fire. Ash thickness was recorded at every point where hydrophobicity was measured on the Moose Fire and at every fifth point on the Hayman Fire. Ash thickness was measured less frequently on the Hayman Fire because it varied less and because of a shortage of time.

**Data analysis for grid based measurements**

Spatial autocorrelation of the grid based soil hydrophobicity measurements was assessed by developing contour maps of hydrophobicity by developing semi-variograms of the grid based hydrophobicity and by calculating Moran's I statistic.

The contour maps were developed using a kriging routine in the Surfer software program (Golden Software Inc.), in which all default settings were used. The linear variogram model appeared to be most appropriate and is displayed in the text, however exponential and spherical models were analyzed as well. Variogram analysis in the grid-

based study was conducted as in the transect-based study (see page 11), however,

multidirectional variograms were also considered in the grid-based analysis.

1

$$\hat{\gamma} = (h) \frac{1}{2N(h)} \sum_{(i,j)|h_{ij}=h} (z_i - z_j)^2$$

Where h = the distance between pairs and N(h) = the number of pairs h untis

apart.

Moran's I statistic is based on the sample correlogram and is similar to the

Pearson's correlation coefficient, with values ranging from –1 to 1. Clustering leads to

positive values while negative autocorrelation leads to negative values. The permutation

test for Moran's I was calculated using 1000 permutation simulations of random

permutations of soil hydrophobicity to establish the rank of the observed statistic in

relation to the 1000 simulation values. In this study $x_i$ and $x_j$ are the variables of interest

in regions i and j and $W_{ij}$ is a measure of connectivity between all $(i,j)$ pairs of region. We

used a $2^{nd}$ order connectivity matrix in which $i$ is considered to be a neighbor of region $j$

if they share a common boundary or if they are diagonal to each other and < 1.4 m away.

2

$$I = \frac{n}{S_0} \frac{\sum_i \sum_j W_{ij}(V_i - \overline{V})(V_j - \overline{V})}{\sum (V_i - \overline{V})}$$

Where n = the sample size, $W_{ij}$ = 1 if sites $i,j$ are neighbors and 0 if sites $i, j$ are not neighbors, $S_0$ = twice the number of neighbors, and $V_i$ = the continuous response at site $i$.

Analysis of the patch characteristics in each grid and the spatial relationships between patches was conducted using the Fragstats spatial analysis software program (McGarigal et al., 2002). The calculated metrics included the number of hydrophobic patches, the mean size of the patches, the mean distance between patches, and the connectivity between patches within the grid. The distance between patches was defined in terms of the mean of the Euclidean Nearest-Neighbor Distance (ENN$_{av}$) where:

3

$$ENN_{av} = \frac{1}{N} \sum_{i=1}^{N} h_i$$

$h_i$ = the distance (meters) from hydrophobic patch $i$ to the nearest neighboring hydrophobic patch, based on the patch edge to edge distance, computed from cell center to cell center, and N = the number of hydrophobic patches. The Euclidean Nearest Neighbor metric has been extensively used as a measure of patch isolation, and as such it provides a useful metric of the potential effectiveness of patchy hydrophobicity in generating contiguous overland flow.

The connectivity among all patches in the grid was defined in terms of the connectance index (CI):

$$CI = \left[ \frac{\sum_{j=k}^{n} c_{jk}}{\frac{n(n-1)}{2}} \right] .100$$

where $c_{jk} = 1$ if two patches j and k are functionally joined and $c_{jk} = 0$ if they are not, n = the total number of possible joinings between patches (McGarigal et al., 2002). A functional joining is defined as one in which two adjacent patches lie within a specified threshold distance of each other, where the threshold distance is defined on the basis of the ecological or hydrologic process under consideration. In the present study a functional joining is one where surface runoff from one patch will be transmitted to the next adjacent patch rather than infiltrating the soil. We defined a threshold distance of 0.5 m, which was the minimum value that could be used given the resolution of our data.

The effects of soil water content, ash depth and soil texture on the spatial distribution of soil hydrophobicity were assessed using a Partial Mantel's test. On the Moose Fire volumetric water content and ash depth were also analyzed together as a factor that might explain spatial variability of soil hydrophobicity. On the Hayman fire this was not possible due to up to 50% missing values for soil moisture content. The Mantel's test is a regression in which the variables are distance or dissimilarity matrices. They summarize pairwise similarities among sample locations. The predictor variable is space, measured as a geographic location. The Mantel's test overcomes two problems associated with traditional methods of analysis. First, because the environmental factors are intercorrelated with each other it is difficult to assess the influence of one variable if a

third is also influencing both. Second, because soil hydrophobicity is autocorrelated, we must distinguish between correlations that are due to overlapping spatial patterns and correlations that are not affected by spatial proximity. Mantel's test of significance is evaluated via a permutation procedure because the elements of a distance matrix are not independent. The permutation procedure uses randomly re-arranged rows and or columns from the distances matrices. The Mantel test (p-values) was calculated using 10000 permutations. In this study $x_i$ and $x_j$ are the variables of interest in regions $i$ and $j$ and $W_{ij}$ is a measure of connectivity between all pairs of region $(i,j)$. For example, $x_i$ and $x_j$ might be soil hydrophobicity and volumetric water content in this study.

5

$$r = \frac{1}{(n-1)} \sum_{i=1}^{m} \sum_{j=1}^{m} \frac{(x_{ij} - \overline{x})}{s_x} - \frac{(y_{ij} - \overline{y})}{s_y}$$

Where m = the number of locations, n = the number of differences, $x$ and $y$ are variables measured at locations $i$ and $j$, and $s_x$ and $s_y$ are standard deviations for variables x and y.

# RESULTS

## Transect based sampling

All of the transects, including those in unburned plots, contained sampling points that were at least slightly hydrophobic. Hydrophobicity occurred as discrete "patches", indicated by two or more adjacent points that were hydrophobic, separated by areas of hydrophilic soil (Figure 5 and Appendix B). The percentage of points along a transect that were hydrophobic generally increased with fire severity ($p =< 0.05$), and ranged from a mean of 23% in the control transects to 69% in the medium severity transects (Table 2), although medium and high severity transects were not significantly different. More of the hydrophobic points in medium severity transects were classified as strongly hydrophobic than in the control, low severity or high severity transects. The size and number of hydrophobic patches per transect generally increased with fire severity. Medium severity transects had significantly larger patches than low severity transects and burned transects had significantly larger patches than control transects ($p =< 0.05$).

Table 2. Mean percentage of points that were hydrophobic by hydrophobicity strength, mean number of patches per transect and mean number of points per patch for transect measurements conducted in unburned control, low, medium and high severity fire sites at the Moose Fire.

|  | Fire Severity | | | |
|---|---|---|---|---|
|  | Unburned | Low | Medium | High |
| Average number of patches per transect | 13 | 16 | 16 | 19 |
| Average number of points per patch | 2 | 2 | 4 | 3 |
| Total Percent Hydrophobic | 23 | 39 | 69 | 59 |
| Percent Hydrophilic | N/A | N/A | N/A | N/A |
| Percent Slightly hydrophobic | 88 | 80 | 52 | 67 |

| | | | | |
|---|---|---|---|---|
| Percent Moderately hydrophobic | 7 | 10 | 25 | 25 |
| Percent Strongly hydrophobic | 4 | 10 | 21 | 8 |
| Percent Very strongly hydrophobic | 1 | 1 | 3 | 0 |

Thirteen of sixteen directional semi-variograms constructed using the transect

data indicated that hydrophobicity was autocorrelated. The strength and geographical

distance at which soil hydrophobicity was correlated did not vary with fire severity. The

distance at which soil hydrophobicity was autocorrelated ranged from <0.25 m to 4 m
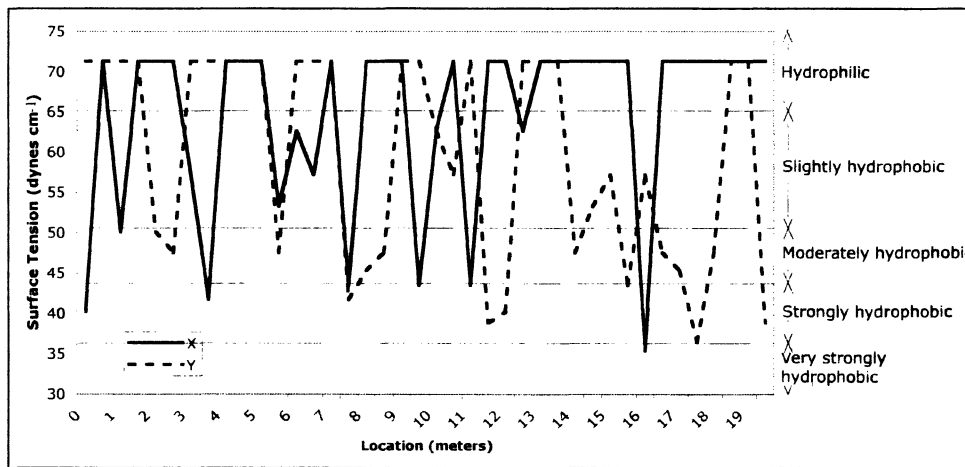
(Figure 6 and Appendix D).



Figure 5. Hydrophobicity values along distance in low severity transect L3. X represents the transect that is perpendicular to slope and Y represents the transect that is parallel to slope (see Appendix C for the rest of the transect profiles).

gamma

60

50

40

30

20

10

0

objective = 102.9818

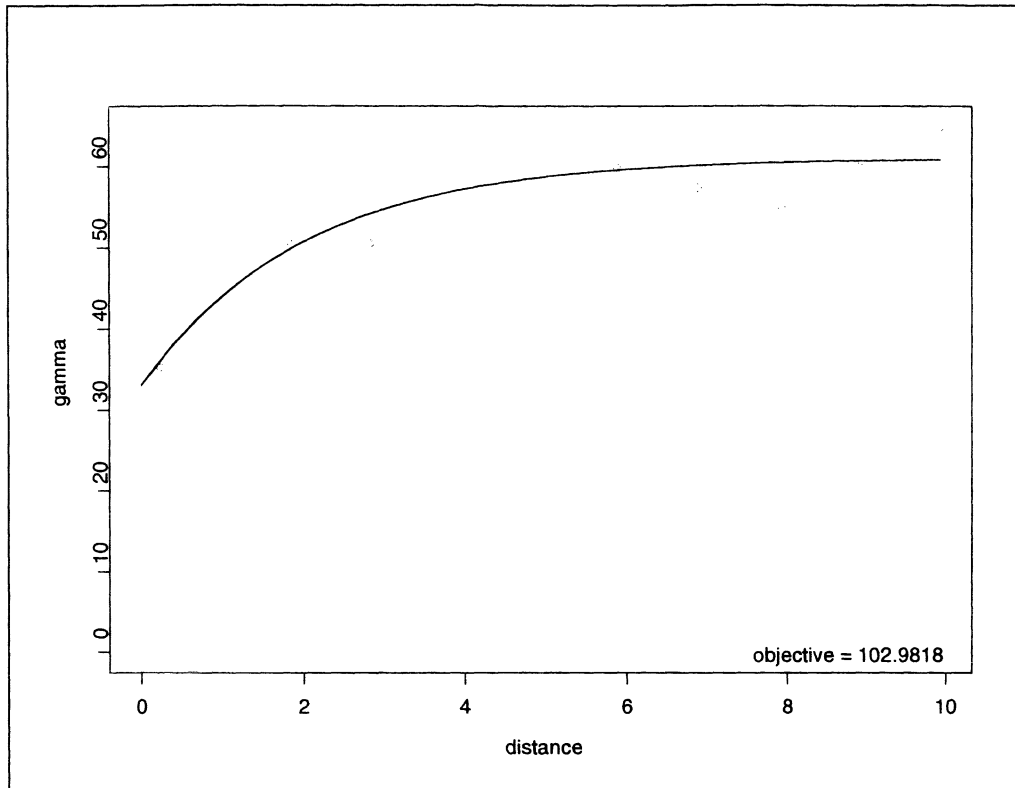0          2          4          6          8          10

distance

Figure 6. This is an example of a typical Directional semi-variogram of soil hydrophobicity based on the six high severity transects oriented perpendicular to the slope. In this example, the range is 2.4 m, the sill is 30 (dynes cm$^{-1}$)$^2$ and the nugget is 33. On high severity transects soil hydrophobicity was autocorrelated over an average distance of 2.4 m.

Volumetric water content was correlated with transect based hydrophobicity measurements (p = 0.019, r = - 0.38) when data from all transects were combined. However, when looked at independently, there was no evident correlation by plot or fire-severity (Figure 7). It appears that soil water content increases with increased soil hydrophobicity. This positive correlation may be due to sampling technique or other factors not accounted for, such as a decreased evaporation rate. The hydrosense probe measures the percentage of water in the soil between the surface and a depth of 12 cm. It would be more appropriate to measure water content at the surface where hydrophobicity is measured. Volumetric water content may not be the best measure of soil water when

correlating it with soil hydrophobicity. Another potential reason for these unexpected

results is that the hydrophobic layer at the surface inhibits evaporation, as found by
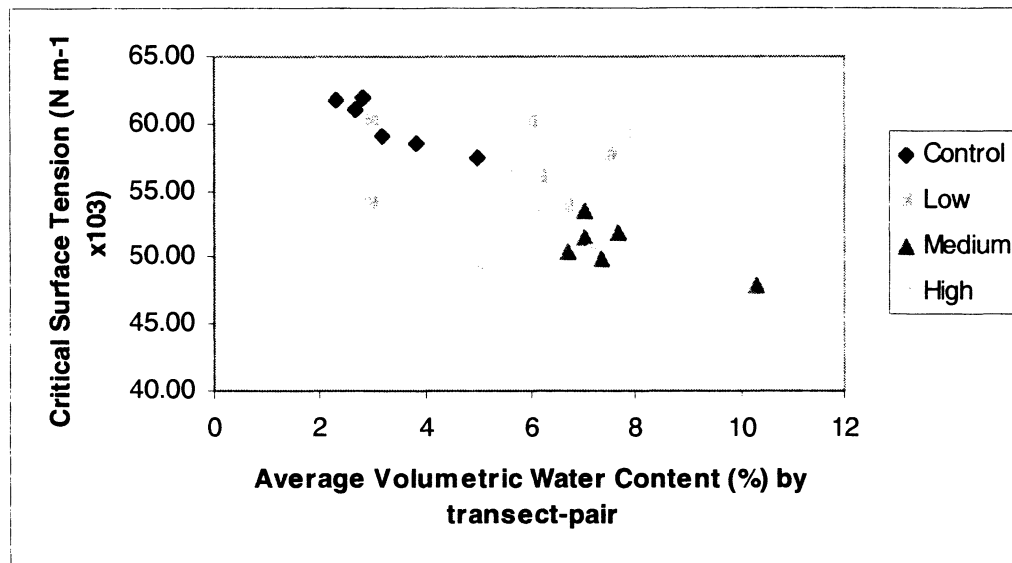
Bachmann et. al, 2001.



Figure 7. Critical surface tension appears to be negatively correlated with average
volumetric water content (p = 0.019, r = - 0.38).

## Areal Variability of Soil Hydrophobicity

A 1 m sampling interval was chosen for the grid-based sampling of soil

hydrophobicity based on the distances over which hydrophobicity was correlated in the

transect-based measurements. Sampling at a 0.25 m spacing within one 1 m x 1 m grid in

each larger grid provided more detailed information regarding the continuity of soil

hydrophobicity inside and outside of hydrophobic patches, and ensured that the distance

at which soil hydrophobicity was spatially autocorrelated would be captured even if this

distance decreased below levels previously seen during transect based sampling. Site

characteristics were measured at each grid (Appendix E)


*Large grid plots*

All of the large (225 m$^2$) plots at both study sites, including the unburned controls,

had areas that were hydrophobic at the surface (CST values < 65 dynes cm$^{-1}$). Moran's I

statistic indicated that in five of the eight grid plots (M1, MC, H1, H2 and H3),

hydrophobicity was significantly possitively autocorrelated (p < 0.05). In other words, if

a point was hydrophobic, then an adjacent point was also likely to be hydrophobic (Table

3). And conversely, if a point was hydrophilic and adjacent point was also likely to be

hydrophilic.

Table 3. Results of Moran's I nearest neighbor similarity test to assess the spatial autocorrelation of soil hydrophobicity. A neighbor was defined as either being next to (1 m away) or diagonally adjacent to ($\approx 1.4$ m away) from the original point.

| Site | Permutation p-value | Correlation (r) |
|---|---|---|
| M1 – Moose Fire medium-severity | 0.02 | 0.06 |
| M2 – Moose Fire medium-severity | 0.26 | 0.02 |
| M3 – Moose Fire medium-severity | 0.06 | 0.05 |
| MC – Moose Fire control (unburned) | 0.01 | 0.08 |
| H1 – Hayman Fire medium-severity | <0.005 | 0.10 |
| H2 – Hayman Fire low-medium-severity | <0.005 | 0.23 |
| H3 – Hayman Fire high-medium-severity | <0.005 | 0.17 |
| HC – Hayman Fire control (unburned | 0.22 | 0.02 |

All but one of the large plots contained between 10 and 23 patches. The exception was plot M1, which contained just two patches (Table 4). While the number of patches was similar in burned and unburned plots, the patches were up to 3 times larger in the burned plots. Mean patch size in all of the burned plots except M1 ranged from 2.0 to 5.7 $m^2$, compared to 1.8 and 2.4 $m^2$ in the two control plots. Plot M1 had a mean patch size of 86.5 $m^2$. In all of the grids, some patches extended beyond the grid boundary, so the estimates of patch size are likely an underestimate of the true mean patch size. This is especially the case for plots with larger patches, such as grid M1. In addition to being larger, the hydrophobic patches in the burned areas were also closer together than in the control plots. The $ENN_{av}$ (Euclidian Nearest neighbor distance) for the six large burned plots ranged from 0.45 m to 1.2 m, compared to 1.51 and 1.60 m in the control plots.

The larger mean patch size and smaller distances between patches meant that a greater area of the burned plots was hydrophobic compared to the control plots (Figures 7 and 8). In five of the six burned plots, from 19% to 38% of the plot was hydrophobic, compared to just 11% in the two control plots. In the sixth burned plot, M1, the proportion of the area that was hydrophobic was much greater, at 76%. The burned plots were also more strongly hydrophobic than the control plots. All of the hydrophobicity in the control plots was classified as either slight or moderate, whereas up to 3% of burned plots H1, H2 and M3 were strongly hydrophobic, and 11% of plot M1 was either strongly or very strongly hydrophobic (Figure 9).

The connectivity index (CI), which is a measure of the potential for contiguous overland flow generation, was very low in all but one of the large plots. In both control plots the CI was zero, and in five of the six burned plots the CI ranged from 0.4 to 1.7,

indicating a very low potential for runoff generation. The exception was plot M1 which

had a CI of 100, indicating that the two large patches in this plot were spatially joined.

Overall, the results from the large grids indicate that there is a low potential for surface

runoff generation due to reduced infiltration on hydrophobic areas of soil.

Table 4. Patch characteristics for large and small plots in the Moose and Hayman fire study sites.

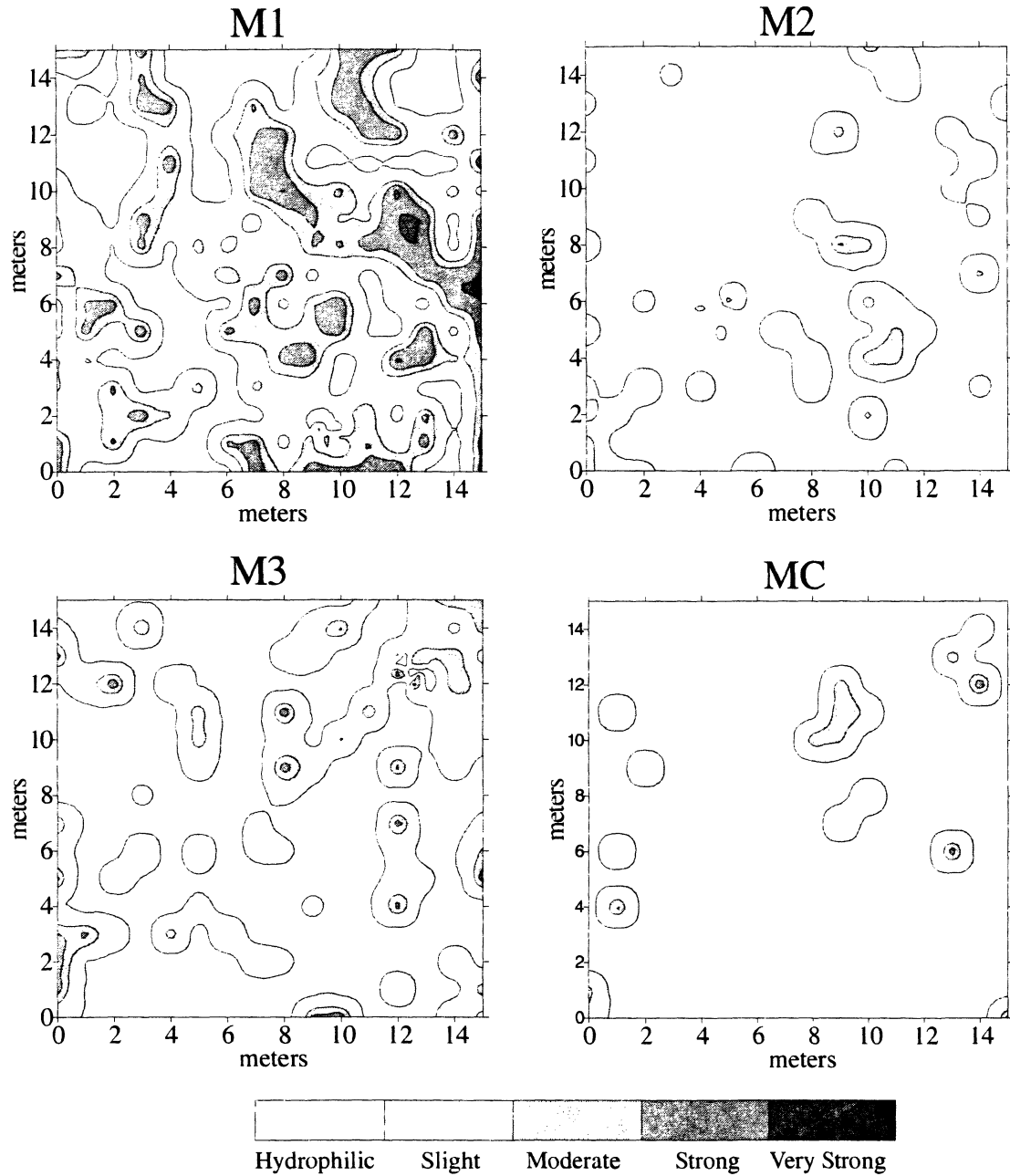| Plot | No. of patches | Mean patch size ($m^2$) | $ENN_{av}$ (m) | CI |
|------|------|------|------|------|
| H1 | 15 | 5.1 | 0.87 | 1.9 |
| H2 | 16 | 4.6 | 0.89 | 1.7 |
| H3 | 13 | 5.7 | 0.88 | 1.3 |
| HC | 15 | 1.8 | 1.51 | 0 |
| M1 | 2 | 86.5 | 0.45 | 100 |
| M2 | 23 | 2.0 | 1.20 | 0.4 |
| M3 | 18 | 4.7 | 0.82 | 1.3 |
| MC | 10 | 2.4 | 1.60 | 0 |
| H1 | 1 | 0.94 | - | 0 |
| H2 | 2 | 0.33 | 0.14 | 100 |
| H3 | 1 | 0.46 | - | 0 |
| HC | 0 | - | - | - |
| M1 | 2 | 0.38 | 0.30 | 0 |
| M2 | 3 | 0.85 | 0.68 | 0 |
| M3 | 2 | 0.40 | 0.15 | 100 |
| MC | 0 | - | - | - |

Figure 8. Contour plots of soil hydrophobicity in plots M1, M2, M3 and MC in the Moose Fire study site. Each grid is 15 m x 15 m (225 m2).
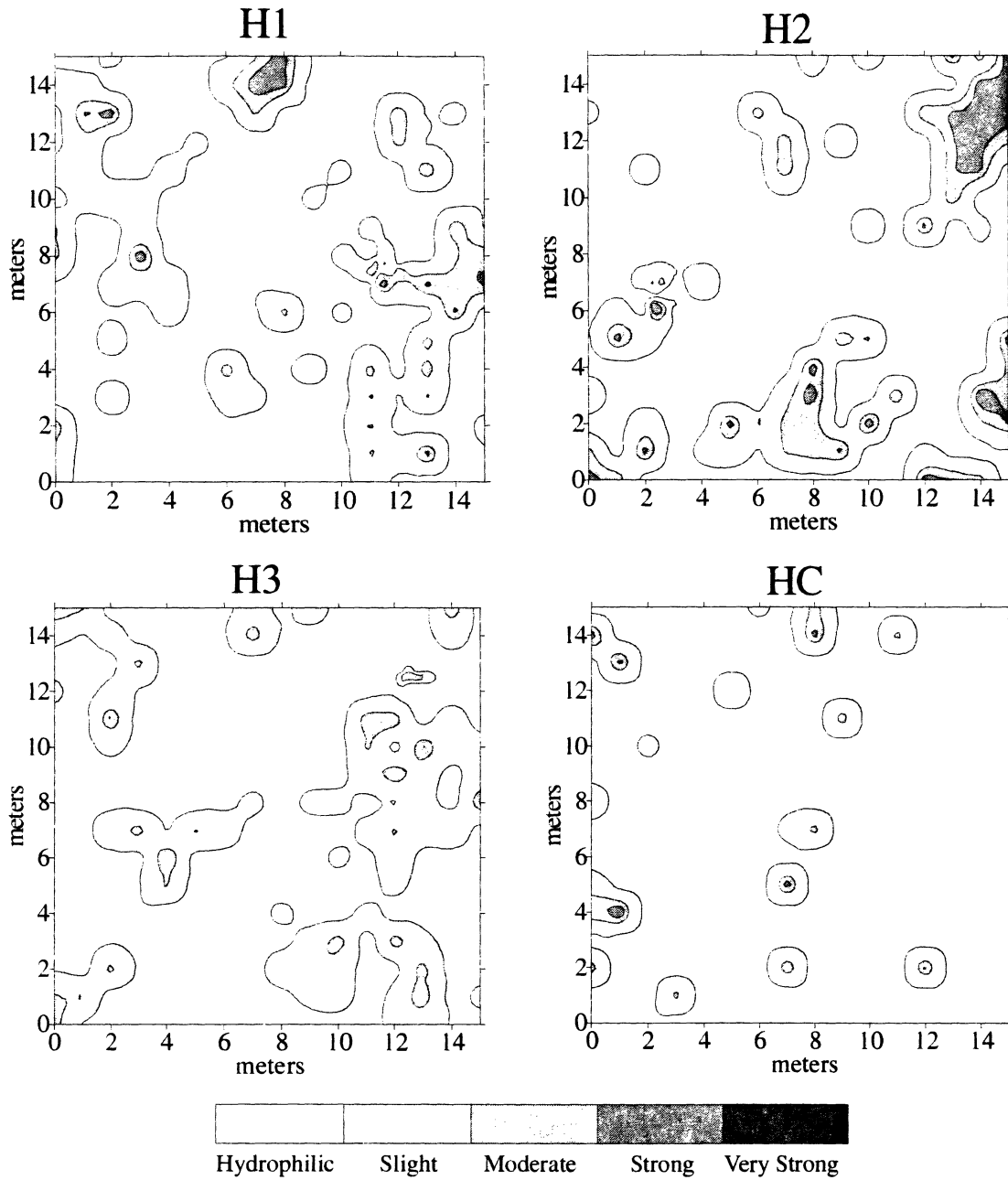
Figure 9. Contour plots of soil hydrophobicity in large plots H1, H2, H3 and HC at the Hayman Fire site. Each grid is 15 m x 15 m (225 m2).
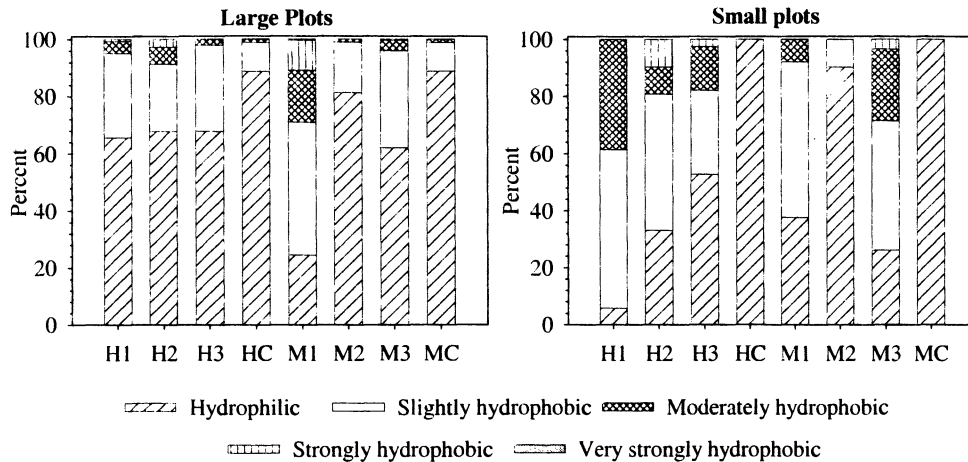
Figure 10. Percentage of sites that were hydrophilic, slightly, moderately, strongly and very strongly hydrophobic in large and small grid plots at the Moose and Hayman fire sites.

*Small grid plots*

Since the $1m^2$ plots were smaller than most of the patches, the proportion of the small plot area that was hydrophobic largely depended on whether a plot overlapped one or more hydrophobic patches. Both of the small control plots were completely hydrophilic because they fell outside the boundaries of a patch whereas all six of the burned plots were partially hydrophobic because they overlapped portions of up to three hydrophobic patches (Figure 10). The proportion of the small burned plots that was hydrophobic was more variable than in the large plots, ranging from 10% in M2 to 94% in H1. Most of the hydrophobicity was classified as slight to moderate, but 0.2 to 10% of plots H2, H3, M1 and M3 were strongly hydrophobic (Figure 9).

Since the $1m^2$ plots were smaller than most of the hydrophobic patches, they did not capture the spatial characteristics of soil hydrophobicity. The calculated mean patch sizes, which range from 0.33 $m^2$ in H2 to 0.94 $m^2$ in H1 are an underestimate of the true patch size because part of almost every patch lies outside the plot. The distance between patches, based on the $ENN_{av}$, is also an underestimate of the true value because only

29

patches that are < 1 m apart lie within the same plot. Since the small plots include a maximum of three patches, the connectivity index (CI) values do not represent the overall connectivity between patches.
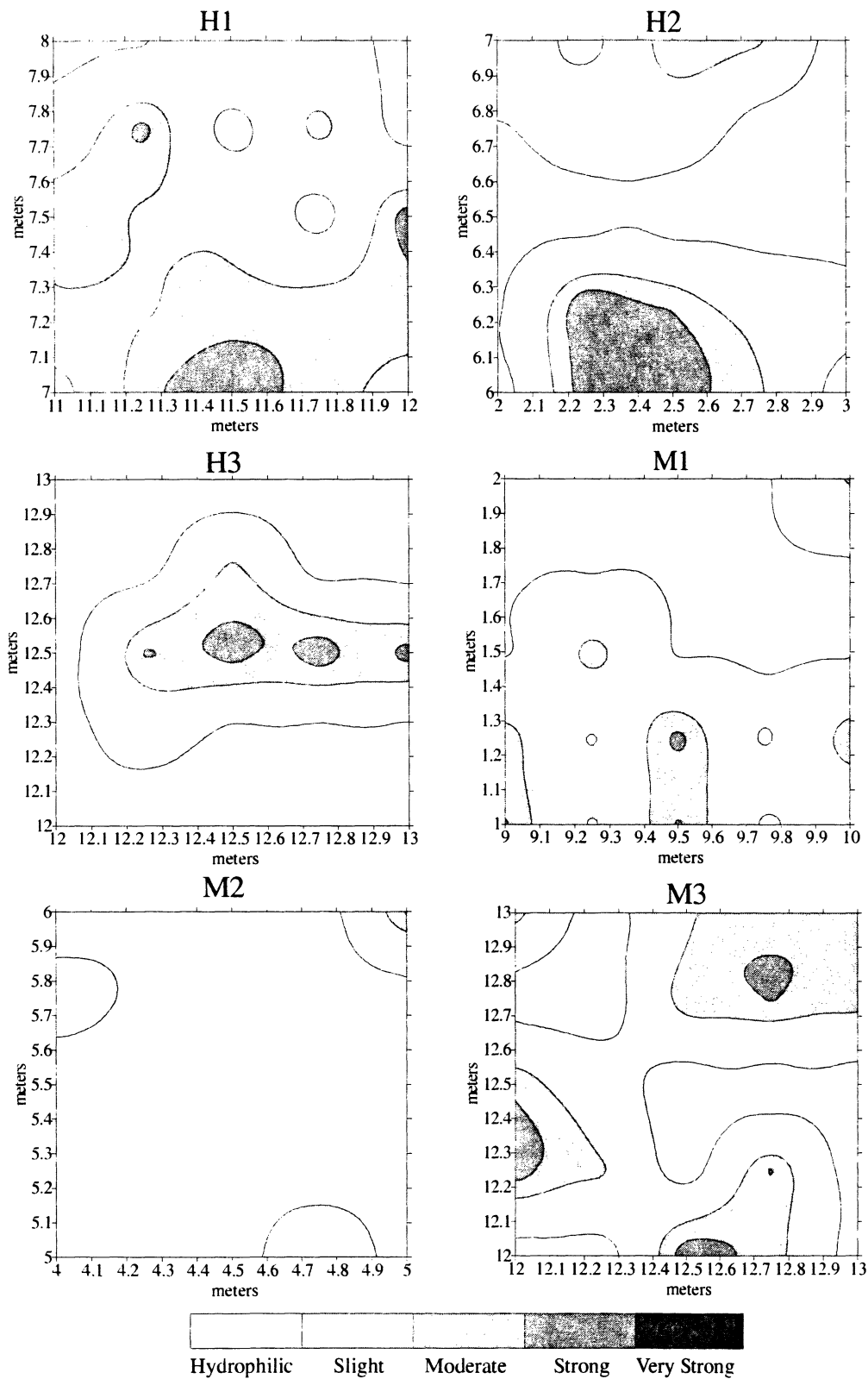
Figure 11. Contour plots of soil hydrophobicity in the small (1 m x 1 m) grids at sites M1, M2, M3, H1, H2 and H3. Neither of the control plots (MC and HC) contained any hydrophobicity.

*Isotropy of soil hydrophobicity*

Only four sampling grids (M1, M2, MC and HC) provided clear semi-variogram structures, and the results of these analyses indicate that hydrophobicity is generally isotropic. The data met both weak and intrinsic stationarity assumptions when analyzed using moving windows statistics to assess the homogeneity of the mean and variance in soil hydrophobicity. Soil hydrophobicity in grids M1, M2, MC, and HC showed evidence of spatial autocorrelation at distances of 1 to 3 meters (Figure 11 and Appendix F). The variograms from the other grids did not exhibit spatial autocorrelation of soil hydrophobicity. Several variograms had an initial point that was much higher than the rest of the points in the variogram (Appendix F). This is likely due to the fact that this point was based off of the small grid data, which was composed of only 24 pairs. It is possible that this first point is erratic because either there is not enough pairs to make a good assessment of its value or because there is greater variation in small grids at a finer scale. Several of the variograms with a clear spherical or exponential structure only exhibited that structure because of the value of the first point. Because the variogram results are so different from those of the Moran's I statistic, and because the value of the first point in the variograms is in question, it may be best to consider the results of Moran's I rather than the variograms when assessing the spatial autocorrelation of soil hydrophobicity. Another reason for the difference in variogram and Moran's I values may be due to the fact that Moran's I uses a binary data set while the variograms use the entire range of surface tension values. A hydrophobic point may be likely to be adjacent to another hydrophobic point, however, it may be unlikely to have a similar degree of hydrophobicity. Some variograms showed evidence of a hole effect. A hole effect occurs when the sill of a variogram exhibits wavy pattern. This is caused by similarity of

32

hydrophobicity values from two (or more) patches separated by an area that is

hydrophilic or of a different degree of hydrophobicity. The variogram below may exhibit

a very mild hole effect, however this effect is more evident in other variograms
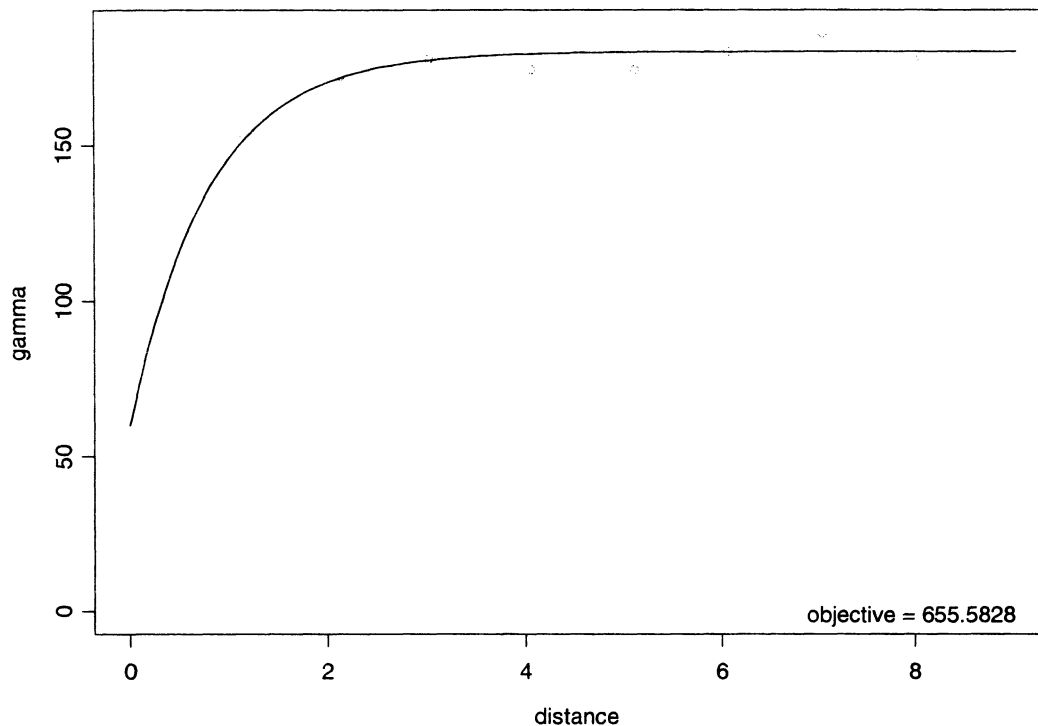
(Appendix F)



Figure 12. Semi-variogram of hydrophobicity from grid M1, fitted to an exponential
curve function. The semivariogram has a range of 0.8, a sill of 120, and a nugget of 60,
indicating that in grid M1, soil hydrophobicity is correlated up to a distance of 0.8 m.

**Variability in hydrophobicity with depth**

Soil hydrophobicity in the burned areas was generally strongest at the surface and

declined rapidly with depth (Figure 12). In plots H1 and H2 at the Hayman Fire site the

soil was hydrophilic within 4 cm of the surface. A similar decline in hydrophobicity with

depth was observed in the 0 to 3 cm depth interval of plot H3, but a moderately

hydrophobic layer occurred between 4 and 6 cm depth. Plot M1 at the Moose Fire site

was similar to the Hayman Fire plots and had slightly hydrophobic soil to 4 cm, whereas in plots M2 and M3 the hydrophobicity declined more rapidly und only extended to 1 cm and 3 cm depth, respectively. These results indicate that soil hydrophobicity measurements at the surface, which were previously described, represent the strongest hydrophobicity at most plot locations. Because soil hydrophobicity was only sampled at depth if the point above a particular depth was found to be hydrophobic, it is possible that soil hydrophobicity might be present at depths greater than those which I measured, and also that it may be present at depth when it is not present at the surface.


**Factors controlling soil hydrophobicity**

The variables measured at each of the sites in an effort to identify the factors controlling soil hydrophobicity were ash depth, volumetric water content, soil texture, and microtopography. On the Hayman fire ash thickness ranged from 0 to 2.2 cm and on the Moose fire it ranged from 0 to 17 cm. In looking at Ash Depth plotted against Surface Tension (Appendix H) it appears that the two are correlated on both fires. However, when the effects of spatial autocorrelation and space are corrected for with the Mantel Test, this correlation dwindles. Ash thickness was significantly positively correlated ($p < 0.05$) with hydrophobicity on plot H3 only. The lack of correlation between ash depth and soil hydrophobicity in most of the plots suggests that ash depth does not affect soil hydrophobicity at these sites (Appendix H and J).

Volumetric water content at the Hayman Fire sites ranged from 1 to 6 % indicating that the soils were very dry during sampling. Soils at the Moose Fire were slightly wetter than at the Hayman Fire with water contents that ranged from 2 to 17 %.

34

In looking at volumetric water content plotted against surface tension (appendix G) they

appear to be negatively correlated. However, after correcting for the effects of

autocorrelation and space with the Mantel's Test (Appendix J), this correlation

disappeared. Instead we find that volumetric water content is positively correlated with
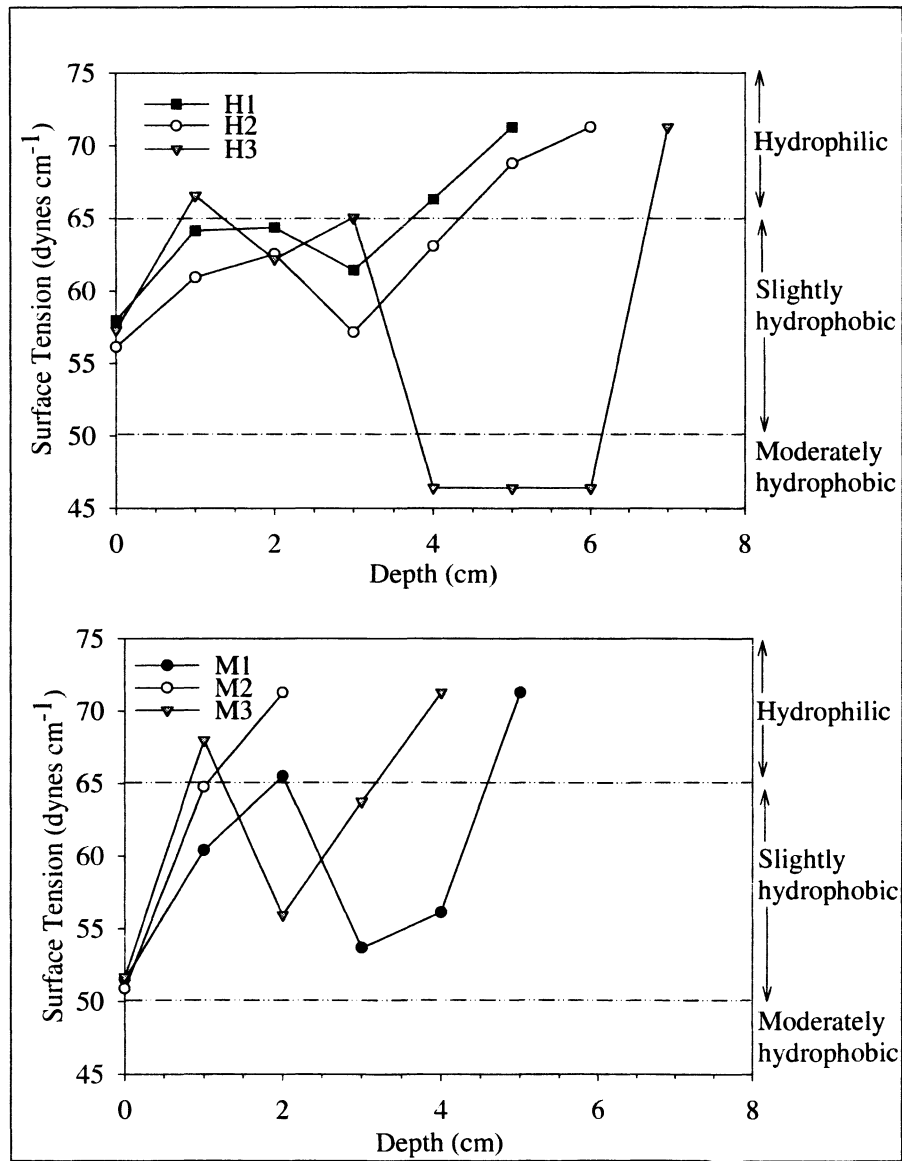
surface tension on grids M3, and H1 ($p=<0.05$).



Figure 13. Variability in soil hydrophobicity with depth in burned plots at the Hayman (H1, H2 and H3) and Moose (M1, M2 and M3) fire sites.

Soils at the two sites had strongly contrasting soil textures. The plots at the Hayman Fire site contained an average of 62 to 72% sand, whereas the soils at the Moose Fire site contained less sand and more silt. Despite the wide range in soil textures in the study plots, there was no relationship between soil hydrophobicity and any metric of soil texture (percent sand, percent silt or percent clay) (Appendix I)

Micotopography was recorded on the Moose Fire, but was not present on the Hayman Fire. Although sites that were described as dips were slightly wetter and slightly less hydrophobic than sites that were described as humps, they did not appear to be significantly different.

# DISCUSSION

## Spatial Variability of Soil Hydrophobicity

Spatially intensive transect and plot based measurements conducted after the Moose Fire in Montana and the Hayman Fire in Colorado indicated that burning results in an increase in the degree and spatial contiguity of soil hydrophobicity, and that the hydrophobicity is spatially variable at two scales. Within the transects and plots, hydrophobicity occurred as discrete patches ranging in size from $< 1m^2$ to $> 10\ m^2$, indicating spatial variability at the $10^0$ to $10^1$ m scale. In addition, the intensity and spatial contiguity varied between sites, indicating variability at the $10^1$ to $10^2$ m or larger scale. Increased water repellency after fire has been noted previously in the Rocky Mountain region (Robichaud, 2000; Huffman et al., 2001; Macdonald and Huffman, 2004) and elsewhere (Imeson et al., 1992; Doerr et al., 1996; Mataix-Solera et al., 2002), and has been identified as a causal mechanism for increases in runoff and erosion from burned areas (Scott and Van Wyk, 1990; Benavides-Solorio and MacDonald, 2001). Spatial variability of soil hydrophobicity at a range of scales has been observed in burned and unburned Arizona chaparral soils (Brock and DeBano, 1990), in sandy soils in Portugal (Doerr et al., 1998), in dune sands in the Netherlands (Dekker et al., 2000), and in calcareous soils in southeastern Spain (Mataix-Solera and Doerr, 2004). However, this is the first study to quantify the spatial variability of fire-induced soil hydrophobicity at sites in the Intermountain West of the United States.

## Factors Leading to Spatial Variability

Fire severity was clearly the most important factor affecting the larger scale spatial variability in soil hydrophobicity in this study. This is illustrated by the data from the transects at the Moose Fire, where there was a two to three-fold increase in the proportion of points that were hydrophobic and an increase in the strength of hydrophobicity in moderate and high severity fire locations compared to unburned sites. The higher hydrophobicity in medium severity transects compared to high severity transects is consistent with the results obtained in a study conducted in Colorado by MacDonald and Huffman (2004), and is presumably due to a partial loss of hydrophobicity at very high soil temperatures. In a laboratory study, DeBano and Krammes (1966) found that the soil hydrophobicity increased with temperature at soil temperatures of up to 800°C. However, exposure of the soil to temperatures of 800 to 900°C for at least twenty minutes resulted in a complete loss of soil hydrophobicity. The high severity transects on the Moose Fire may have been exposed to temperatures and durations above the thresholds described by DeBano and Krammes, resulting in reduced hydrophobicity relative to medium severity sites. The loss of hydrophobicity at very high temperatures may also explain why high severity transects had a larger number of patches but smaller mean patch size than the medium severity transects. Under high fire severity conditions, large patches created at lower soil temperatures may have been broken into a larger number of smaller segments.

The burned grid plots were all located in areas deemed to have burned at moderate to high fire severity on the basis of indicators such as ash color and woody debris consumption. However, plot M1 had a much higher percentage of the total area

that was hydrophobic and a higher overall intensity of hydrophobicity than the other five burned plots, suggesting a higher level of fire severity in this plot. There was no evidence for such a difference based on the normal indicators of fire severity, such as ash color and fuel consumption, but this may be due to the fact that the fire severity classifications were made at least a year after the fire when much of the ash had been moved off the site by erosion. Fire severity determinations made immediately after the fire may have enabled a more accurate determination of fire severity at the grid plots, and a clearer understanding of the factors leading to increased soil hydrophobicity in plot M1.

Localized differences in fire severity may have contributed to the smaller scale variability or "patchiness" of soil hydrophobicity observed within the transects and plots. For example, the presence of red ash around a burned log in grid H3 indicated high fire severity, and soil hydrophobicity was high in the area surrounding the log. However hydrophobicity was lower directly beneath the log, where temperatures were presumably even higher. Exposure of the soil beneath the log to higher temperatures for a longer period of time may have eliminated some of the hydrophobicity, while heating around the log was sufficient to create an intensely hydrophobic response.

In addition to fire severity, the strength of post-fire soil hydrophobicity has been related to ash depth, soil texture, and soil moisture (Meeuwig, 1971; DeBano, 1981; Doerr and Thomas, 2000). However, over the range of conditions encountered in the present study, none of these factors had a significant effect on soil hydrophobicity. With regard to the effect of ash depth, this may be due to the fact that the data were collected 1 to 2 years after the fires, so that much of the ash on the site had been either removed or relocated by overland flow and erosion. In most cases, ash on the study sites had

accumulated in depressions on the surface, indicating that it had likely moved since the fire.

The absence of a relationship between hydrophobicity and soil texture, despite strong contrasts in sand and silt content, may be due to the small sample size used in the analysis. Alternatively, differences in soil hydrophobicity due to other factors, such as fire severity, may have overwhelmed more subtle differences due to the effects of soil texture.

The fact that soil moisture was significantly correlated with soil hydrophobicity in just two out of the six burned grids indicates that soil moisture was generally not an important control on soil hydrophobicity. These results may have been somewhat affected by difficulties encountered while measuring soil moisture content. The rocky soil at the Hayman Fire site made it difficult to insert the Hydrosense probe. At many places, measurements could not be obtained or the probe had to be inserted at an angle to avoid rocks. This resulted in fewer and possibly less accurate measurements of soil hydrophobicity at the Hayman Fire site. Another reason for this lack of correlation may be due to the method used to measure soil water levels. Other methods of measuring soil water content should be tried, such as soil water holding capacity. Soil water holding capacity measures the availability of water in the soil (usually for plants). Although soil hydrophobicity is not dependant on removing water from the soil as plants are, it may still be affected by soil water holding capacity, which varies with particle size.

Work conducted in Colorado indicates that, rather than there being a linear relationship between soil hydrophobicity and soil moisture, there is a threshold value for soil moisture above which the hydrophobicity is no longer present (MacDonald and

Huffman, 2004). This threshold was found to be 26% for areas burned at moderate to high severity. None of the sites in the present study had moisture contents greater than 17% on grid M1. Therefore, even with more intensive sampling, it would not have been possible to determine whether the threshold values observed at the Colorado sites also applied at the Moose and Hayman fire sites.

Differences in vegetation and duff characteristics may lead to differences in soil hydrophobicity because of their effect on soil temperatures during a fire and the types of hydrophobic compounds introduced into the soil. This study attempted to control for these variables by selecting sites with similar vegetation and duff characteristics. However, data from the control plots at the Moose Fire site suggest that differences in these characteristics may still have affected the soil hydrophobicity measurements. Transects C1, C2, and C3, which are in pure lodgepole pine forests with a well developed O horizon had significantly higher frequency of hydrophobicity than transects C4, C5, and C6, which are in a mixed lodgepole stand with younger trees, a barely developed O horizon and exposed mineral soil in many places. Similar differences in vegetation and duff characteristics may have occurred in the burned areas, leading to additional spatial variability in soil hydrophobicity.

**Variability of hydrophobicity with depth**

The depth at which hydrophobicity occurs in the soil depends on the magnitude and the duration of the heat pulse generated by the fire (Letey, 2001). In general, hotter fires result in the hydrophobic layer being driven more deeply in the soil profile (Scholl, 1975; Robichaud and Hungerford, 2000). Since dry soils are poor conductors of heat,

41

temperature gradients in the soil are very steep so that fire-induced hydrophobicity rarely occurs below 50 cm depth (Doerr et al., 2000). In this study, hydrophobicity was generally strongest at the surface, declined rapidly with depth, and was not detectable below 6 cm from the surface. These results are generally consistent with the depth profiles of soil hydrophobicity measured after fires in Colorado (Huffman et al., 2001). They suggest either that the temperatures generated by the two fires were quite moderate or that the fire was moving rapidly and only generated a brief heat pulse in the soil.

**Variability in hydrophobicity over time**

The plot based measurements were conducted 12 and 22 months after the Hayman and Moose Fires, respectively. Since hydrophobicity declines with time since burning, the results obtained in this study almost certainly do not represent the maximum extent or severity of hydrophobicity that occurred at these two sites. The reduced percentage of points at the Moose Fire that were hydrophobic in the plot sites compared to the transect sites, where data were collected 9 months after the fire, shows that there was a decline in hydrophobicity in the year between the two sets of measurements. However, both data sets indicated the presence of patchiness in soil hydrophobicity. This suggests that while water repellency may have been stronger and more contiguous immediately after the Moose and Hayman fires, spatial variability ("patchiness") is an inherent characteristic of post-fire soil hydrophobicity unless patchiness is an outcome of time and change.

**Hydrologic Implications of Patchy Soil Hydrophobicity**

Increased soil hydrophobicity after fire results in a decrease in the infiltration rate and a corresponding increase in the potential for generating infiltration excess overland flow (Burch et al., 1989; Letey, 2001; Wang et al., 2000). However, overland flow generated by intense rainfall on a hydrophobic patch will infiltrate when it reaches an adjacent hydrophilic area, or a root channel or crack that provides a conduit along which water can flow into the soil (Shakesby et al., 2000). The potential for continuous overland flow therefore depends in part on the spatial contiguity of hydrophobic soil patches.

In all but one of the burned plots hydrophobicity occupied less than 40% of the plot area and the hydrophobic patches were far enough apart that they were spatially isolated, as indicated by the low connectivity index scores. Runoff generated from hydrophobic patches in these plots would most likely infiltrate before reaching another patch, and continuous overland flow would not occur. The exception was Plot M1, in which 68% of the points were hydrophobic and the two patches in the plot were spatially joined. Runoff from this plot would be quite likely to generate continuous overland flow. Presumably there is a threshold value for the percentage area of the plot or hillslope that is hydrophobic above which continuous overland flow is likely to occur. The data obtained from this study indicates that this threshold is greater than 37%, the second highest percent area hydrophobic after plot M1, and less than 68%. A more precise estimate of this threshold could enable forest managers to determine the potential for hydrophobicity induced overland flow and erosion on the basis of a random sample of points from across a hillslope. The percentage of points noted to be hydrophobic would

then be an indicator of whether the percent area hydrophobic exceeded the threshold value.

The patchiness of hydrophobicity observed in our study supports the hypothesis presented by Shakesby et al., (2000) regarding the relationship between hydrophobicity and the scale dependency of runoff observed in burned areas. The magnitude and variability of runoff measured in small ($1m^2$) plots is often substantially greater than that measured in larger plots or small catchments (Doerr et al., 2003). This is likely due at least in part to the fact that, as the scale of measurement increases, so too does the potential for the plot to include areas of hydrophilic soil or root holes and cracks. Small runoff plots may be located completely within or completely outside a hydrophobic patch, so they will substantially overestimate both the magnitude of runoff and the range of variability. Measurements from small catchments, while logistically more challenging to obtain, provide a better estimate of the magnitude and variability of runoff because they integrate the effects of spatial variability in soil hydrophobicity and macropores such as root channels and cracks.

**Management Implications and Future Research**

The observed spatial variability of soil hydrophobicity has important implications for the assessment of soil hydrophobicity using field measurements. Field characterization of soil hydrophobicity is usually based on point measurements. This is the approach most commonly used by Burn Area Emergency Rehabilitation teams to characterize fire effects on soils. While point measurements provide a measure of the overall mean and variance of the hydrophobicity, they do not characterize the spatial

44

contiguity of hydrophobic patches. As the data from our small (1 m$^2$) plots demonstrate, even spatially intensive measurements are inadequate if the scale of measurement is less than the scale of variability. The design of field measurement programs to characterize soil hydrophobicity should be based on transect based pilot data that characterizes the scale of variability and the distance over which values are spatially correlated. Failing this, we suggest a similar sampling protocol to that used in our large plots, with measurements conducted at 1 meter spacing across areas of > 100 m$^2$. If it is not possible to conduct such detailed sampling, then an estimate of the proportion of the ground surface that is hydrophobic can be obtained from point measurements. Our data suggest that hydrophobicity is unlikely to be spatially contiguous enough to generate overland flow if less than 35% of the points are hydrophobic. If more than 70% of the points are hydrophobic, then it is highly likely that the hydrophobicity is spatially contiguous. Using these values as a guide, Burn Area Emergency Rehabilitationteams may assess the risk for overland flow from burned areas.

Significant questions still remain regarding the spatial variability of soil hydrophobicity in different areas, changes over time in the spatial characteristics of soil hydrophobicity, and the factors contributing to spatial variability in soil hydrophobicity. Future work should include additional plot based measurements in a range of different soil and vegetation types. These measurements should be conducted immediately after fires and then repeated periodically in the same locations for up to 2 years afterwards to track changes over time. Additional measurements such as these will also help to constrain the threshold value at which soil hydrophobicity becomes sufficiently spatially contiguous to generate overland flow.

Determining the effects of fire severity, vegetation cover, soil texture and soil moisture on the spatial variability of soil hydrophobicity is probably not possible in an uncontrolled field environment due to the difficulty involved in isolating the effect of any one variable. Burning experiments in which soils are exposed to a range of fire severities by manipulating the fuel load may offer considerable insight as to the effect of fire severity on the spatial variability of soil hydrophobicity. Similar experiments should be conducted using a range of soil textures and soil moisture levels to analyze the effects of variability in these characteristics. Experiments like these, along with additional spatially intensive measurements, will continue to expand our knowledge of the spatial variability of soil hydrophobicity and its role in post-fire runoff and erosion.

# CONCLUSIONS

Spatially intensive measurements of soil hydrophobicity at sites in western Montana and Colorado indicate that post fire soil hydrophobicity generally occurs as discrete patches $<1m^2$ to $>10m^2$ in area. However, the intensity of soil hydrophobicity varies within these patches. The size and contiguity of the patches generally increases with fire severity, and this leads to additional spatial variability at the $10^1$ to $10^2$ meter scale. Under the circumstances observed in this study, where sites had burned at medium to high fire severity 1 to 2 years previously, soil hydrophobicity was unlikely to affect runoff and erosion rates because runoff from hydrophobic areas would infiltrate when it reached an adjacent hydrophilic area of soil. Factors such as ash depth, soil texture, and soil moisture did not affect soil hydrophobicity under the range of conditions observed in this study. More work is needed to determine the role of these factors in determining the spatial variability of soil hydrophobicity.

Isolated point measurements and measurements from small ($1m^2$) plots do not adequately quantify the spatial variability of soil hydrophobicity. However, given the logistical limitations inherent in conducting spatially intensive measurements across large areas, we suggest a threshold in the range from 35 to 70% for the percentage of point measurements at which the water repellency is sufficiently spatially contiguous to generate continuous overland flow. Since hydrophobic patches are generally larger than $1m^2$, small runoff plots are likely to overestimate the magnitude and variability of runoff from burned catchments. More work is needed to characterize the spatial characteristics of soil hydrophobicity in a range of settings, its variability over time, and the factors

controlling it. This can be achieved through repeated spatially intensive measurements at

a variety of sites and controlled burning experiments.

# APPENDIX

## A. Site characteristics for transect-based sampling

| Site | Slope | Aspect | Date | Location | Altitude (meters) | Air Temp. (degrees Celsius) |
|------|-------|--------|------|----------|-------------------|------------------------------|
| c1 | 14% | 348 | 7/20/2002 | N48$^\circ$ 40.573'<br>W114$^\circ$17.933' | 1170 | 77 |
| c2 | 23% | 328 | 8/9/2002 | N48$^\circ$ 40.575'<br>W114$^\circ$ 17.902' | 1173 | 75 |
| c3 | 16% | 318 | 8/8/2002 | N48$^\circ$ 40.574'<br>W11$^\circ$ 17.889' | 1173 | 77 |
| c4 | 35% | 346 | 8/9/2002 | N48$^\circ$ 40. 634'<br>W114$^\circ$ 19. 507' | 1191 | 83 |
| c5 | 32% | 343 | 8/10/2002 | N48$^\circ$ 40.632'<br>W114$^\circ$ 19.526' | 1185 | 80 |
| c6 | 30% | 23 | 8/11/2002 | N48$^\circ$ 40.635<br>W114$^\circ$ 19.552 | 1191 | 69 |
| l1 | 22% | 183 | 7/6/2002 | N48$^\circ$ 40.670'<br>W114$^\circ$ 16.534' | 1305 | 83 |
| l2 | 30% | 173 | 7/6/2002 | N48$^\circ$ 40.671'<br>W114$^\circ$ 16.570 | 1320 | 81 |
| l3 | 30% | 173 | 7/13/2002 | N48$^\circ$40.773'<br>W114$^\circ$16.60 | 1335 | 95 |
| l4 | 26% | 20 | 7/14/2002 | N48$^\circ$ 40.285'<br>W114$^\circ$ 17.170' | 1170 | 90 |
| l5 | 26% | 20 | 7/14/2002 | N48$^\circ$ 40.285'<br>W114$^\circ$ 17.170' | 1170 | 90 |
| l6 | 33% | 13 | 7/15/2002 | N48$^\circ$ 40. 312'<br>W114$^\circ$ 17.159' | 1197 | 89 |
| m1 | 36% | 233 | 6/29/2002 | N48$^\circ$ 39.696'<br>W114$^\circ$ 17.758' | 1248 | 77 |
| m2 | 36% | 233 | 7/4/2002 | N48$^\circ$ 39.609'<br>W114$^\circ$ 17.839' | 1248 | 68 |
| m3 | 25% | 223 | 7/13/2002 | N48$^\circ$ 39.613'<br>W114$^\circ$ 17.777' | 1248 | 81 |
| m4 | 18% | 253 | 7/15/2002 | N48$^\circ$ 40.336'<br>W114$^\circ$ 16.272' | 1257 | 81 |
| m5 | 27% | 253 | 7/15/2002 | N48$^\circ$ 40. 369'<br>W114$^\circ$ 16.258' | 1257 | 90 |
| m6 | 15% | 253 | 7/16/2002 | N48$^\circ$ 40.392'<br>W114$^\circ$ 17.281' | 1248 | 68 |
| h1 | 26% | 58 | 7/21/2002 | W114$^\circ$ 13.816'<br>W114$^\circ$ 13.816' | 1179 | 68 |
| h2 | 35% | 58 | 7/21/2002 | N48$^\circ$ 39.215'<br>W114$^\circ$ 13.775' | 1209 | 76 |

| | | | | N48° 39.229' | | |
|---|---|---|---|---|---|---|
| h3 | 30% | 58 | 7/21/2002 | W114° 13.748' | 1221 | 76 |
| h4 | 43% | 303 | 7/22/2002 | N48° 39. 176'<br>W114° 18. 397' | 1347 | 76 |
| h5 | 27% | 278 | 7/25/2002 | N48° 39. 155'<br>W114° 18. 375' | 1314 | 87 |
| h6 | 30% | 313 | 7/25/2002 | N48° 39.147'<br>W114° 18.391' | 1464 | 91 |

## B. Patch information for transect-based sampling

| Transect-pair | # of hydrophilic points | average # of points per hydrophobic patch | # of Patches | Mean surface tension |
|---|---|---|---|---|
| c1 | 63 | 1.83 | 18 | 58.49301 |
| c2 | 49 | 2.17 | 24 | 57.37467 |
| c3 | 64 | 2.14 | 14 | 59.0799 |
| c4 | 90 | 2 | 3 | 61.84583 |
| c5 | 90 | 1.2 | 5 | 61.93335 |
| c6 | 82 | 1.08 | 14 | 61.08349 |
| l1 | 64 | 1.68 | 19 | 57.56618 |
| l2 | 40 | 2.5 | 20 | 53.89833 |
| l3 | 57 | 2.17 | 18 | 55.97939 |
| l4 | 74 | 1.62 | 13 | 60.09037 |
| l5 | 77 | 2 | 9 | 60.17871 |
| l6 | 82 | 3.24 | 17 | 54.10092 |
| m1 | 20 | 5.07 | 15 | 50.50504 |
| m2 | 22 | 5.15 | 13 | 49.93296 |
| m3 | 29 | 4.4 | 15 | 51.85926 |
| m4 | 43 | 2.08 | 24 | 53.47268 |
| m5 | 34 | 3.65 | 17 | 51.45736 |
| m6 | 26 | 5 | 14 | 47.94673 |
| h1 | 33 | 2.54 | 24 | 53.60916 |
| h2 | 43 | 2.65 | 20 | 56.10157 |
| h3 | 50 | 2.19 | 21 | 56.66229 |
| h4 | 17 | 5.27 | 15 | 49.08978 |
| h5 | 22 | 4.1 | 18 | 50.38237 |
| h6 | 70 | 1.75 | 16 | 59.16227 |

## C. CST Values along Transects.
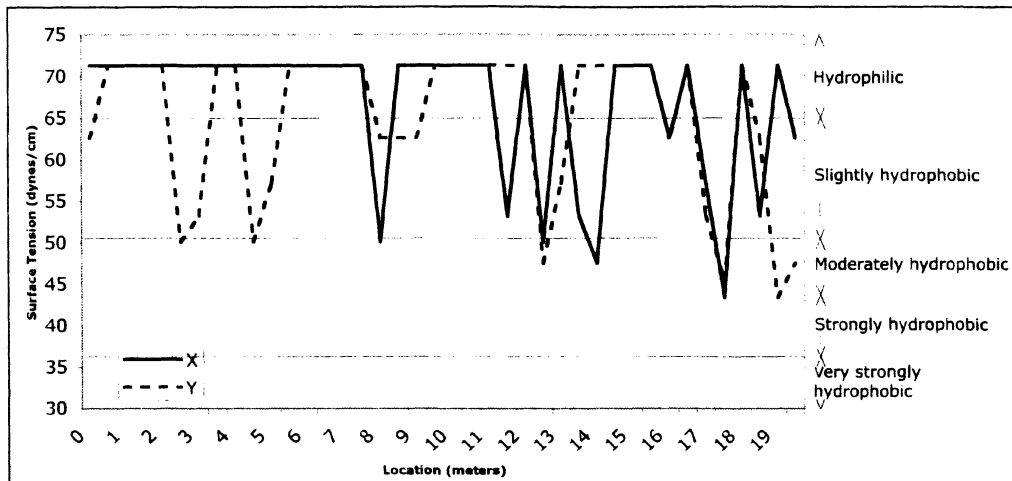


Control transect-pair C1
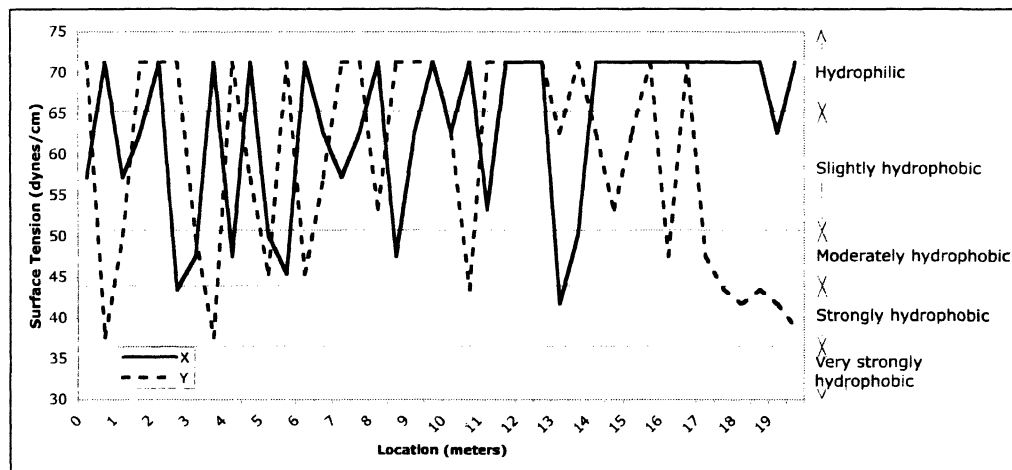


Control transect-pair C2
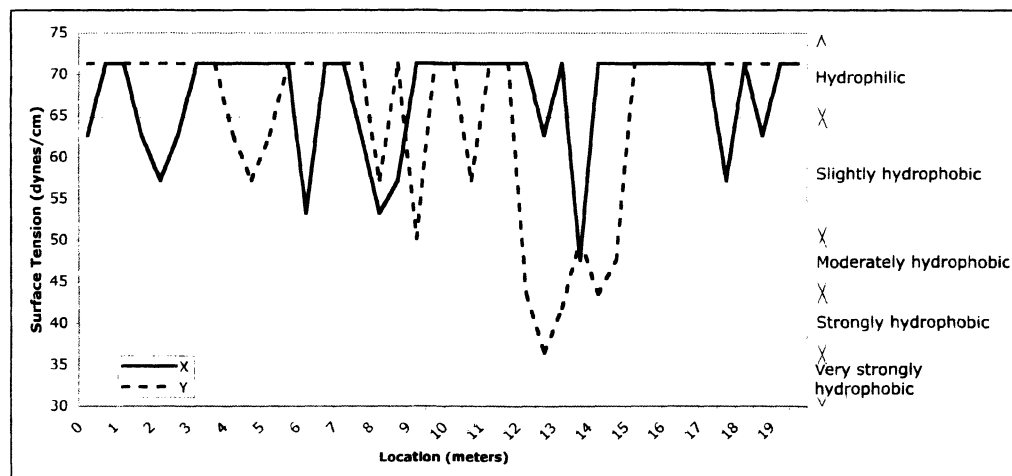


Control transect-pair C3

51
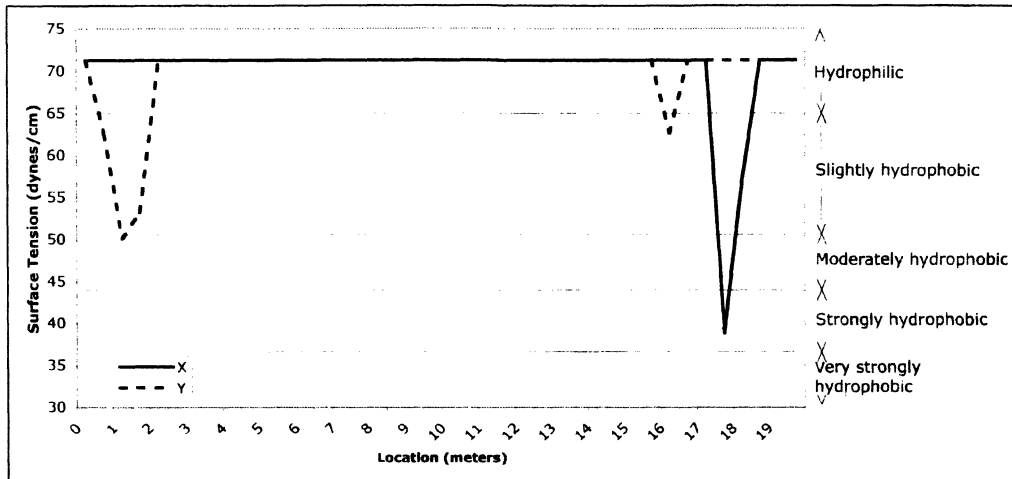
Control transect-pair C4
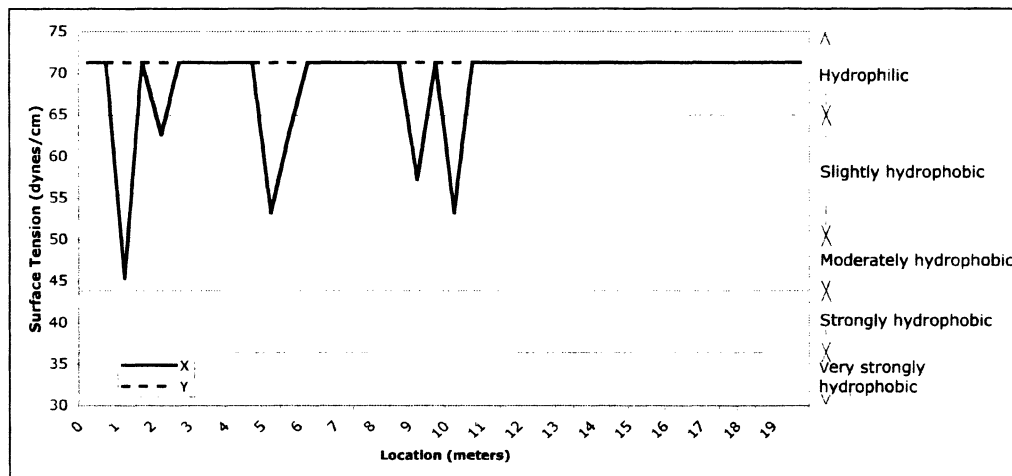


Control transect-pair C5
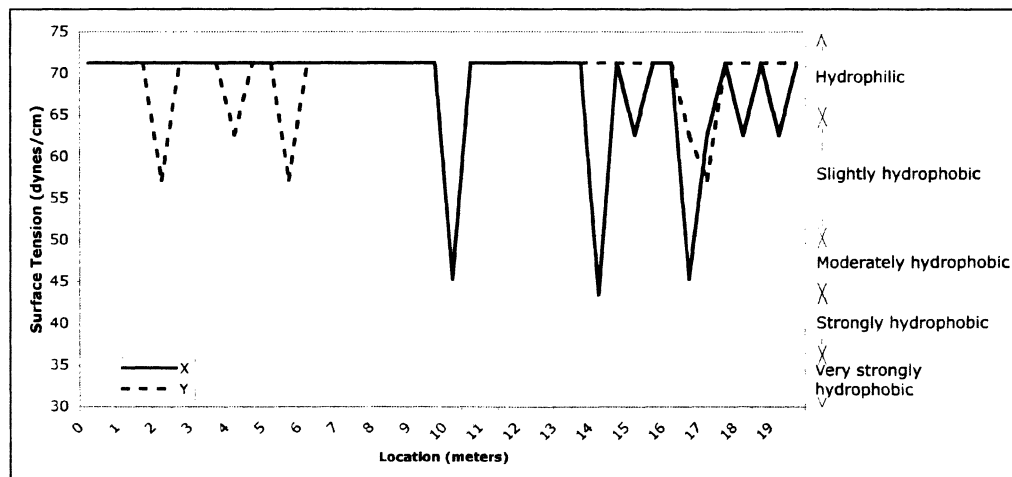


Control transect-pair C6

52
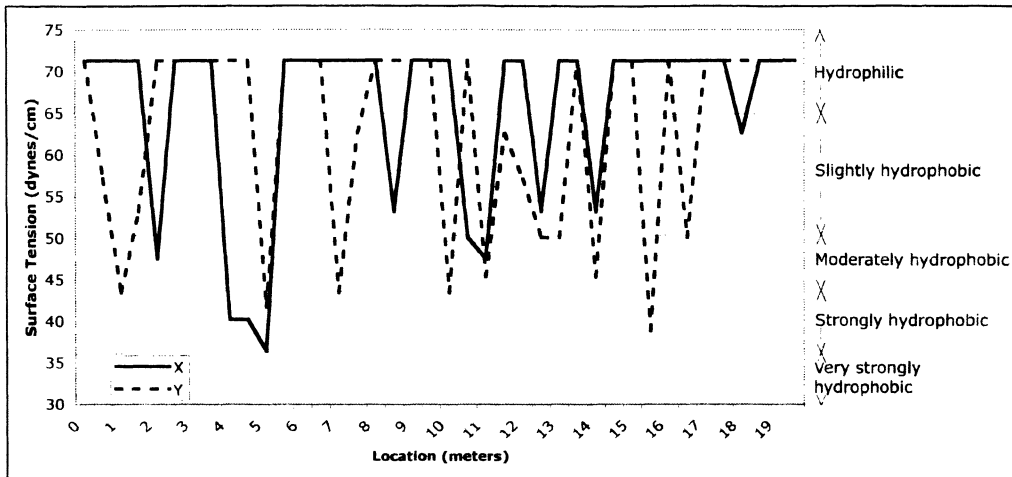
Low-severity transect-pair L1
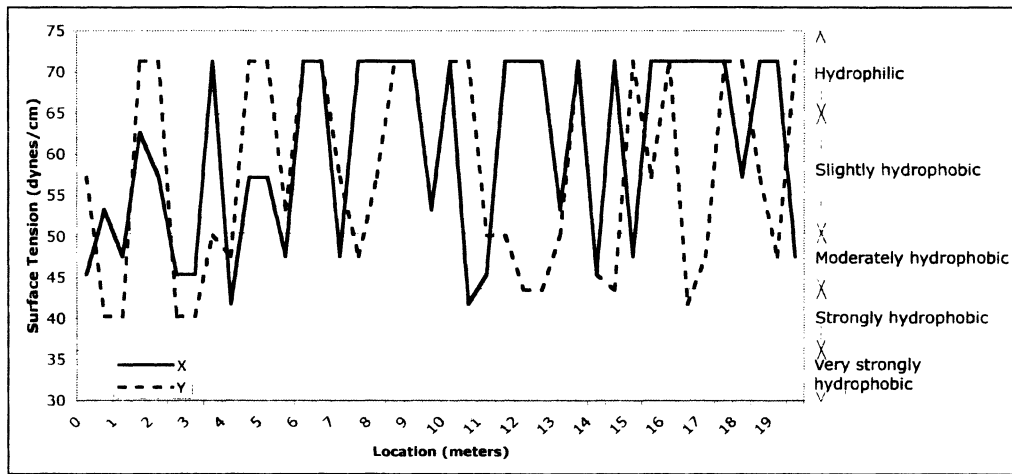


Low-severity transect-pair L2
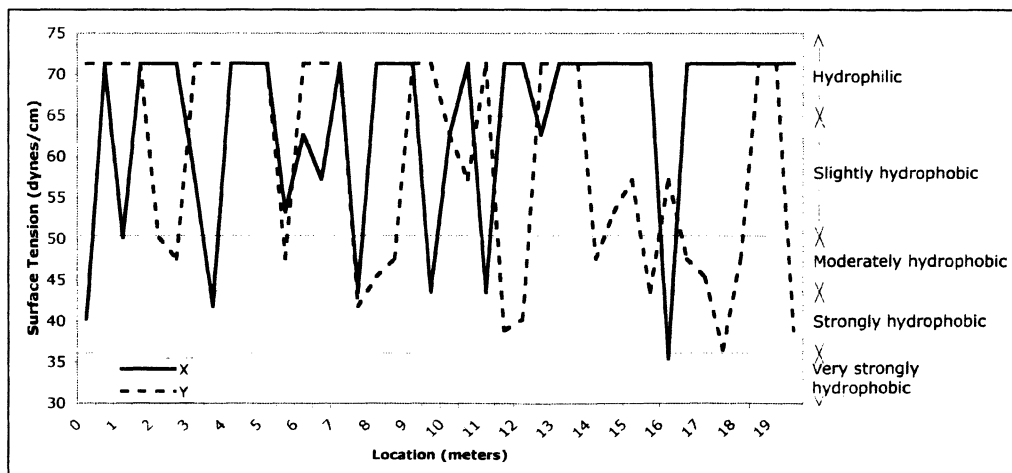


Low-severity transect-pair L3
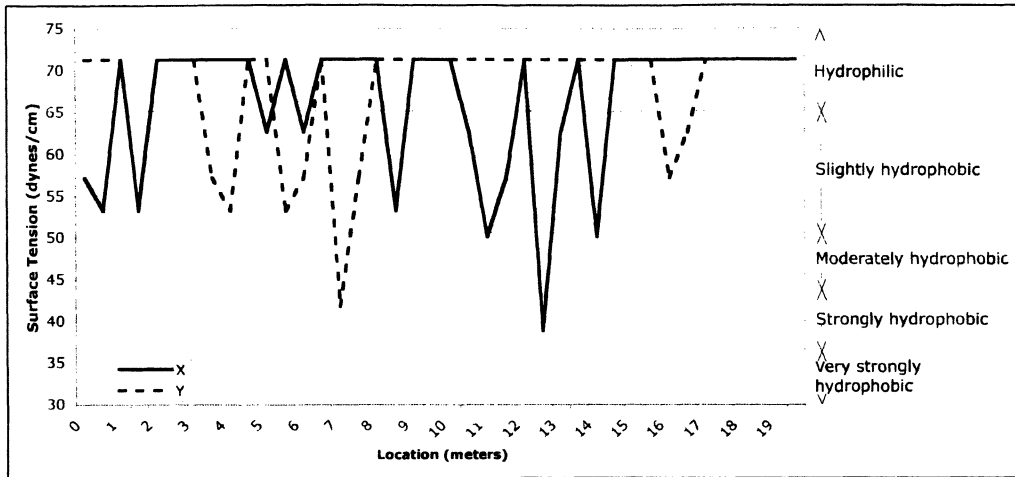
Low-severity transect-pair L4
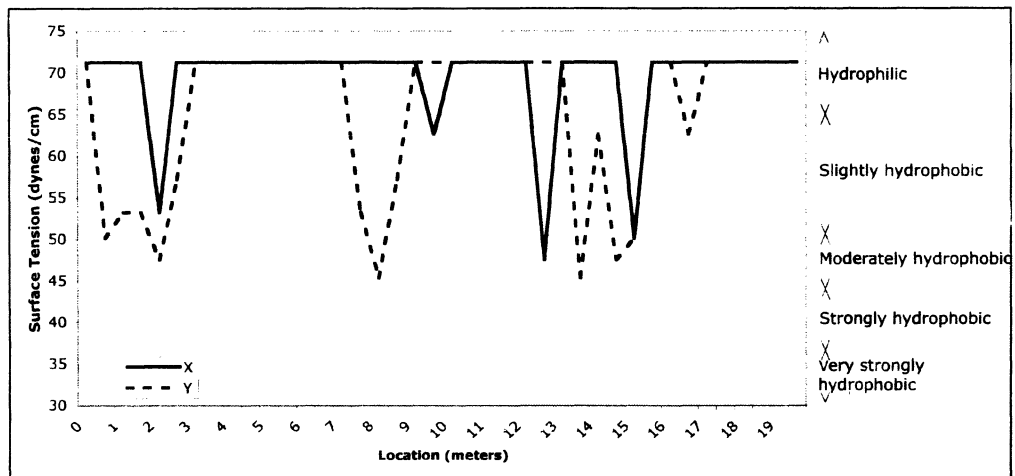


Low-severity transect-pair L5
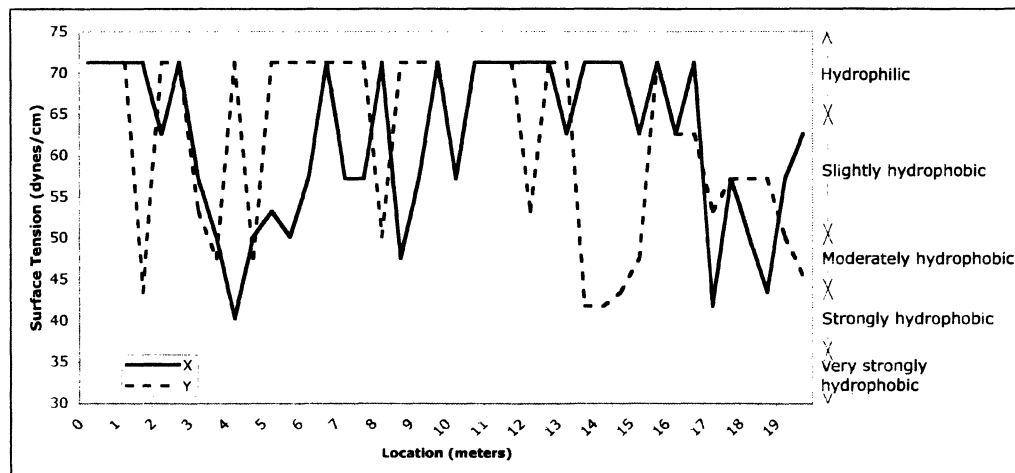


Low-severity transect-pair L6

54
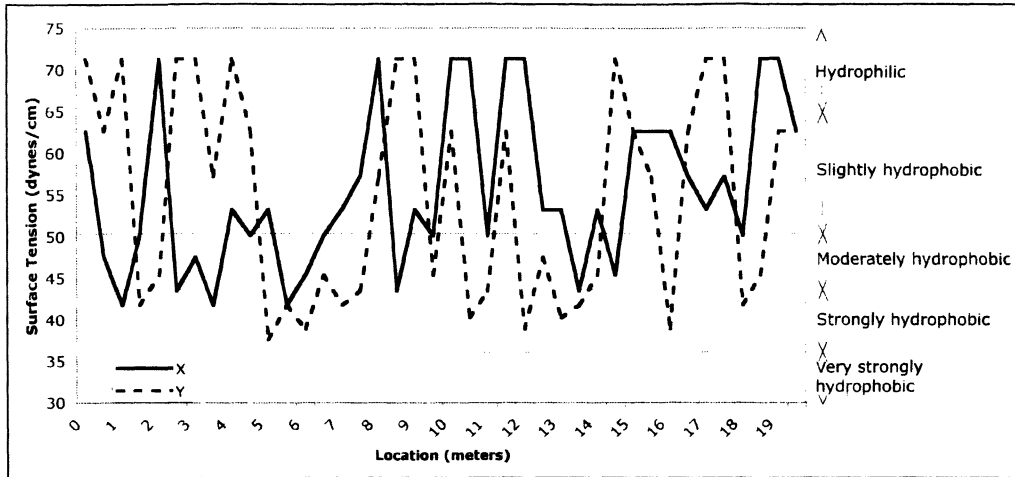
Medium-severity transect-pair M1
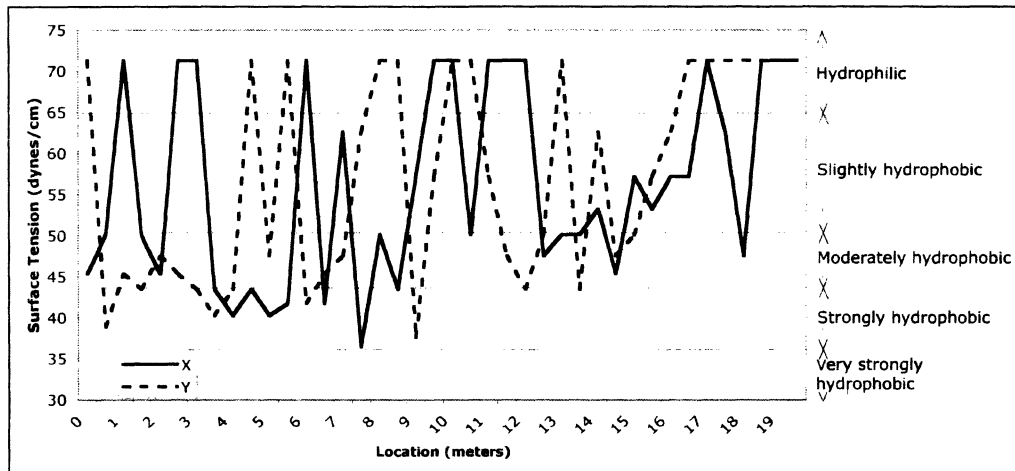

Medium-severity transect-pair M2
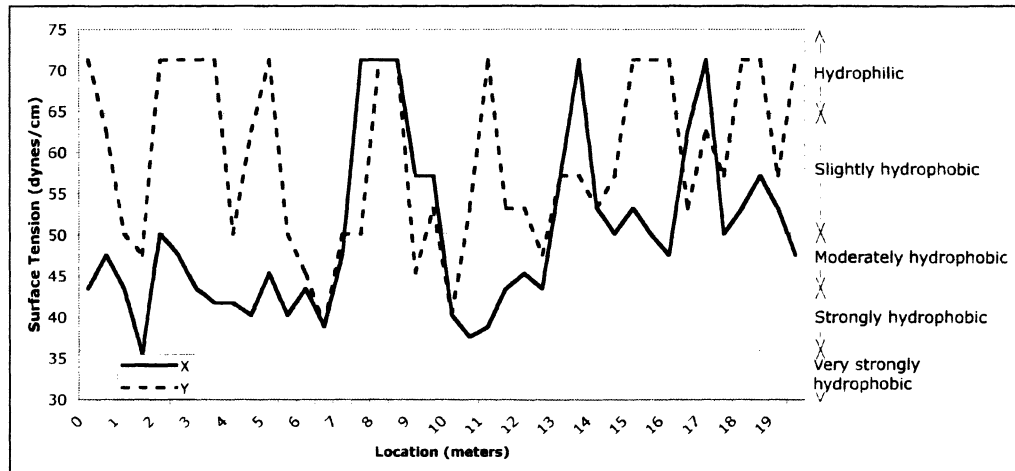

Medium-severity transect-pair M3
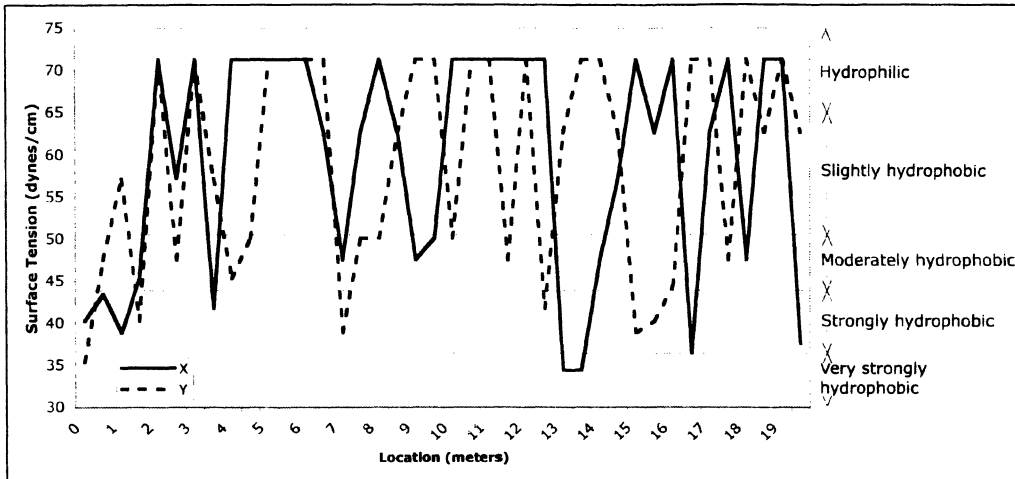
Medium-severity transect-pair M4
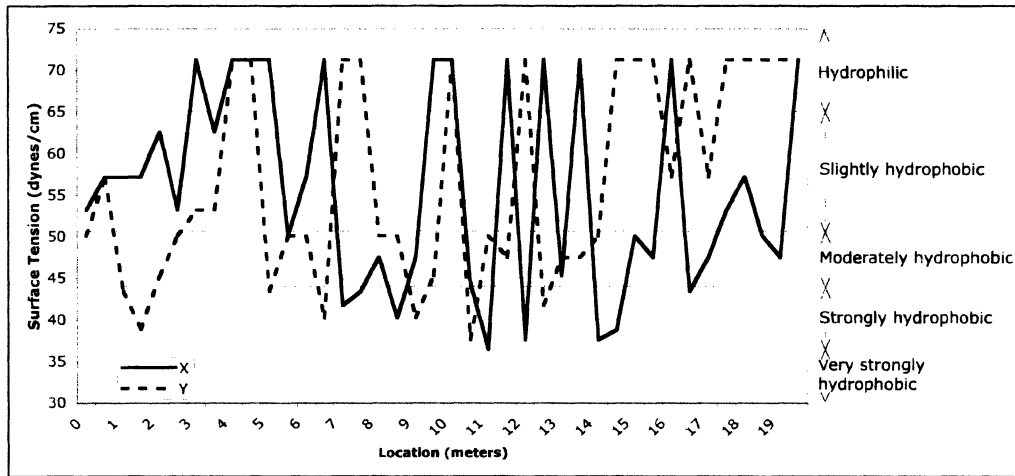
Medium-severity transect-pair M5
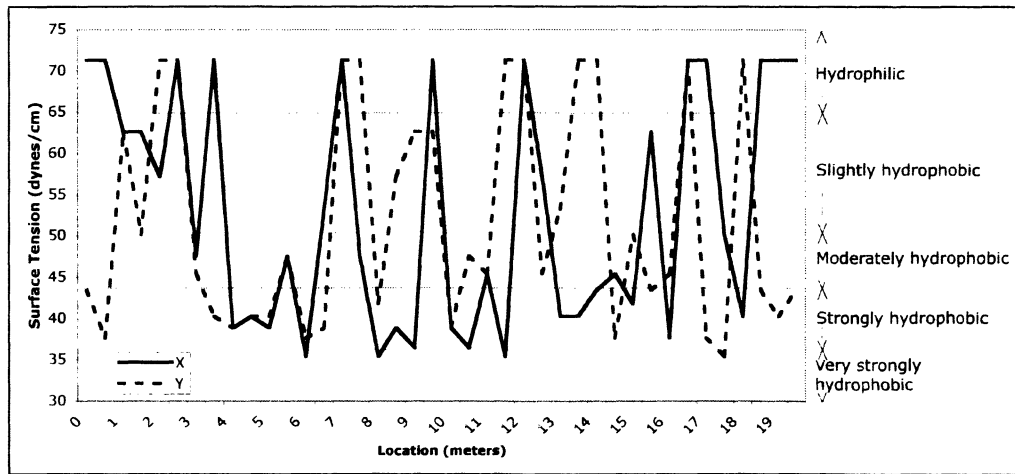
Medium-severity transect-pair M6
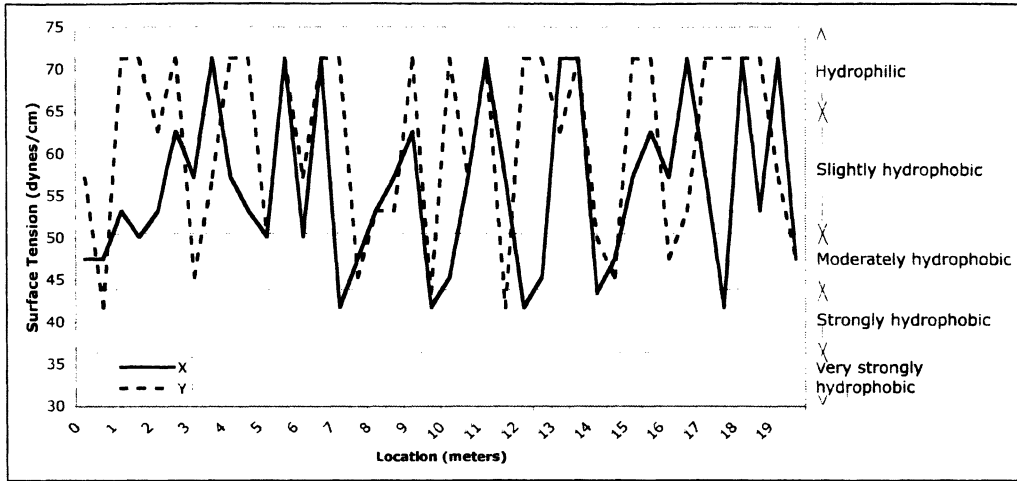
High-severity transect-pair H1
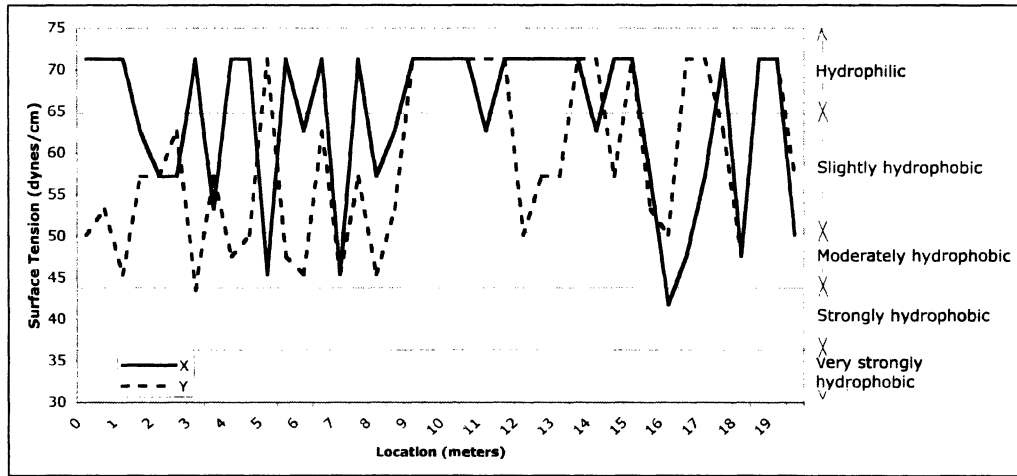


High-severity transect-pair H2
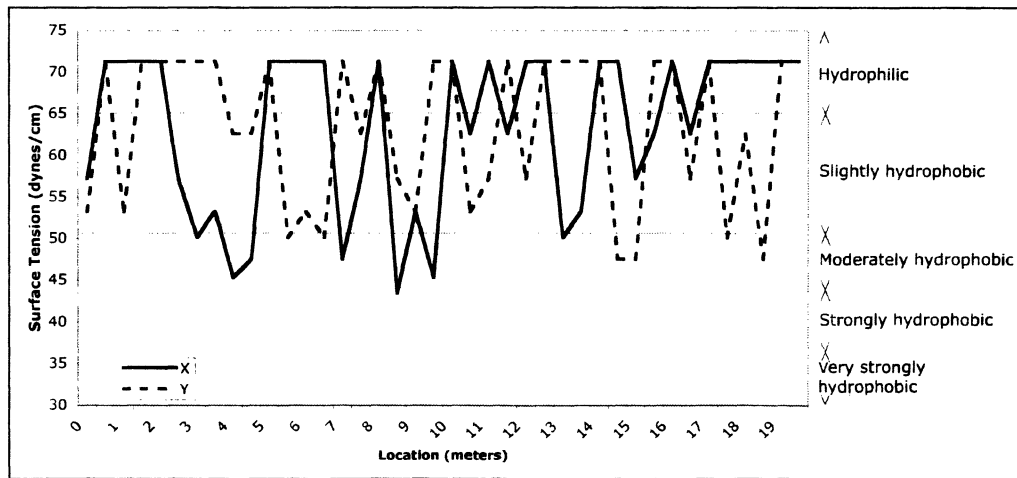


High-severity transect-pair H3

57
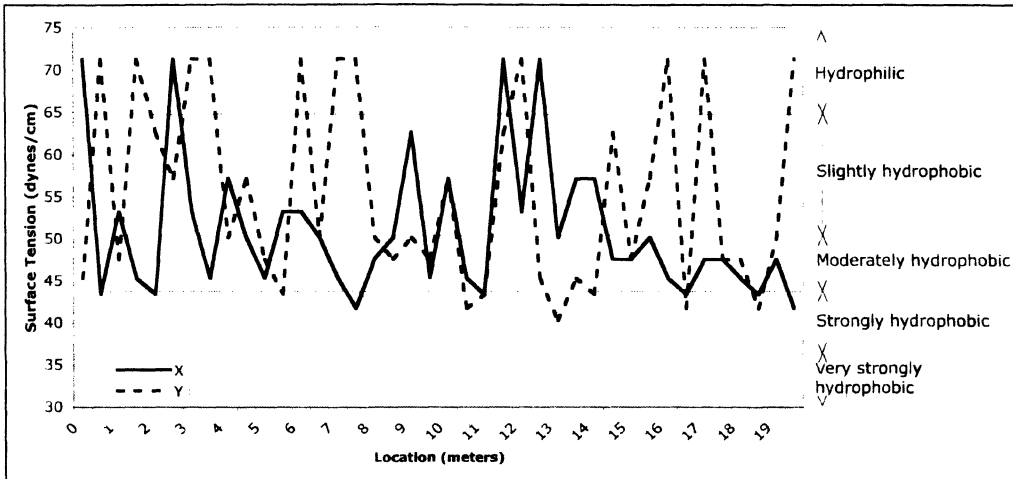
High-severity transect-pair H4
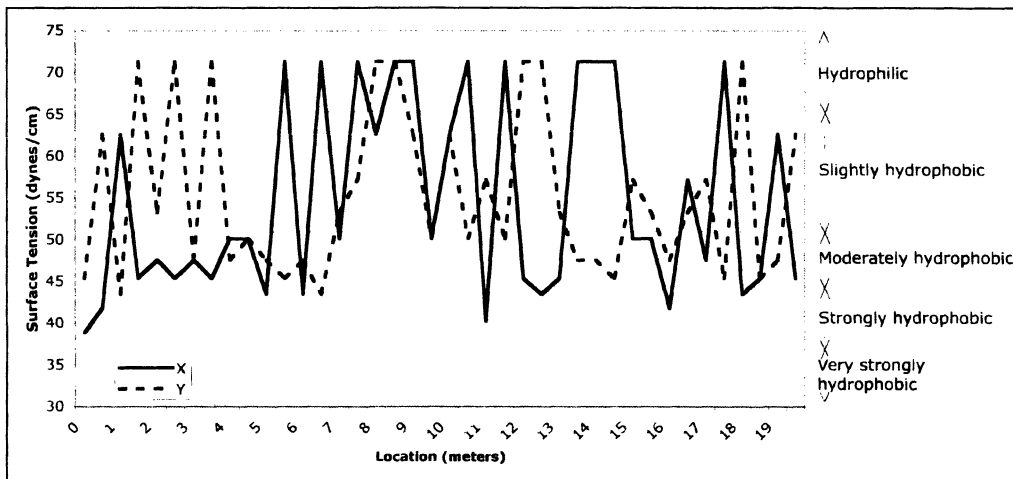


High-severity transect-pair H5
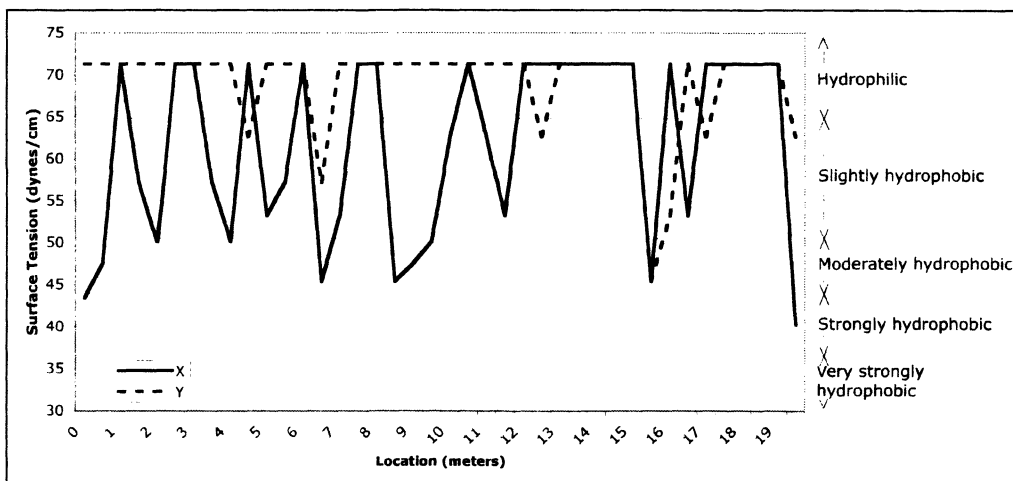


High-severity transect-pair H6

58

## D. Variograms of CST for transects

Each variogram is composed of 3 transects in either the X or Y direction from the same severity class. Each severity class has two sites, A or B.

### Variogram Control A, Y Direction
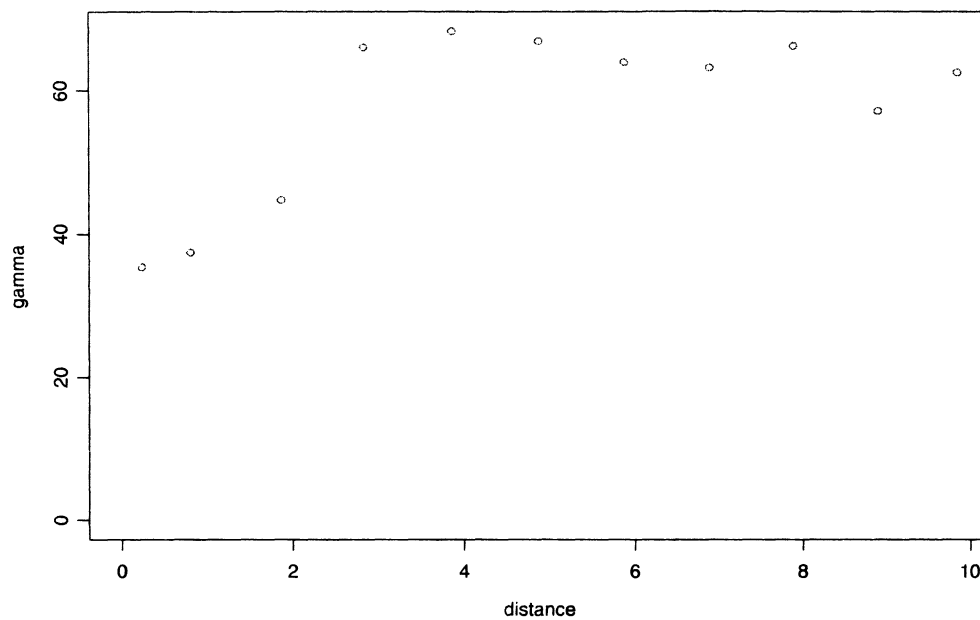


### Variogram Control A, X Direction
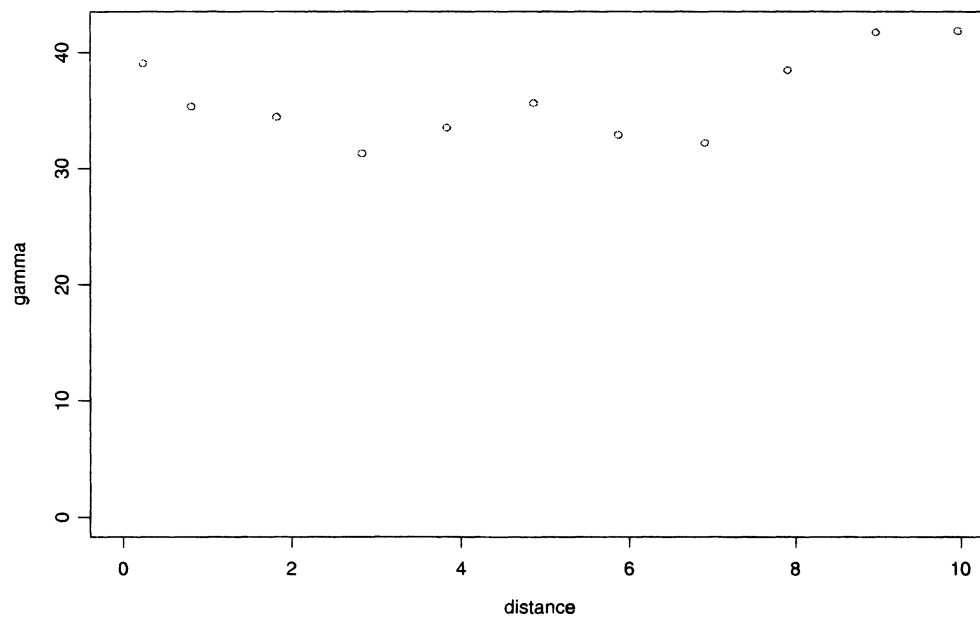
## Variogram Control B, X Direction
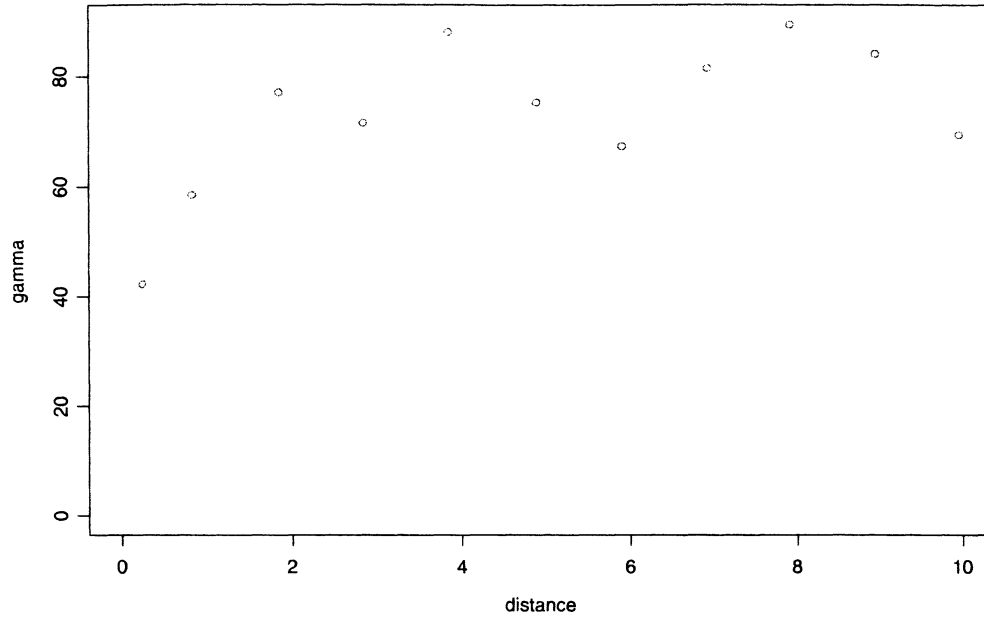


## Variogram Control B, Y Direction
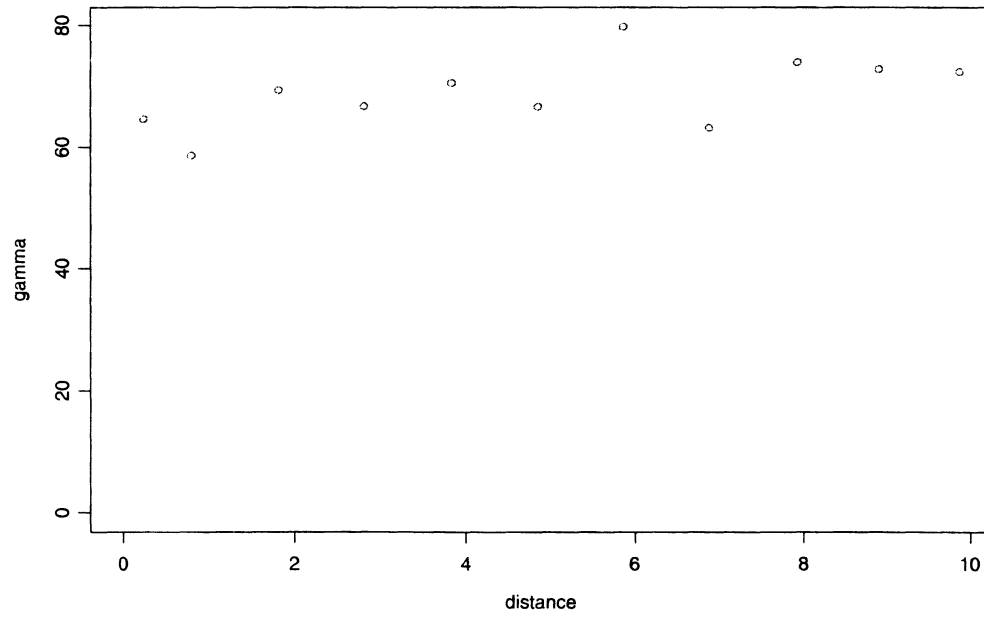
## Variogram Low Severity A, X Direction
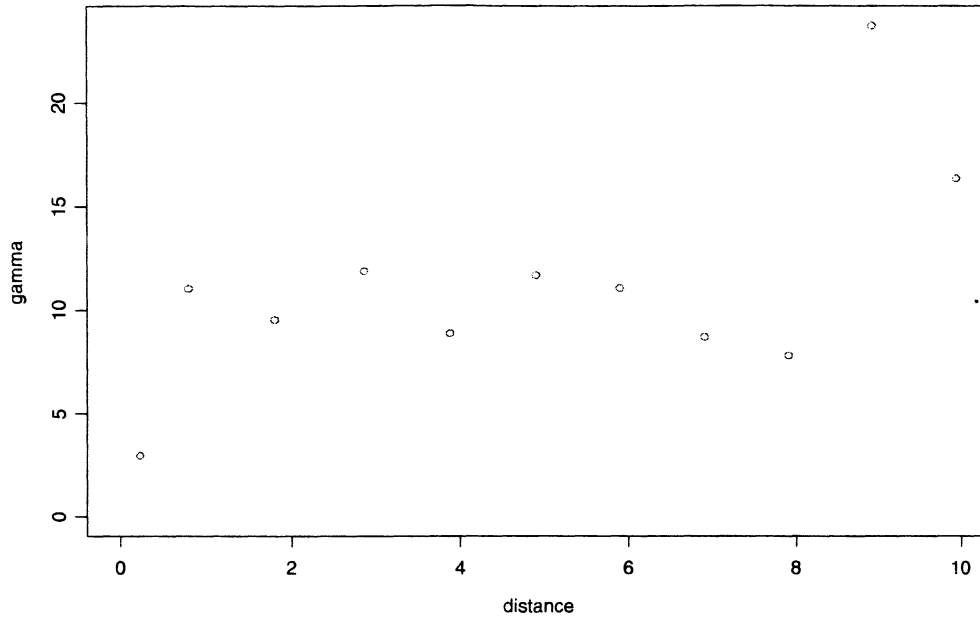


## Variogram Low Severity A, Y Direction
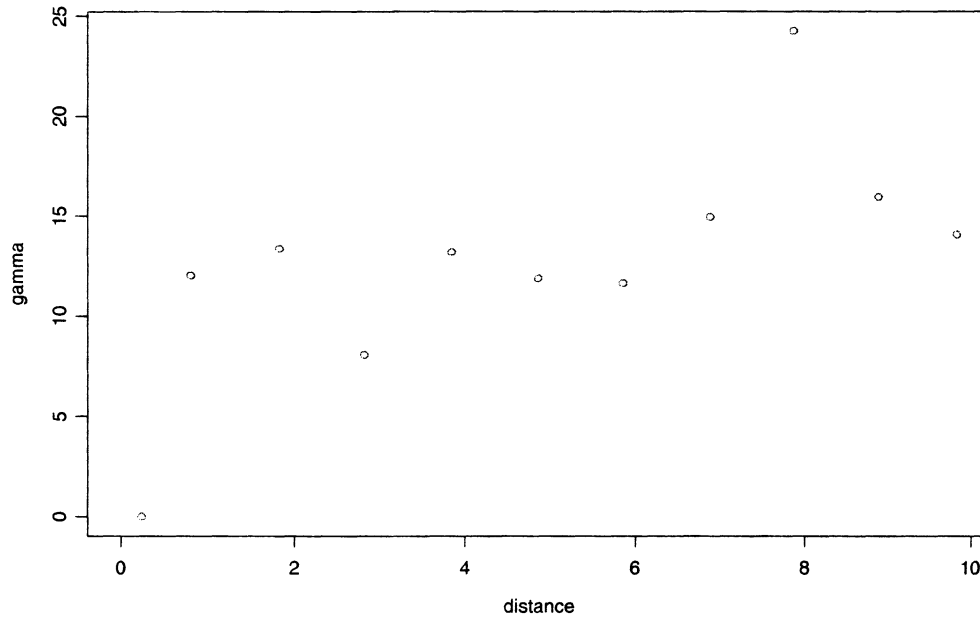
## Variogram Low Severity B, X Direction
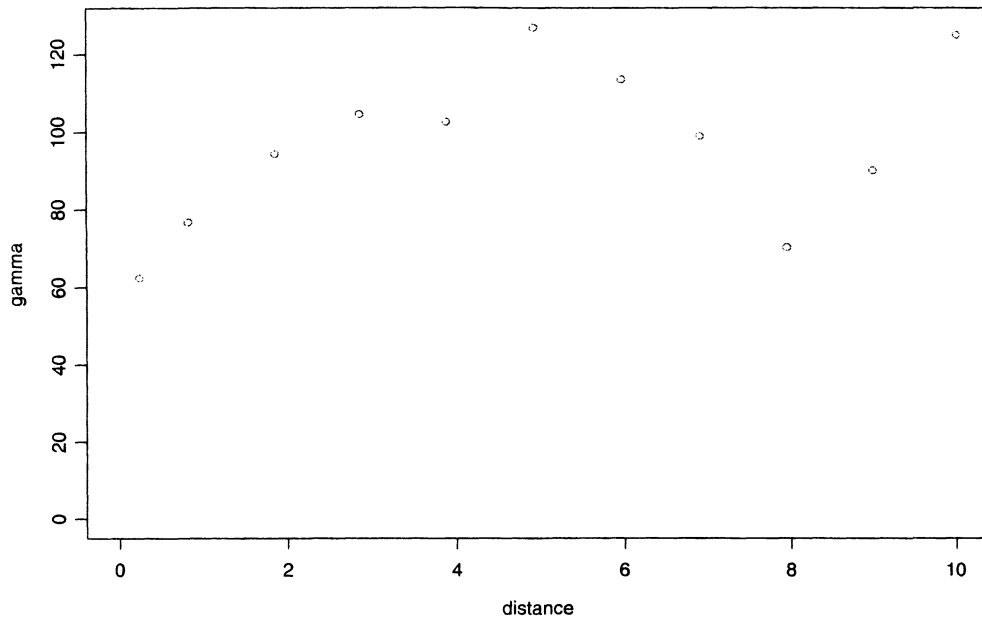


## Variogram Low Severity B, Y Direction
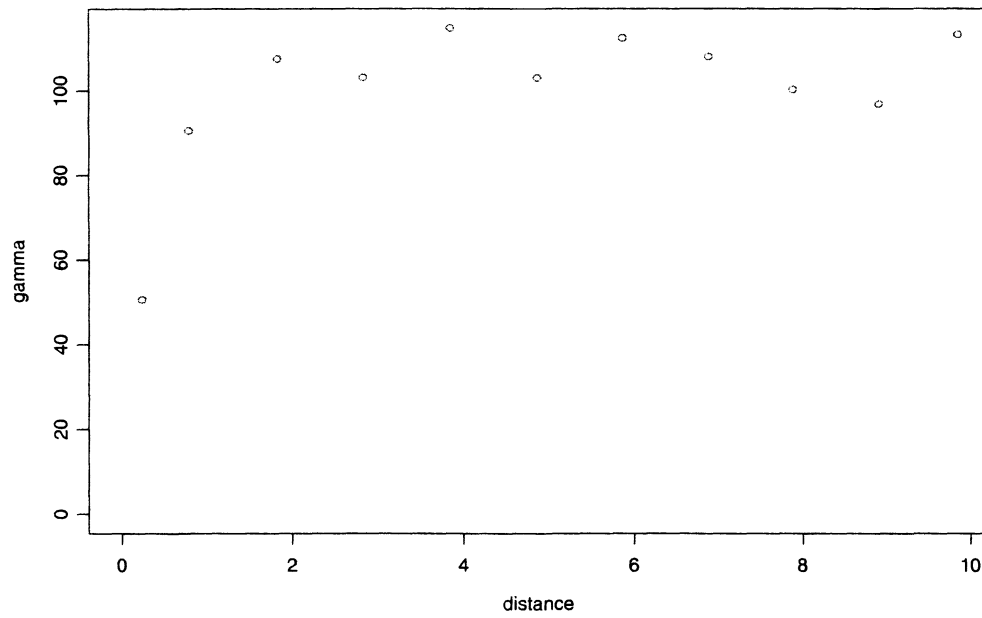
## Variogram Medium Severity A, X Direction
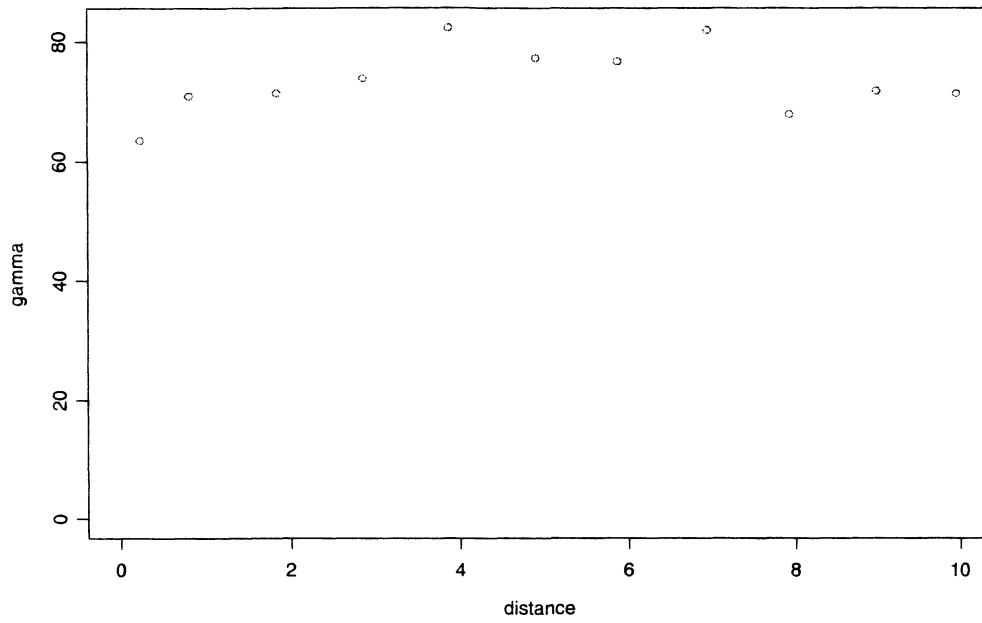


## Variogram Medium Severity A, Y Direction
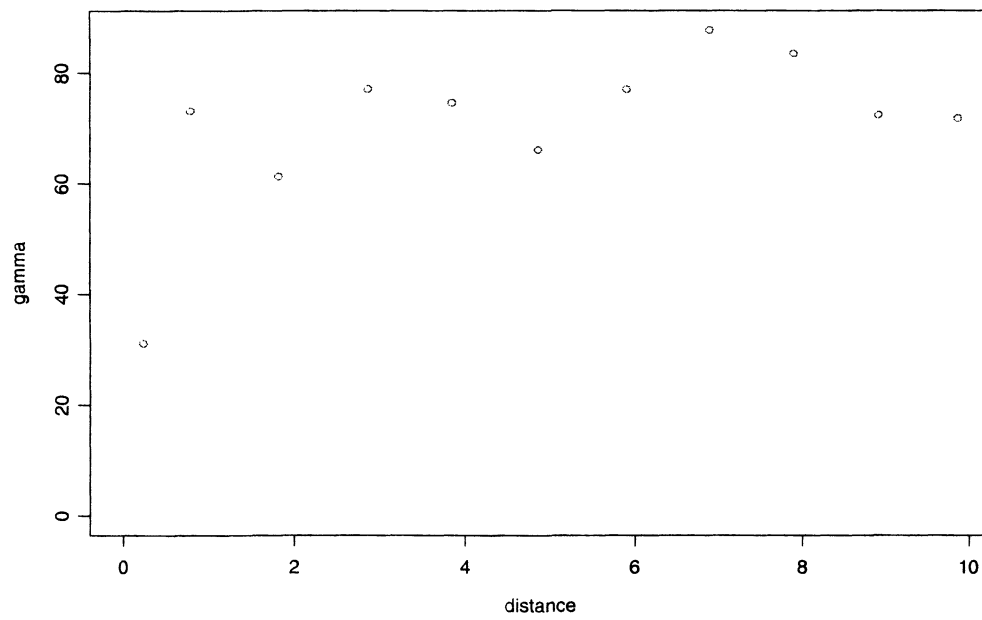
## Variogram Medium Severity B, X Direction
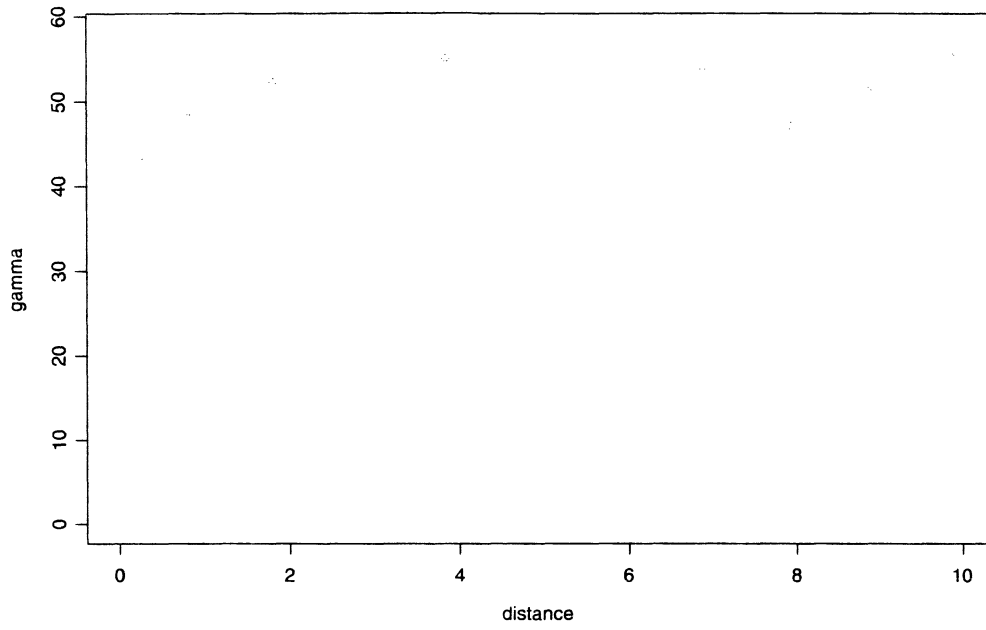


## Variogram Medium Severity B, Y Direction
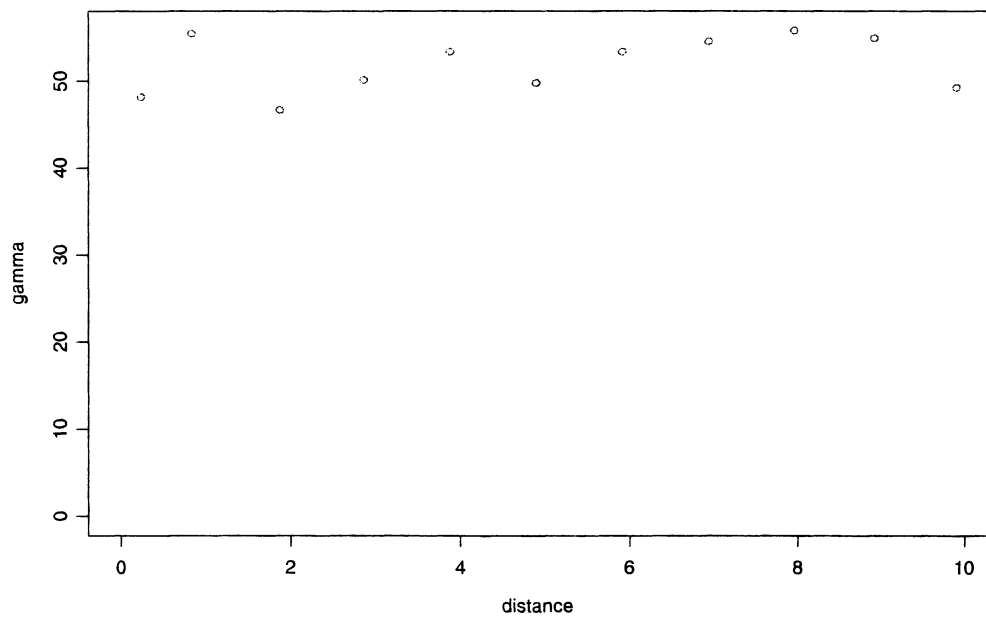
## Variogram High Severity A, X Direction
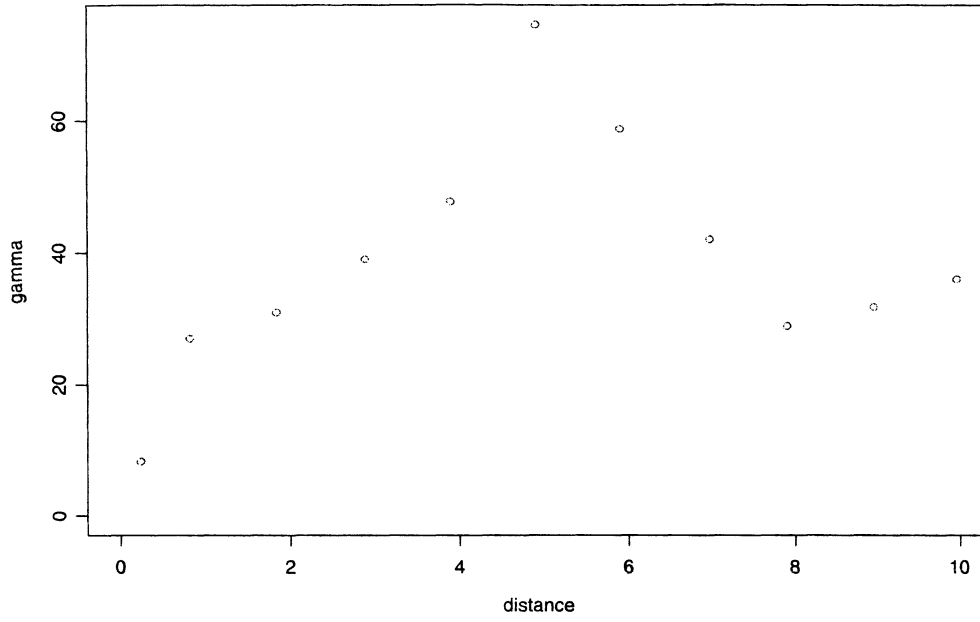


## Variogram High Severity A, Y Direction
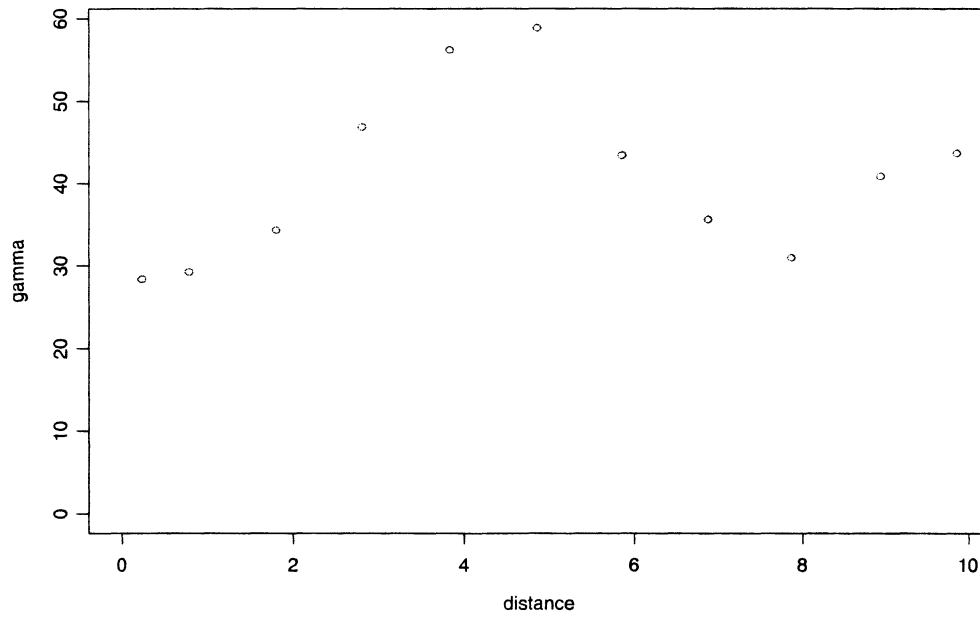
## Variogram High Severity B, X Direction
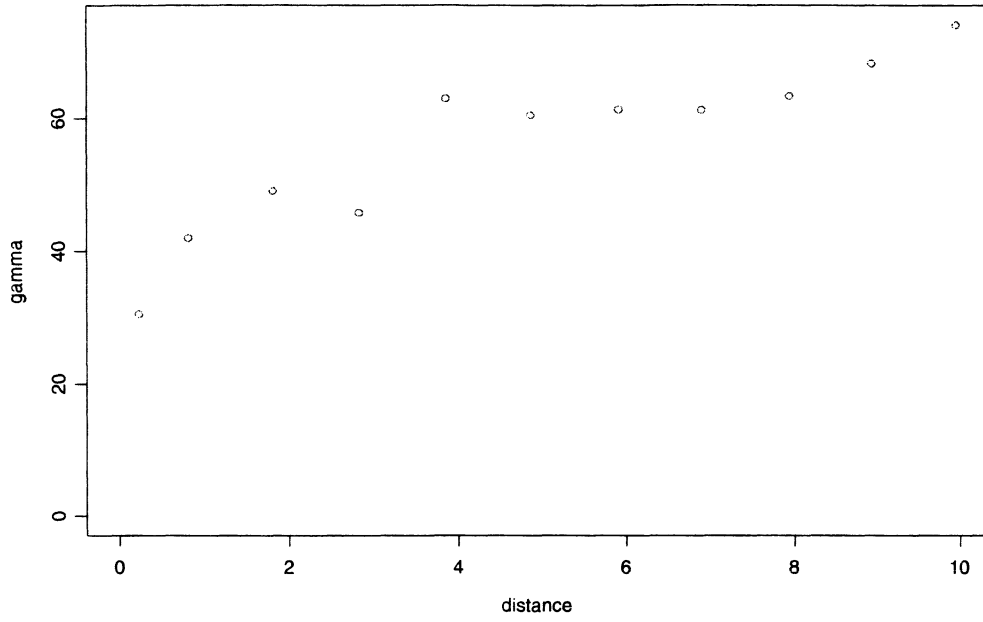


## Variogram High Severity B, Y Direction
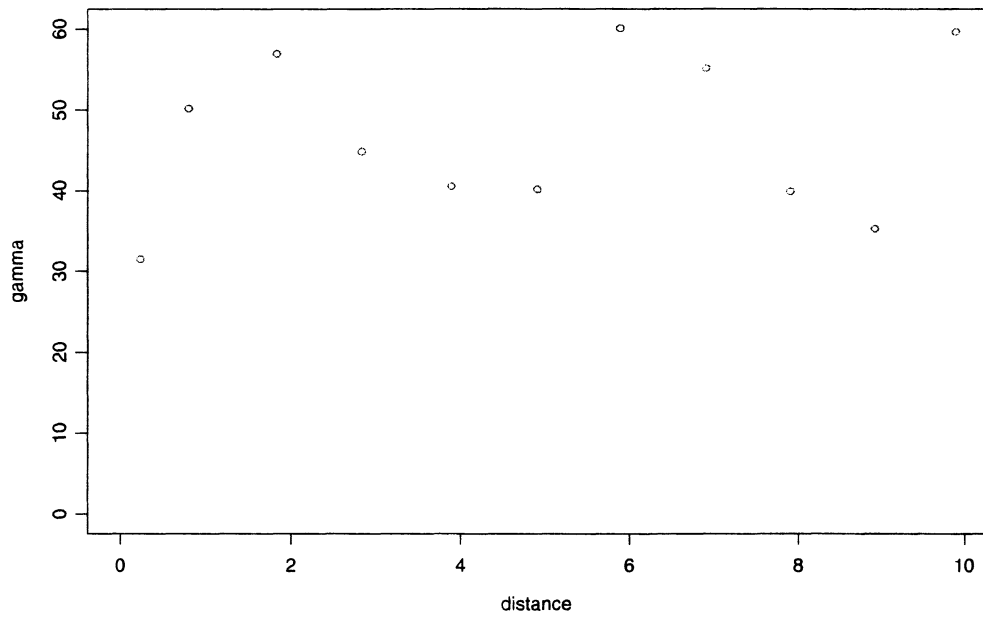
## E. Site characteristics for grid-based sampling

| Site | Slope | Aspect | Date | Location | Air Temperature |
|------|-------|--------|------|----------|-----------------|
| M1 | 24 | 87 | 6/12/2003 | N48.660434<br>W114.296666 | 67 |
| M2 | 19 | 83 | 6/2003 | N48.660434<br>W114.296666 | 69 |
| M3 | 26 | 327 | 6/2003 | N48.653360<br>W114.305029 | 72 |
| MC | 17 | 327 | 6/2003 | N48.675956<br>W114.298661 | 79 |
| H1 | 8 | 337 | 7/19/2003<br>7/20/2003 | N39 17 59.68"<br>W105 13' 52.88" | 83 |
| H2 | 17 | 357 | 7/20/2003<br>7/21/2003 | N 39 17' 5.83"<br>W 105 14' 46.51" | 70 |
| H3 | 18 | 92 | 7/22/2003 | N 39 17' 52.01 "<br>W 105 14' 4.87 | 84 |
| HC | 12 | 62 | 7/23/2002 | N 39 17' 49.39"<br>W 105 16' 0.21 | 78 |

# F. Directional and omnidirectional variograms for grids

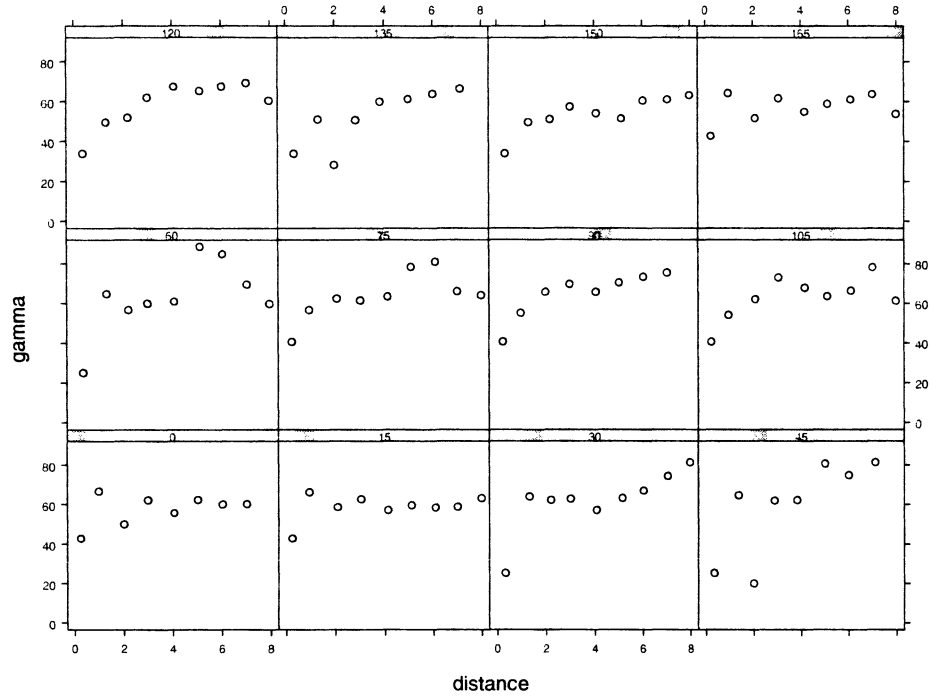Directional variograms of CST values - Grid M1
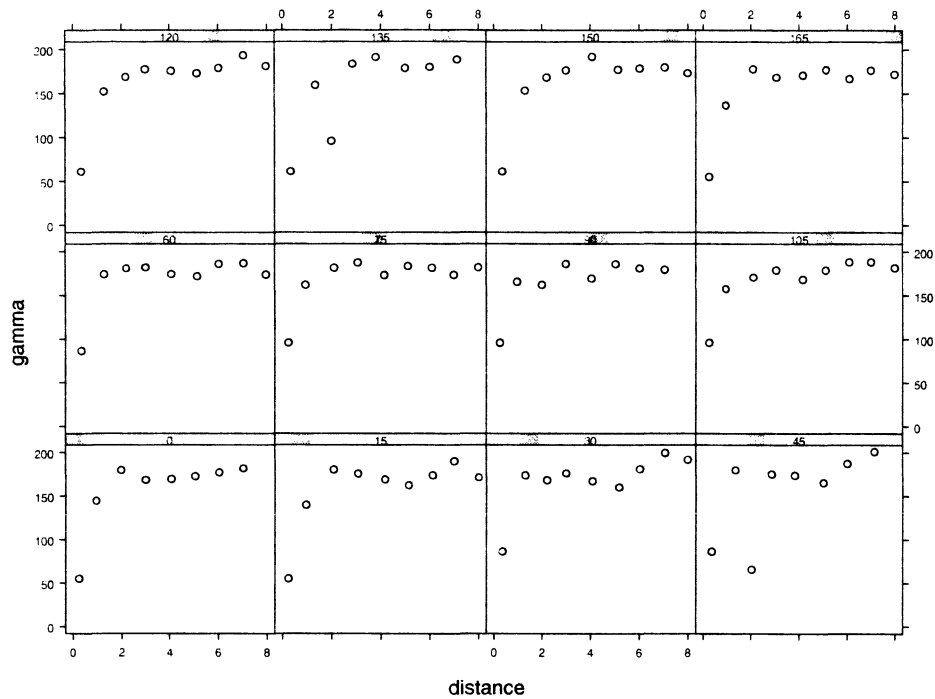


In viewing the above directional variograms, the direction of maximum spatial continuity appears to be around the azimuths of 120 and 135.

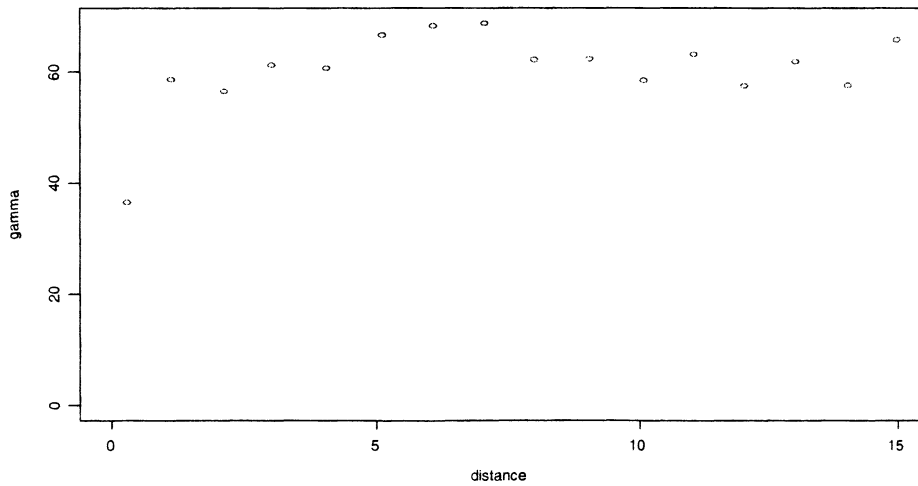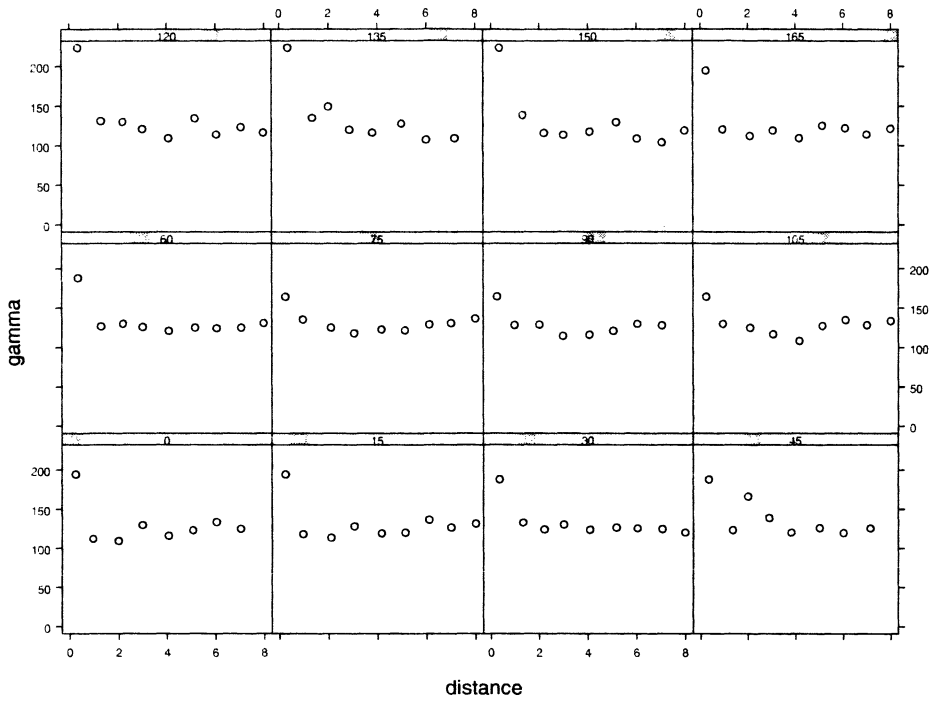Omnidirectional Variogram of CST Values - Grid M1
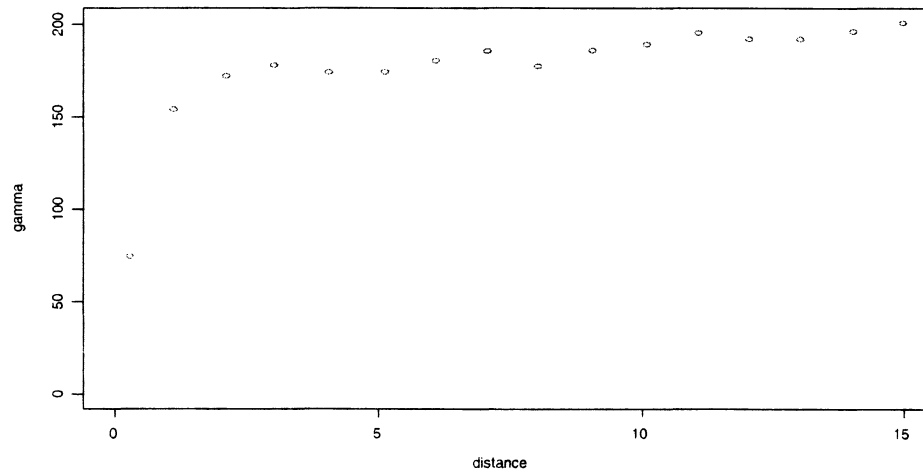


The above omnidirectional variogram shows a sill at 170 and a maximum spatial continuity at a distance of 2 meters.

68

Directional variograms of CST values - Grid M2



In viewing the above directional variograms, the direction of maximum spatial continuity appears to be around the azimuths of 120, 135, and 150.

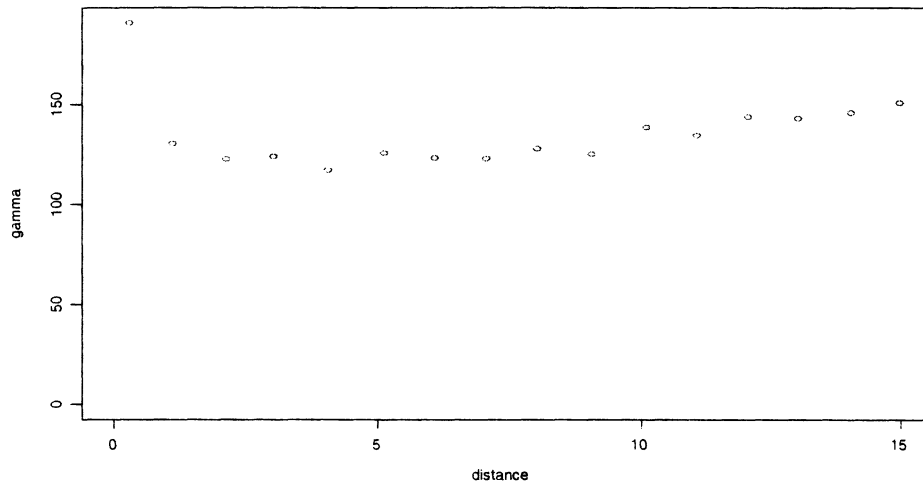Omnidirectional Variogram of CST Values - Grid M2



The above omnidirectional variogram shows a sill at 60 and a maximum spatial continuity at a distance of 2 meters. The sill shows evidence of a hole effect.

69

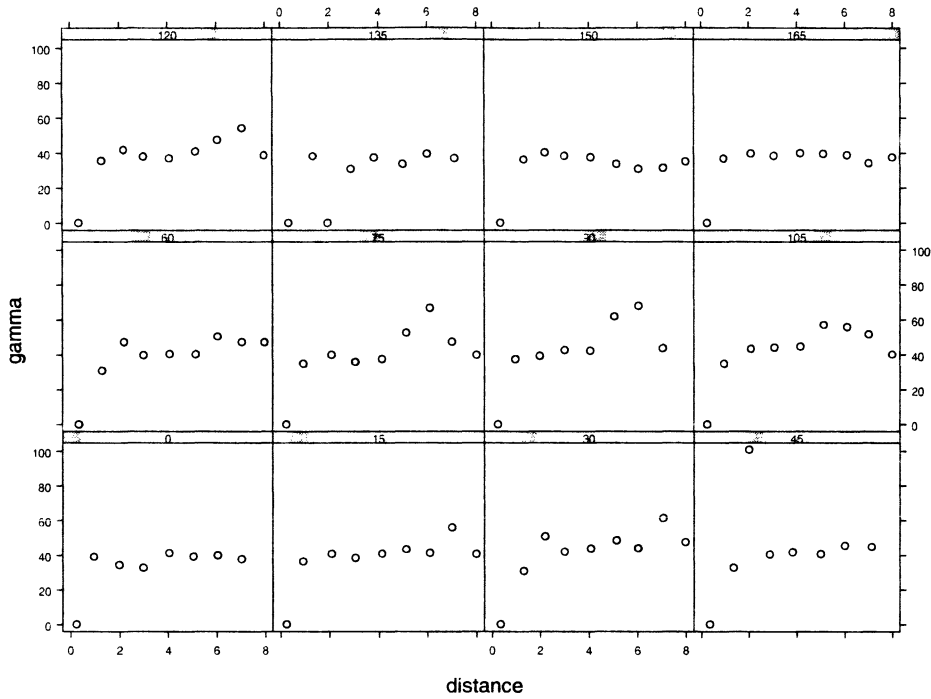Directional variograms of CST values - Grid M3

In viewing the above directional variograms, the direction of maximum spatial continuity appears to be around the azimuth of 90.



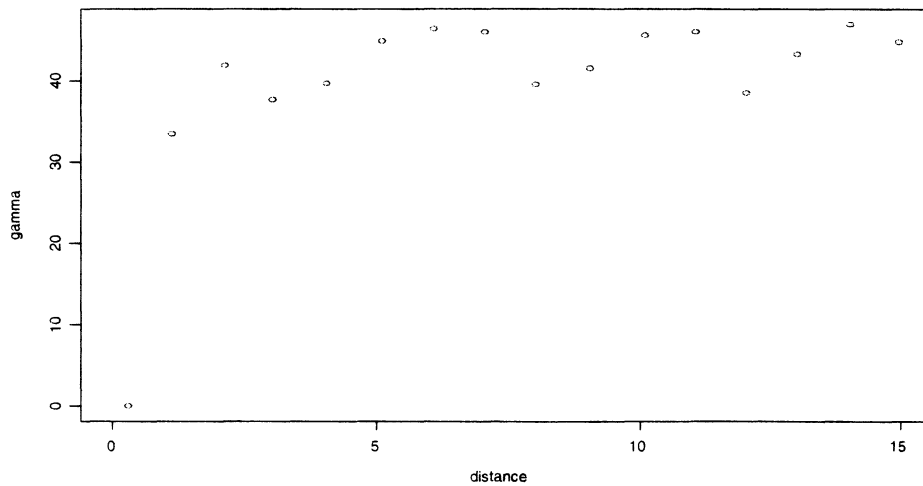Omnidirectional Variogram of CST Values - Grid M3

The above omnidirectional variogram shows a sill at 60 and a maximum spatial continuity at a distance of 2 meters. The sill shows evidence of a hole effect.

70

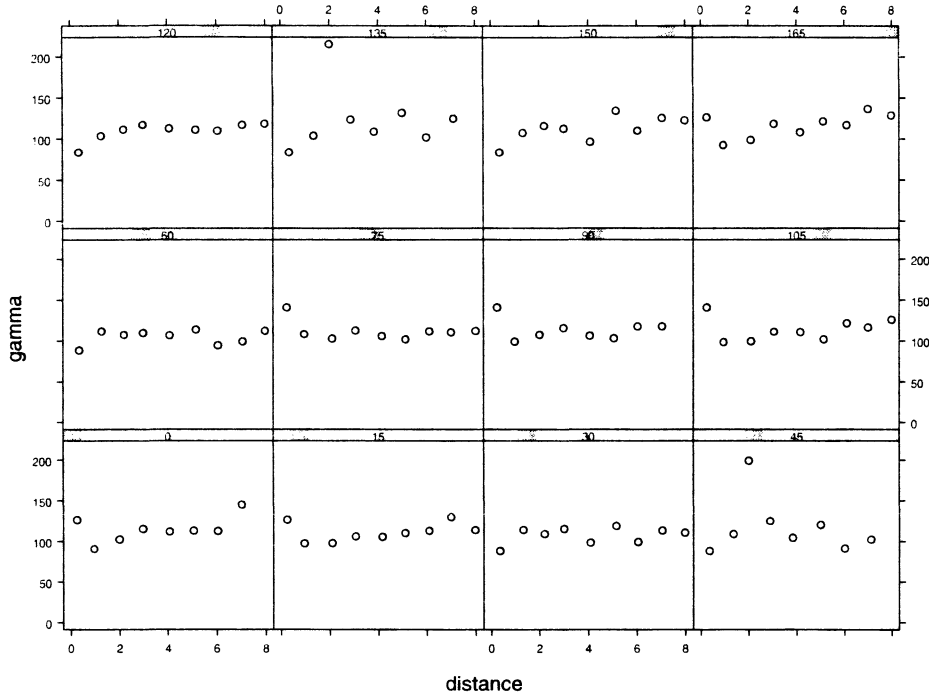Directional variograms of CST values - Grid MC

In viewing the above directional variograms, the direction of maximum spatial continuity appears to be around the azimuths of 30, 45, and 60.

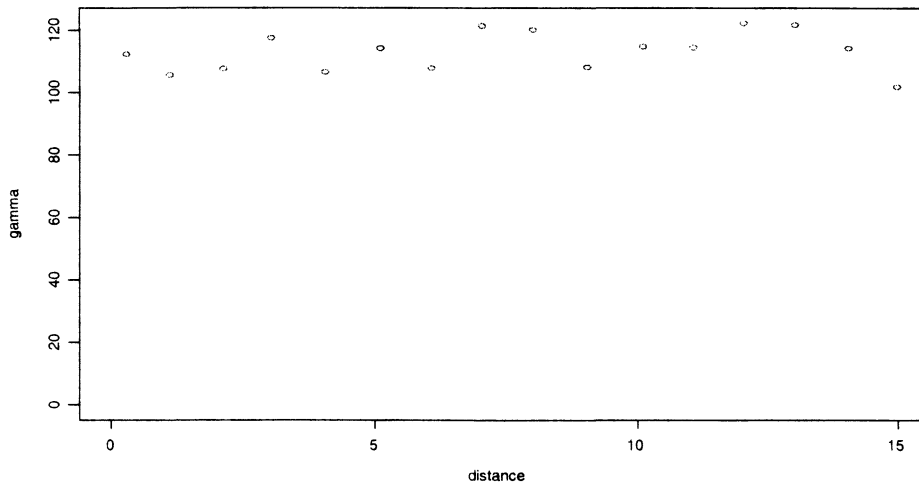Omnidirectional Variogram of CST Values - Grid MC



The above omnidirectional variogram shows a sill at 40 and a maximum spatial continuity at a distance of 3 meters. It also shows evidence of a hole effect.

71

Directional variograms of CST values - Grid H1



In viewing the above directional variograms, the direction of maximum spatial continuity appears to be around the azimuths of 90.

Omnidirectional Variogram of CST Values - Grid H1



The above omnidirectional variogram does not have a clear sill.
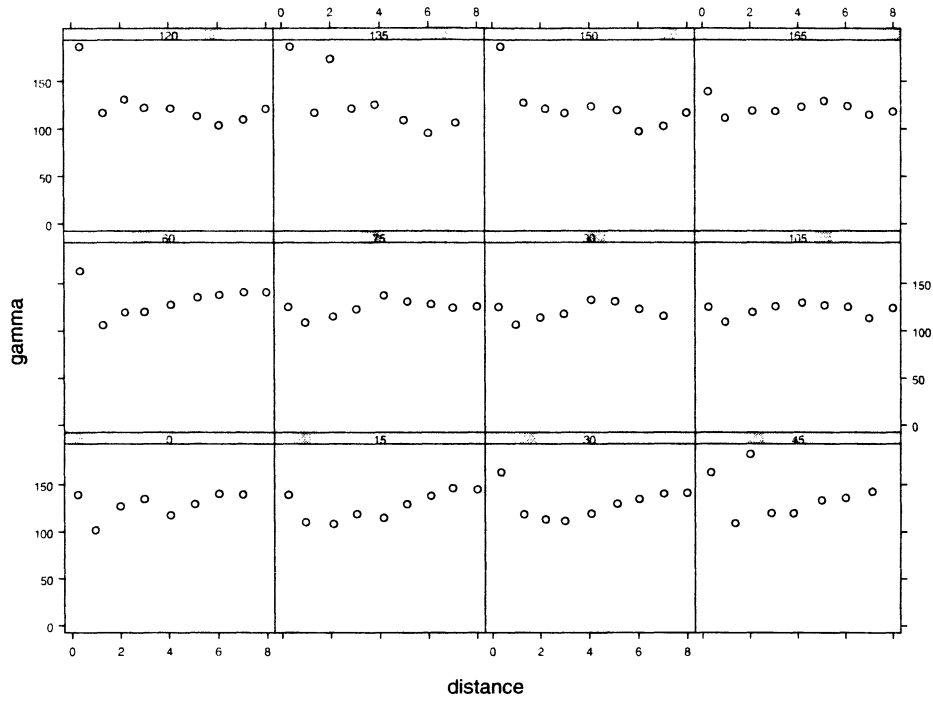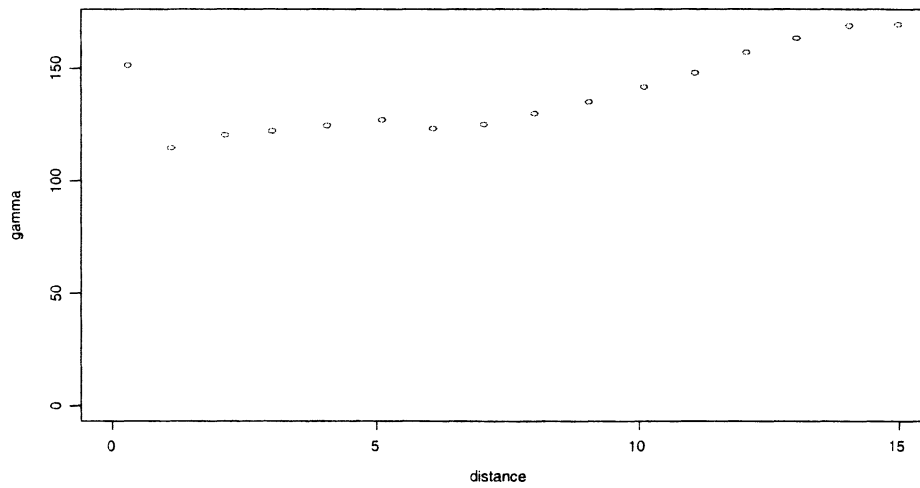
Directional variograms of CST values - Grid H2



In viewing the above directional variograms, the direction of maximum spatial continuity appears to be around the azimuths of 150.

Omnidirectional Variogram of CST Values - Grid h2



The above omnidirectional variogram does not show a clear sill.

73

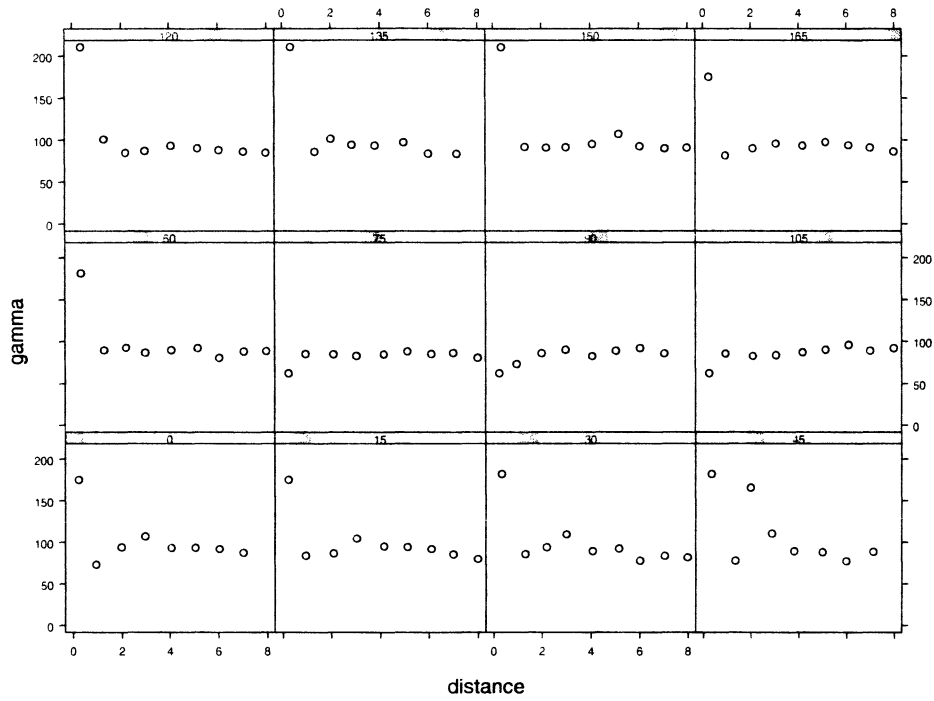## Directional variograms of CST values - Grid H3



**In viewing the above directional variograms, the direction of maximum spatial continuity appears to be around the azimuth of 105.**

## Omnidirectional Variogram of CST Values - Grid H3



**The above omnidirectional variogram does not show a clear sill.**

Directional variograms of CST values - Grid HC



In viewing the above directional variograms, the direction of maximum spatial continuity appears to be around the azimuth of 120.

Omnidirectional Variogram of CST Values - Grid HC
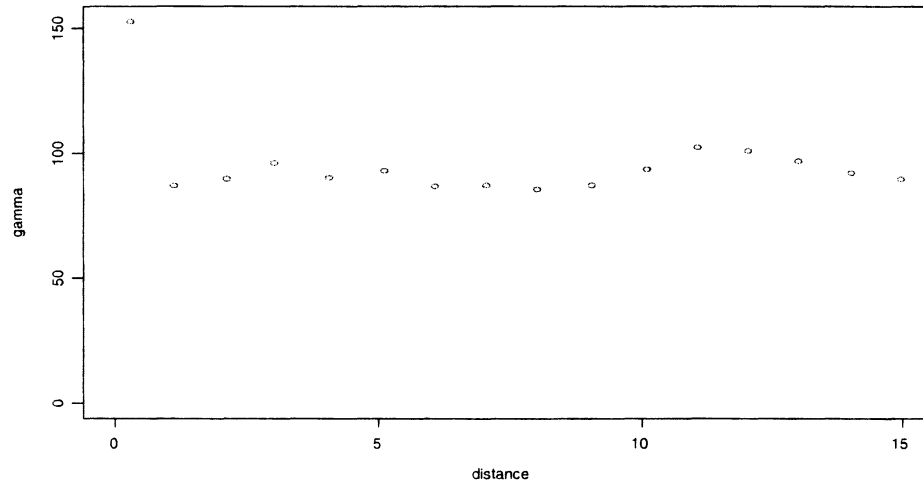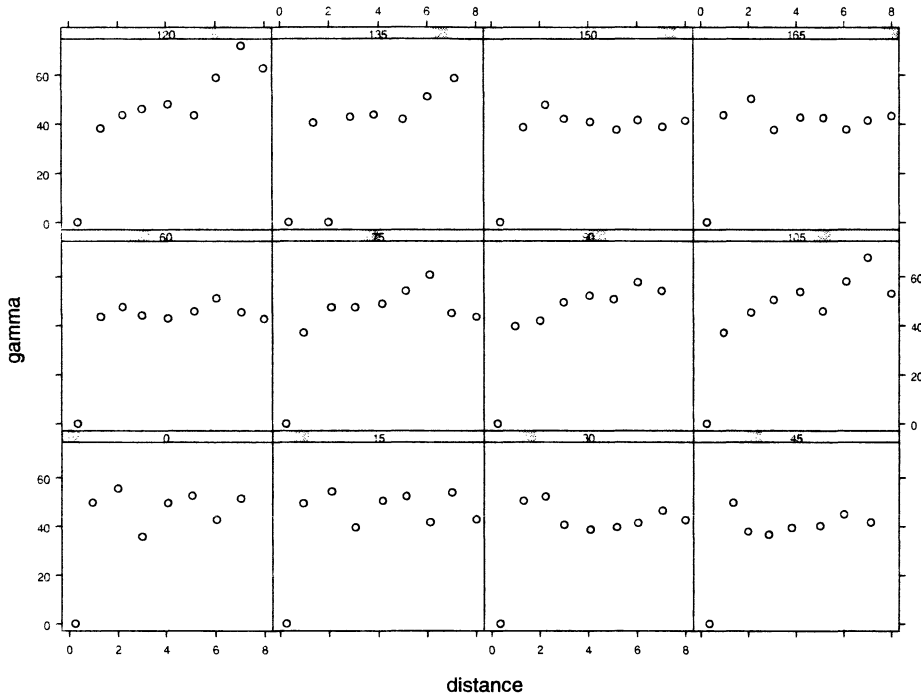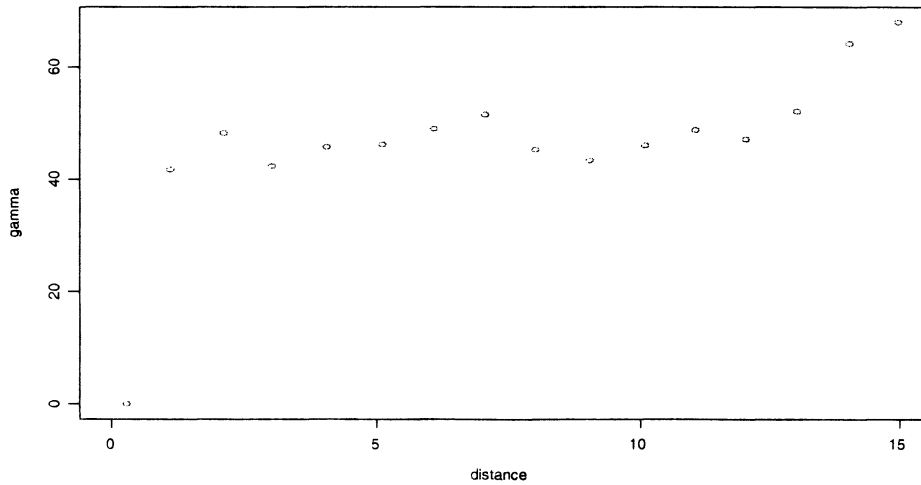


The above omnidirectional variogram shows a sill at 45 and a maximum spatial continuity at a distance of 1 meter.

# G. Plot of volumetric water content and CST.
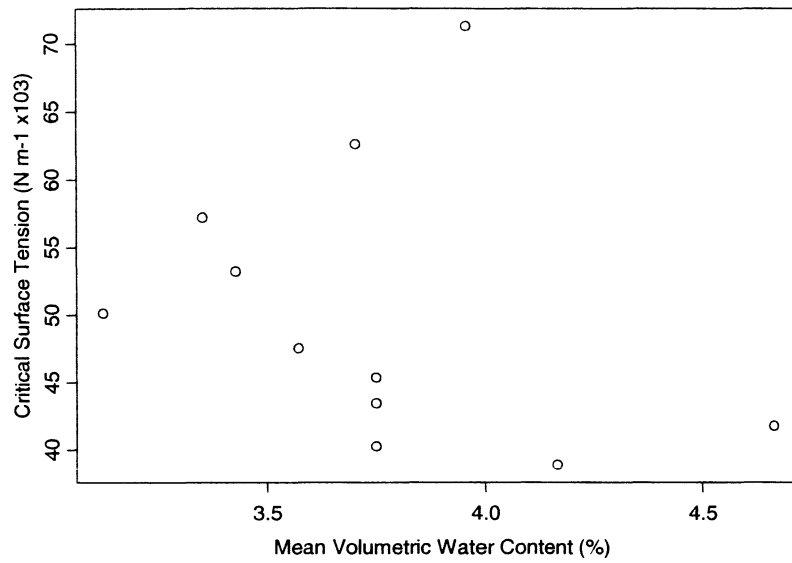


Scatter plot of critical surface tension against mean volumetric water content on the Moose Fire plots.
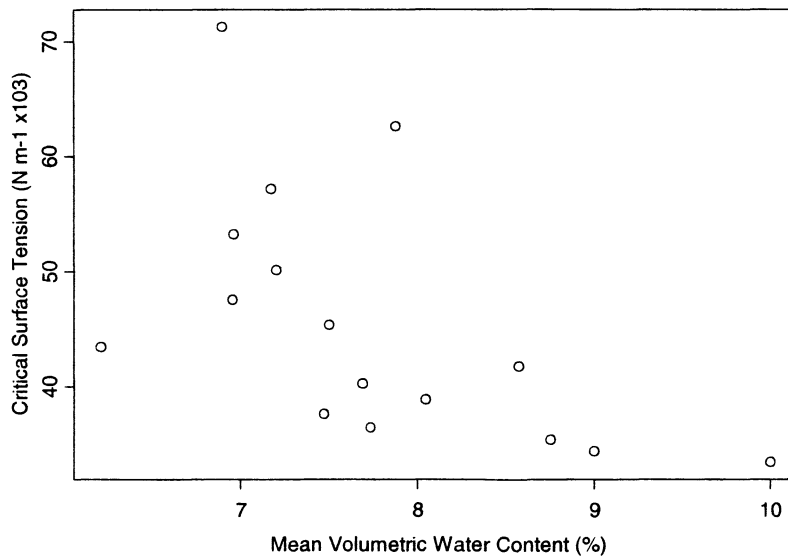


Scatter plot of critical surface tension against mean volumetric water content on the Hayman Fire plots .

## H. Plot of ash depth and CST.
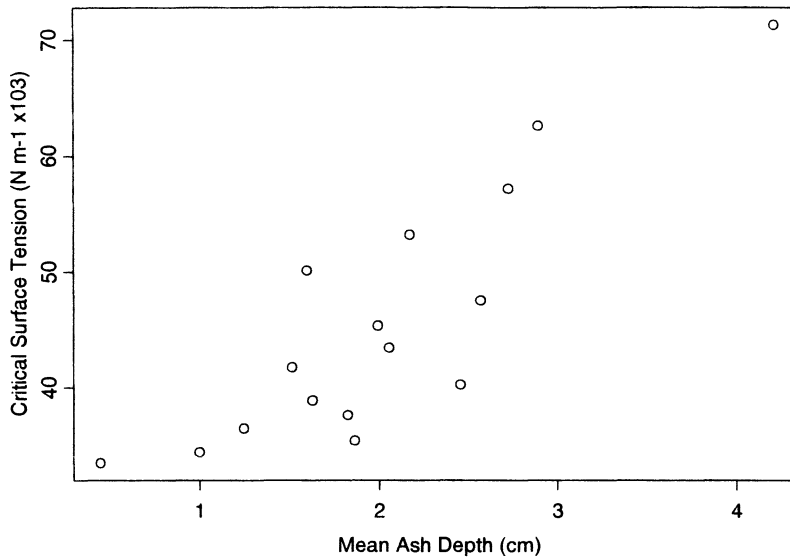


**Scatter plot of critical surface tension against mean ash depth for the Moose Fire plots.**



**Scatter plot of critical surface tension against mean ash depth for the Hayman Fire plots.**

77
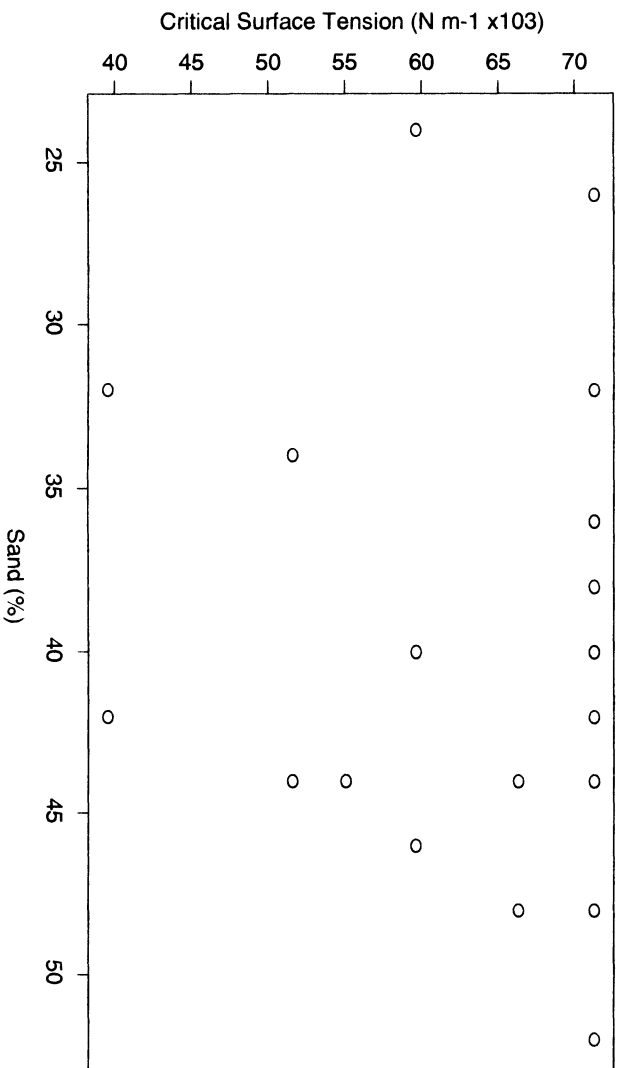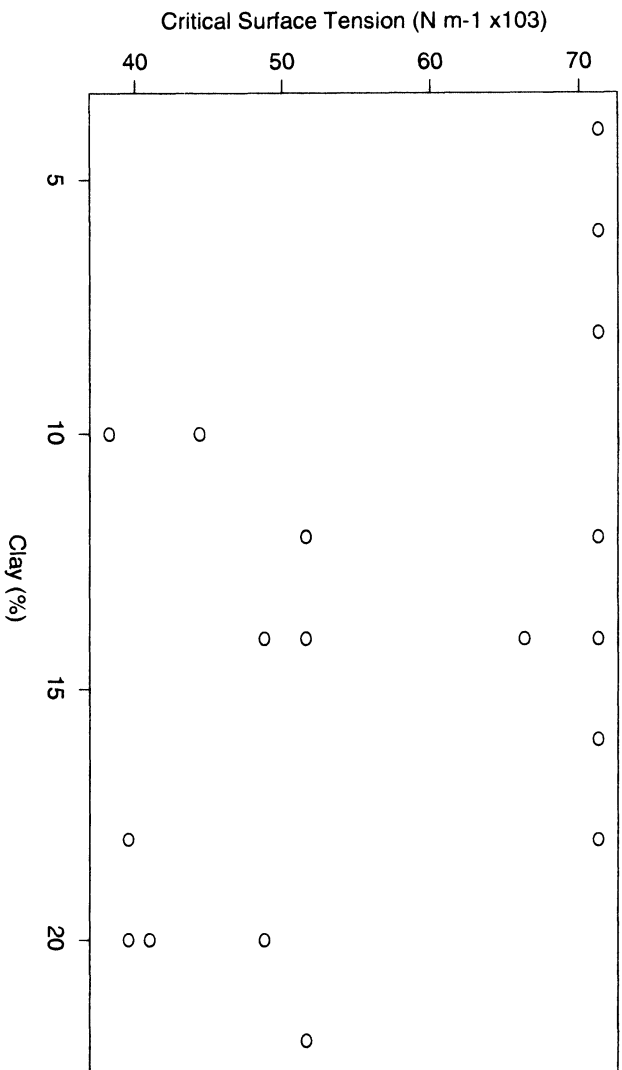
Moose Fire
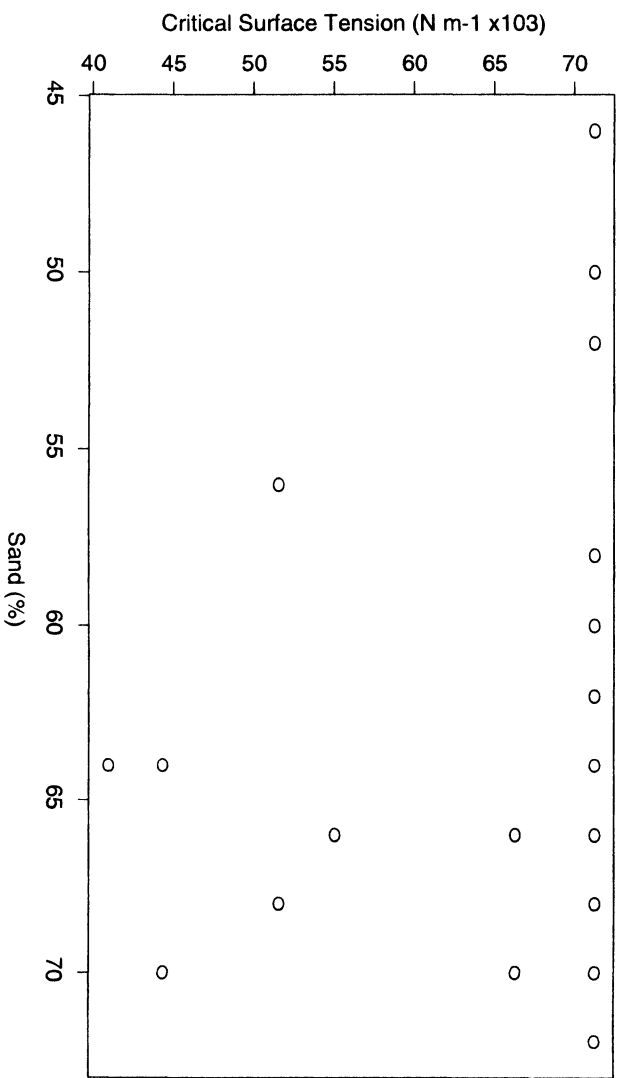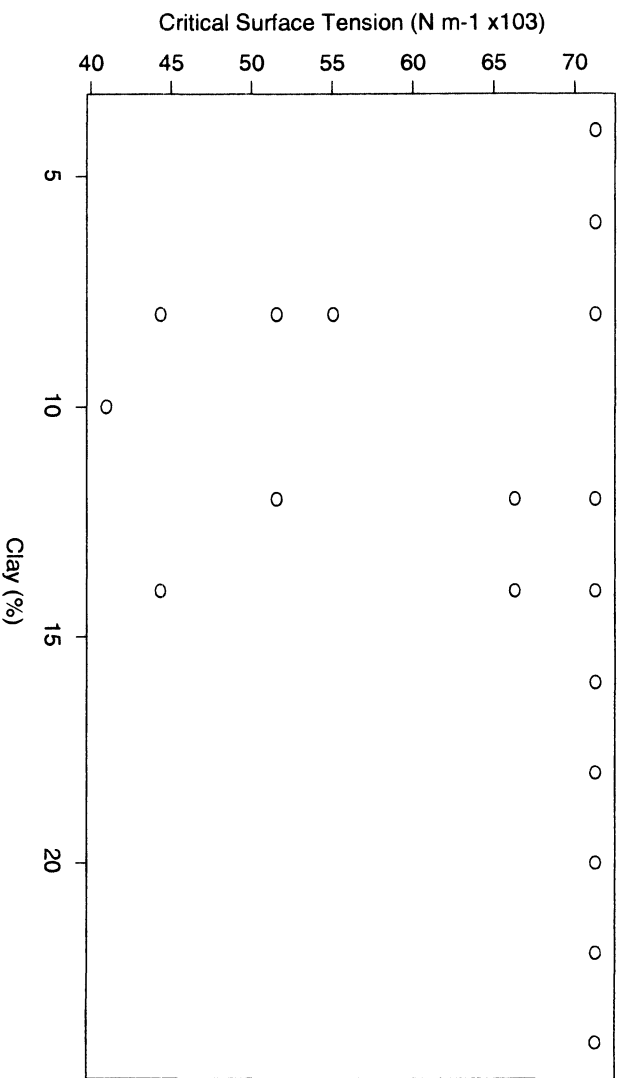
Percent sand, silt, and clay by grid
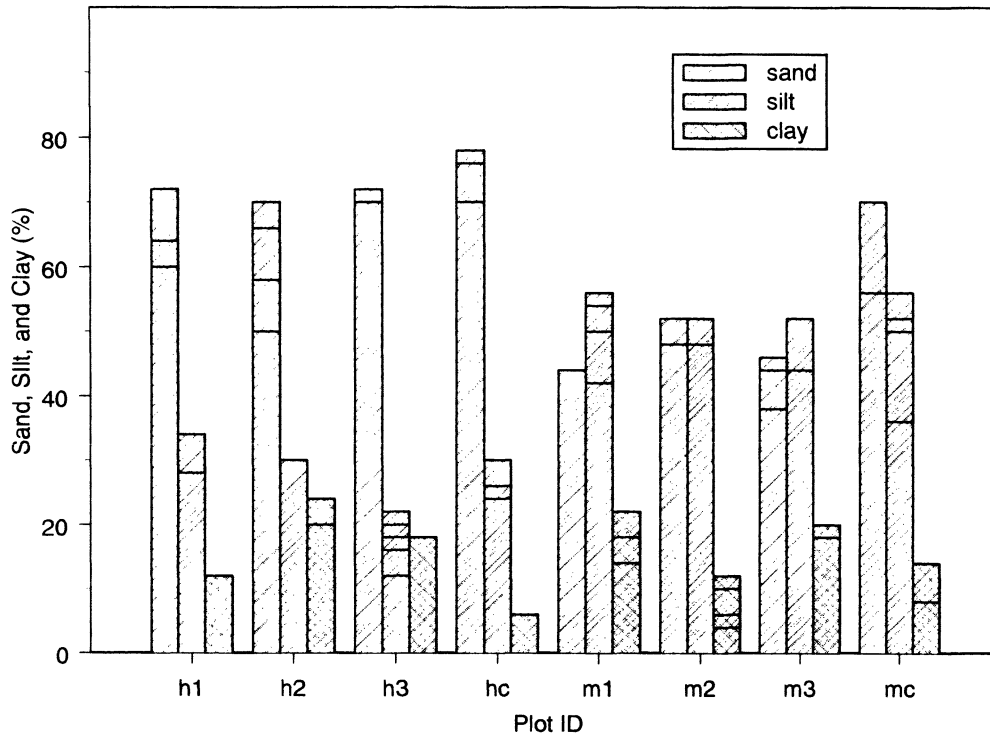
**J. Mantel Test p-values and correlation coefficients (r) based on 10,000 permutations.**

Correlation of % sand and space with CST while controlling for sand and space.

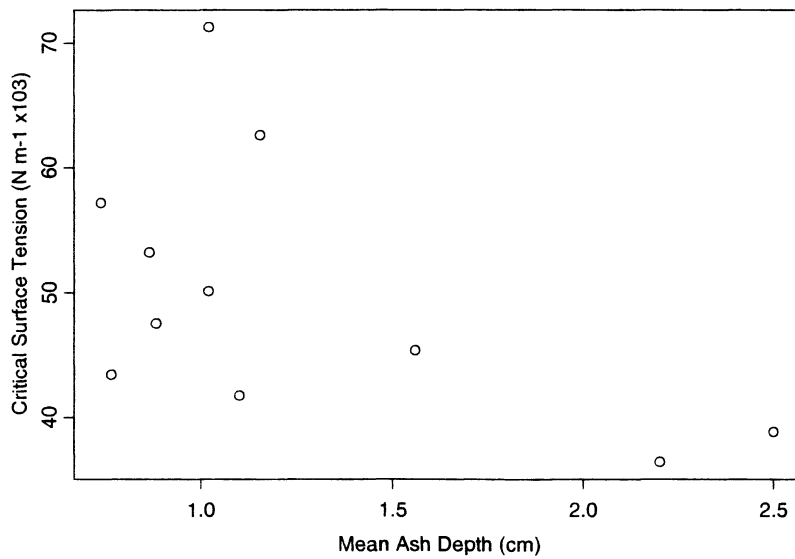| Site | St vs sand/space | St vs space/sand | St vs space |
|---|---|---|---|
| M1 M2 M3 | r=0.012 p=0.357 | r=-0.015 p=0.459 | r=-0.015 p=0.466 |
| H1 H2 H3 | r=-0.104 p=0.084 | r=-0.005 p=0.521 | r=-0.008 p=0.505 |

Correlation of CST and Space while controlling for Volumetric Water Content (VWC) and Ash Depth.

| Site | St vs space/vwc | St vs space/ash |
|---|---|---|
| M1 | r=0.033 p=0.0003 | r=0.032 p=0.0006 |
| M2 | r=0.009 p=0.329 | r=0.009 p=0.321 |
| M3 | r=0.058 p=0.002 | r=0.058 p=0.002 |
| MC | r=0.027 p=0.137 | |
| H1 | r=1.000 p=0.0001 | r=0.030 p=0.245 |
| H2 | r=0.067 p=0.008 | r=0.061 p=0.125 |
| H3 | r=0.053 p=0.016 | r=0.394 p=0.0001 |
| HC | | |

81

Correlations of CST with volumetric water content (VWC) while controlling for ash and space; and correlations of CST with ash depth while controlling for space and VWC.

| Site | St vs vwc/space | St vs vwc/ash | St vs ash/space | St vs ash/vwc |
|------|-----------------|---------------|-----------------|---------------|
| M1 | r= 0.0067<br>p= 0.199 | r=0.016<br>p=0.080 | r= -0.0067<br>p= 0.194 | r=0.108<br>p=0.0001 |
| M2 | r=0.028<br>p=0.103 | r=0.019<br>p=0.125 | r=0.024<br>p=0.193 | r=0.010<br>p=0.321 |
| M3 | r=0.033<br>p=0.006 | r=0.015<br>p=0.100 | r=0.02<br>p=0.075 | r=0.02<br>p=0.075 |
| MC | r=0.041<br>p=0.079 | | | |
| H1 | r=0.0105<br>p=0.0017 | r=0.259<br>p=0.0001 | r=0.093<br>p=0.0369 | r=0.283<br>p=0.0001 |
| H2 | r=0.025<br>p=0.261 | r=0.257<br>p=0.0002 | r=-0.039<br>p=0.307 | r=0.213<br>p=0.001 |
| H3 | r=-0.051<br>p=0.077 | r=0.215<br>p=0.0001 | r=0.187<br>p=0.0001 | r=0.309<br>p=0.0001 |
| HC | NA | | | |

# REFERENCES

Bachmann, J., R. Horton, R., and van der Ploeg, R.R. 2001. *Isothermal and Nonisothermal Evaporation from Four Sandy Soils of Different Water Repellency* Soil Sci Soc Am. 65: 1599-1607

Benavides-Solorio, J., and MacDonald, L.F. 2001 Post-fire runoff and erosion from simulated rainfall on small plots, Colorado Front Range. Hydrologic Processes. 15: 2931-2952

Brock, John H.; DeBano, Leonard F. 1990. Wettability of an Arizona chaparral soil influenced by prescribed burning. In: Krammes, J. S., technical coordinator. Effects of fire management of Southwestern natural resources: Proceedings of the symposium; 1988 November 15-17; Tucson, AZ. Gen. Tech, Rep. RM-191. Fort Collins, CO: U.S. Department of Agriculture, Forest Service, Rocky Mountain Forest and Range Experiment Station: 206-209. [11291]

DeBano, L. F. 2000. *The role of fire and soil heating on water repellency in wildland environments: a review.* Journal of Hydrology 231:195-206.

DeBano, L. F., S. M. Savage, and D. M. Hamilton. 1976. *The transfer of heat and hydrophobic substances during burning.* Soil Science Society of America Journal 40:779-782.

DeBano, L.F., D. G. Neary, and P. F. Folliott. 1998. *Fire's effects on ecosystems.* John Wiley & Sons, New York, New York, USA.

DeBano, L.F., and Krammes, J.S., 1966, *Water-repellent soils and their relation to wildfire temperatures.* Bulletin of the International Association of Scientific Hydrology 11(2):14-19.

DeBano, L.F. 1981. *Water repellent soils: a state-of-the-art.* USDA Forest Service General Technical Report PSW-46, 21pp.

DeBano, L.F., L.D. Mann, and D.A. Hamilton. 1970. Translocation of hydrophobic substances in soil by burning. Soil Sci. Amer. Proc. 34130-133.

DeByle, N.V., 1973, *Broadcast burning of logging residues and the water repellency of soils.* Northwest Science 47(2):77-87.

Dekker, L.W., and Ritsema, C.J. 2000. *Wetting patterns and moisture variability in water repellent Dutch soils.* J. Hydrology 231-232:148-164.

Doerr, S.H., and A.D. Thomas. 2000. The role of soil moisture in controlling water repellency: new evidence from forest soils in Portugal. J. Hydrol. 231–232:134–147.

Doerr, S.H.; Shakesby, R.A.; and Walsh, R.P.D., 2000. *Soil Water Repellency: Its causes, characteristics and hydro-geomorphological significance.* Earth Science review 51:33-65.

Doerr S.H., R.A. Shakesby and R.P.D. Walsh, 1996. Soil Hydrophobicity variations with depth and particle size fraction in burned and unburned *Eucalyptus globux* and *Pinar pinastar* forest terrain in the Aqueda Basin, Portugal. *Cantena* 27:25-47.

Doerr, S.H.; Shakesby, R.A.; and Walsh, R.P.D; 1998 *Spatial Variability of soil hydrophobicity in fire-prone eucalyptus and pine forests,* Portugal. Soil Science 163:313-324.

Doerr, S.H., and A.D. Thomas. 2000. The role of soil moisture in controlling water repellency: new evidence from forest soils in Portugal. J. Hydrol. 231–232:134–147.

Dyrness, C.T., 1976. *Effect of wildfire on soil wettability in the High Cascades of Oregon.* USDA Forest Service, Research Paper PNW-202, 18pp.

Ehrenfeld, J.G. 1997. Invasion of deciduous forest preserves in the New York metropolitan region by Japanese barberry (*Berberis thunbergii* DC.). J. Torrey Bot. Soc. 124:210–215.

Gaston, L.A., M.A. Locke, R.M. Zablotowicz, and K.N. Reddy. 2001. Spatial variability of soil properties and weed populations in the Mississippi Delta. Agron. J. 65:449–459.

Hawley, M.E.; Jackson, T.J.; McCuen, R.H., 1983. Surface Soil Moisture Variation on Small Agricultural Watersheds. Journal of Hydrology 62: 179-200.

Helvey, J. D. 1980. *Effects of a north-central Washington wildfire on runoff and sediment production.* Water Resource Bulletin 16:627-634

Huffman, E.L, MacDonald, L.H., Stednick, J.D. 2001. *Strength and persistence of fire-induced soil hydrophobicity under ponderosa and lodgepole pine,* Colorado Front Range. Hydrologic Processes 15:2877-2892.

Johnson, J.P., Hakonson, T.E., Breshears, D.D. 2001. Post-fire runoff and erosion from rainfall simulation: contrasting forests with shrublands and grasslands. Hydrological Processes15:2953-2965.

Imeson, A.C., Verstraten, J.M., van Mulligen, E.J. and Sevink, J., 1992. *The effects of fire ans water repellency on infiltration and runoff under Mediterranean type forest.* Catena 19:345-361.

Mataix-Solera J.; Doerr S.H. 2004. Hydrophobicity and aggregate stability in calcareous topsoils from fire-affected pine forests in southeastern Spain. Geoderma. 118: 77-88.

Mataix-solere, J., Gomez, I., Navarro- Pedreño, J., Guerrero, C., and Moral, R. 2002. Soil organic matter and aggregates affected by wildfire in a *Pinus halepensis* forest in a Mediterranean environment. International journal of wildland fire. 11:107-114.

Meyer, G.A., and Wells, S.G., 1997, Fire-related sedimentation events on alluvial fans, Yellowstone National Park, U.S.A.: *Journal of Sedimentary Research,* v. A67, p. 776-791.

Letey, J., 2001. *Causes and consequences of fire-induced soil water repellency.* Hydrological Processes 15:2867 – 2875.

MacDonald, L.H., and E.L. Huffman, 2004. Post-fire soil water repellency: persistence and soil moisture thresholds. Soil Science Society of America Journal 68: 1729-1734.

McNabb, D.H., Gaweda, F., Fröhlich, H.A., 1989. Infiltration, water repellency, and soil moisture content after broadcast burning a forest site in southwest Oregon. Journal of Soil and Water Conservation 44, 87-90.

Meyer, G. A., J. L. Pierce, S. H. Wood, and A. J. T. Jail (2001), Fire, storms, and erosional events in the Idaho batholith, *Hydrologic Processes, 15,* 3025-3038.

Meeuwig, R.O., 1971. *Infiltration and water repellency in granitic soils,* U.S.D.A. Forest Service Research Paper INT-111, 20 pp. Moody, J. A., and D. A. Martin, (2001), Post-fire, rainfhll intensity-peak discharge relations ibr three mountainous watersheds in the western USA,

Robichaud, P. R. and Hungerford, R. D. 2000. *Water repellency by laboratory burning of four nothrern Rocky Mountain forest soils.* Jurnal of Hydrolgoy 231-232:207-219

Robichaud P.R., L. MacDonald, J. Freeouf, D. Neary, D. Martin and L. Ashmun, 2003. Postfire rehabilitation of the Hayman Fire. USDA Forest Service Gen. Tech. Rep. RMRS-GTR-114. p.293-313.

Savage, S.M., 1974. *Mechanism of fire-induced water repellency in soil.* Soil Science Society of America Proceedings 38:652-657.

Scholl, D.G. 1975. Soil wettability and fire in Arizona chaparral. Soil Science Society of America proceeding. 39: 356-361.

Scott, D.F., 2000.Soil wettability in forested catchments in South Africa: as measured by different methods and as affected by vegetation cover and soil characteristics. Journal of Hydrology 231-232, 87-104.

Scott, D.F., and Van Wyk, D.B. 1990. Effects of wildfire on soil wettability and hydrological behaviour of an afforested catchment. Journal of Hydrology. 121: 239-256.

Shakesby, A., Doerr, S.H., Walsh, R.P.D. 2000. *The erosional impact of soil hydrophobicity: Current problems and future research directions.* Journal of Hydrology 231-232:178-191.

Shakesby, R.A., C.O.A. Coelho, A.D. Ferreira, J.P. Terry and R.P.D. Walsh, 1993. Wildfire impacts on soil erosion and hydrology in wed Medeterranean forest, Portugal. *International Journal of Wildland Fire* 3(2):95-110.

Soil survey of Flathead national Forest Area, Montana. 1999. vii, 100 p., 106 p. of plates : ill., maps ; Washington, D.C.?

Tiedemann A.R., C.E. Conrad, J.H. Dietrich, J.W. Hornbeck, W.F. Megahan, L.A. Viereck and D.D. Wade, 1979. Effects of fire on water: a state of knowledge review. General Technical Report WO-10, USDA Forest Service.

USDA 2002. Burned Area Report FSH 2509. 13

USDA 2002. Moose Fire Restoration Project: broad-scale viability analysis. USDA Forest Service. Flathead national Forest, Kalispell, MT. 9p.

USDA 2003. Watershed Restoration Plan for Big Creek, Northfork of the Flathead River.

Wells, C. G., Campbell, R. E., DeBano, L. F., Lewis, C. E., Fredriksen, R. L., Franklin, E. C., Froelich, R. C., and Dunn, P. H. 1979. *Effects of fire on soil: A state-of-knowledge review.* General Technical Repeport USDA Forest Serves WO-7. Washington D.C.